ANL/GTRI/TM-14/15

Neutronics Conversion Analyses of the Laue-Langevin Institute (ILL) High Flux Reactor (RHF)

Nuclear Engineering Division

About Argonne National Laboratory
Argonne is a U.S. Department of Energy laboratory managed by UChicago Argonne, LLC under contract DE-AC02-06CH11357. The Laboratory's main facility is outside Chicago, at 9700 South Cass Avenue, Argonne, Illinois 60439. For information about Argonne and its pioneering science and technology programs, see www.anl.gov.

DOCUMENT AVAILABILITY

Online Access: U.S. Department of Energy (DOE) reports produced after 1991 and a growing number of pre-1991 documents are available free via DOE's SciTech Connect (http://www.osti.gov/scitech/)

Reports not in digital format may be purchased by the public from the National Technical Information Service (NTIS):

U.S. Department of Commerce
National Technical Information Service
5301 Shawnee Rd
Alexandria, VA 22312
www.ntis.gov
Phone: (800) 553-NTIS (6847) or (703) 605-6000
Fax: (703) 605-6900
Email: **orders@ntis.gov**

Reports not in digital format are available to DOE and DOE contractors from the Office of Scientific and Technical Information (OSTI):

U.S. Department of Energy
Office of Scientific and Technical Information
P.O. Box 62
Oak Ridge, TN 37831-0062
www.osti.gov
Phone: (865) 576-8401
Fax: (865) 576-5728
Email: **reports@osti.gov**

Disclaimer
This report was prepared as an account of work sponsored by an agency of the United States Government. Neither the United States Government nor any agency thereof, nor UChicago Argonne, LLC, nor any of their employees or officers, makes any warranty, express or implied, or assumes any legal liability or responsibility for the accuracy, completeness, or usefulness of any information, apparatus, product, or process disclosed, or represents that its use would not infringe privately owned rights. Reference herein to any specific commercial product, process, or service by trade name, trademark, manufacturer, or otherwise, does not necessarily constitute or imply its endorsement, recommendation, or favoring by the United States Government or any agency thereof. The views and opinions of document authors expressed herein do not necessarily state or reflect those of the United States Government or any agency thereof, Argonne National Laboratory, or UChicago Argonne, LLC.

ANL/GTRI/TM-14/15

Neutronics Conversion Analyses of the Laue-Langevin Institute (ILL) High Flux Reactor (RHF)

prepared by
A. Bergeron, B. Dionne
Nuclear Engineering Division, Argonne National Laboratory

Y. Calzavara
BPC / Projects Office, Institut Laue Langevin

9/30/2014

[This page intentionally left blank]

Abstract

The following report describes the neutronics results obtained with the MCNP model of the RHF U7Mo LEU reference design that has been established in 2010 during the feasibility analysis. This work constitutes a complete and detailed neutronics analysis of that LEU design using models that have been significantly improved since 2010 and the release of the feasibility report.

When possible, the credibility of the neutronics model is tested by comparing the HEU model results with experimental data or other codes calculations results. The results obtained with the LEU model are systematically compared to the HEU model.

The changes applied to the neutronics model lead to better comparisons with experimental data or improved the calculation efficiency but do not challenge the conclusion of the feasibility analysis. If the U7Mo fuel is commercially available, not cost prohibitive, a back-end solution is established and if it is possible to manufacture the proposed element, neutronics analyses show that the performance of the reactor would not be challenged by the conversion to LEU fuel.

Acknowledgments

The authors would like to acknowledge that the support for this work was provided by the National Nuclear Security Administration (NNSA) Reactor Conversion Program and the U.S. Department of Energy (DOE). This work could not have been possible without the close collaboration with the ILL staff and the RHF conversion team.

Table of Contents

ABSTRACT 5

ACKNOWLEDGMENTS 6

TABLE OF CONTENTS 7

LIST OF FIGURES 9

LIST OF TABLES 11

LIST OF ABBREVIATIONS 14

1. INTRODUCTION 15

2. RHF REACTOR AND NEUTRONICS MODEL 16

2.1. Brief Reactor Description 16

2.2. U7Mo LEU Reference Design 21

2.3. Neutronics Models 24

3. TOOLS AND METHODS 30

3.1. Tools 30
3.1.1. Steady-state Neutronics Calculations – MCNP 30
3.1.2. Depletion Calculations - ORIGEN 30
3.1.3. Monte-Carlo-Depletion - VESTA 30
3.1.4. Nuclear Library 31

3.2. Methods 32
3.2.1. Critical Search 32
3.2.2. Generating MCNP Cards for Discrete Involute Modeling 32
3.2.3. Power Distribution Normalization in MCNP 34

4. NEUTRONICS ANALYSIS 37

4.1. Depletion 37
4.1.1. Model Credibility 37
4.1.2. HEU vs. LEU Cycle Length 38

4.1.3. Fission Rate and Fission Density 39
4.1.4. Heavy Isotopes Inventory 43
4.1.5. Helium Production in Borated Zone 44
4.1.6. Kinetic Parameters Evolution 45

4.2. Neutron flux 48
4.2.1. Model Credibility 48
4.2.2. Neutron Flux at the Beam Tube Entrances 52

4.3. Power Distribution 56
4.3.1. Model Credibility 56
4.3.2. Power Deposition in the Core 58
4.3.3. Power Distribution in the Fuel 59

4.4. In-Pile Reactivity Worth & Feedback Coefficient 65
4.4.1. Experimental Device Worth 66
4.4.2. Power Defect 68
4.4.3. Control Element Differential Worth 71
4.4.4. Safety Rods Worth & Shutdown Margins 72

5. CONCLUSIONS 75

REFERENCES 76

APPENDICES 79

A1. Tabulated Values of Section 4.1 79

A2. Tabulated Values of Section 4.2 86

A3. Tabulated Values of Section 4.3 94

A4. Tabulated Values of Section 4.4 116

List of Figures

Figures in core of the report

Figure 2.1-1 – Cross-section of the RHF reactor [NEA, 2011] 18
Figure 2.1-2 – Top view of the RHF reactor; the fuel element is colored in pink. [NEA, 2011] 19
Figure 2.1-3 – Dimensions of the RHF HEU fuel plate [NEA, 2011] 19
Figure 2.1-4 – Dimensions of the RHF HEU fuel element [NEA, 2011] 20
Figure 2.2-1 – Schematic of RHF HEU and LEU fuel plate and dimensions of the poison belt (mm) 23
Figure 2.3-1 – 3D view of the RHF reflector obtained with a simplified neutronics model 25
Figure 2.3-2 – Top view of the fuel element as modeled 25
Figure 2.3-3 – Model details of unit cell (cladding is cyan, fuel is yellow, coolant channel is blue and side-plates are pink) 26
Figure 3.2-1 – Depletion scheme including critical search used for this study 33
Figure 4.1-1 – Comparison of calculated versus measured control element position of cycle 143; relative error on cycle length is estimated at one day 38
Figure 4.1-2 – Control element position evolution of the HEU and LEU cores depleted at a constant nuclear power of 57.8 MW; relative error on cycle length is estimated at one day 39
Figure 4.1-3 – Evolution of the average and maximum fission rate for HEU and LEU cores.; relative error is estimated at 10% .. 40
Figure 4.1-4 – Evolution of the average and maximum fission density for HEU and LEU cores; relative error is estimated at 10% 41
Figure 4.1-5 – Evolution of the average and maximum ^{235}U consumption for HEU and LEU cores; relative error is estimated at 10% 42
Figure 4.1-6 – Comparison between peak fission density and peak ^{235}U consumption; relative error is estimated at 10% 43
Figure 4.1-7 – Evolution of the neutron flux magnitude and ^{10}B, ^{4}He composition in the borated region; relative error is estimated at 10% 45
Figure 4.1-8 – Evolution of the β_{eff} for the HEU and LEU cores; steady state uncertainty is 6 pcm at one standard deviation; relative error including effect of depletion calculation estimated at 10% 46
Figure 4.1-9 – Evolution of the neutron lifetime for the HEU and LEU cores; steady state uncertainty is 1.3 µs at one standard deviation; relative error including effect of depletion calculation estimated at 10% 47
Figure 4.2-1 – Calculated versus measured axial thermal flux profile at a distance of 23.5, 27.5 and 31.5 cm from the core center; relative error is less than 2% at one standard deviation 49
Figure 4.2-2 – Calculated versus measured axial thermal flux profile at a distance of 35.5, 43.5, 51.5 and 83.5 cm from the core center; relative error is less than 2% at one standard deviation 50
Figure 4.2-3 – ANL versus SAR calculated radial flux distribution in the median plane of the reactor; relative error is less than 2% at one standard deviation 51
Figure 4.2-4 – HEU (52.8 MW) and LEU (57.8 MW) axial profile of the thermal neutron flux at a radial distance of 30 cm (typical distance from beam tube inlet) from the core center; relative error is less than 0.1% at one standard deviation at BOC and estimated at 10% at EOC 54
Figure 4.3-1 – Comparison between measured and calculated axially averaged radial power profile; calculation relative error is less than 0.25% 57
Figure 4.3-2 – Comparison between measured and calculated ratio between local and average power; calculation relative error is less than 0.25% 57
Figure 4.3-3 – 2D representation of the power density in the fuel; from left to right, HEU BOC, HEU EOC, LEU BOC and LEU EOC; calculated relative error is less than 0.25% at BOC and estimated at 10% at EOC 60

Figure 4.3-4 – Power density axial profile in the inner edge of the fuel element; from top to bottom: at BOC, at day 24 and at EOC; calculated relative error is less than 0.25% at BOC and estimated at 10% otherwise. Position of the HEU and LEU core control rod is represented with a black and red rectangle, respectively. 61
Figure 4.3-5 – Power density axial profile in the outer edge of the fuel element; from top to bottom: at BOC, at day 24 and at EOC; calculated relative error is less than 0.25% at BOC and estimated at 10% otherwise 62
Figure 4.3-6 – Evolution of the power density at different location and resulting power density envelope in HEU core; calculated relative error is less than 0.25% at BOC and estimated at 10% otherwise 63
Figure 4.3-7 – Evolution of the power density at different location and resulting power density envelope in LEU core; calculated relative error is less than 0.25% at BOC and estimated at 10% otherwise 63
Figure 4.3-8 – Power density envelope for HEU and LEU cores; calculated relative error is less than 0.25% at BOC and estimated at 10% otherwise 64
Figure 4.4-1 – Reactivity worth of the HEU core in-pile experimental devices in cold and hot conditions; relative error is less than 15 pcm at one standard deviation 66
Figure 4.4-2 – Reactivity worth of the HEU and LEU cores in-pile experimental devices in cold conditions; relative error is less than 15 pcm at one standard deviation 67
Figure 4.4-3 - Reactivity worth of the HEU and LEU cores flooded beam tubes in cold conditions; relative error is less than 15 pcm at one standard deviation 68
Figure 4.4-4 – Reactivity change due to passage from cold to full power conditions; relative error is less than 15 pcm at one standard deviation 70
Figure 4.4-5 – Differential worth of the control element; relative error is less than 15 pcm at one standard deviation 71
Figure 4.4-6 – Reactivity change due to the insertion of the four less efficient safety rods; relative error is less than 40 pcm at one standard deviation 74

Figures in appendices

Figure A2 - 1 – relative error associated to the calculated HEU core thermal neutron flux presented in table A2 -3 and A2 - 4 at one standard deviation 89
Figure A2 - 2 – relative error associated to the calculated HEU core neutron flux presented in table A2 -1 at one standard deviation 91
Figure A2 - 3 – relative error associated to the calculated HEU and LEU cores neutron flux presented in table A2 - 6 at one standard deviation 93

List of Tables

Tables in core of the report

Table 2.3-1 – Materials temperature, pressure and density for the cold and hot states 26
Table 2.3-2 – Axial discretization used for the HEU and LEU fuel (1 = top; 46 = bottom)..... 27
Table 2.3-3 – Lateral discretization used for the HEU fuel, borated regions and LEU fuel (1 = inner side; 13 = outer side)..... 27
Table 2.3-4 – Axial discretization used for the HEU and LEU borated regions (1 = top; 3 or 4 = bottom) 27
Table 2.3-5 – Comparison of the fresh HEU fuel as used in the neutronics model..... 28
Table 2.3-6 – Composition of the fresh borated regions in the HEU neutronics model 28
Table 2.3-7 – Composition of the LEU fuel as used in the neutronics model 29
Table 2.3-8 – Composition of the fresh poison belt as used in the LEU neutronics model..... 29
Table 3.2-1 – Individual contribution to the nuclear power and methods to evaluate them..... 34
Table 4.1-1 – Inventory of Uranium, Neptunium and Plutonium isotopes at BOC and EOC; relative error is estimated at 10% ... 43
Table 4.2-1 – Categories of beam tubes defined by the presence or absence of cold/hot sources 52
Table 4.2-2 – Ratio LEU/HEU core peak neutron flux at BOC, EOC and at different power; relative error is less than 1% at BOC and estimated at 10% at EOC 53
Table 4.2-3 – Ratio BOC/EOC peak neutron flux of HEU and LEU cores; relative error estimated at 10%. 55
Table 4.3-1 – Distribution of power at BOC and EOC for both the HEU and LEU cores; calculated relative error is less than 1% at BOC and estimated at 10% at EOC..... 58
Table 4.4-1 – Reactivity worth of in-pile components and temperature and void coefficient; relative error is less than 1% at one standard deviation..... 65
Table 4.4-2 - Critical configurations tested prior to cycle 143 72
Table 4.4-3 - Results of the modeling of the critical configurations tested prior to cycle 143 73

Tables in appendix A1

Table A1 - 1 – Cycle 143 experimental and calculated critical control element position 79
Table A1 - 2 – Calculated critical control rod position for HEU and LEU reference design core depleted at a constant power of 57.8 MW and without beam tube IH4 80
Table A1 - 3 – Calculated fission rate for HEU and LEU reference design core depleted at a constant power of 57.8 MW and without beam tube IH4..... 81
Table A1 - 4 – Calculated fission density for HEU and LEU reference design core depleted at a constant power of 57.8 MW and without beam tube IH4..... 82
Table A1 - 5 – Calculated ^{235}U consumption for HEU and LEU reference design core depleted at a constant power of 57.8 MW and without beam tube IH4..... 83
Table A1 - 6 – Calculated neutron flux, ^{10}B and ^{4}He density evolution in most limiting boated region for HEU and LEU reference design core depleted at a constant power of 57.8 MW and without beam tube IH4 84
Table A1 - 7 – Calculated kinetic parameters evolution for HEU and LEU reference design core depleted at a constant power of 57.8 MW and without beam tube IH4 85

Tables in appendix A2

Table A2 - 1 – Digitized experimental axial neutron flux profile data at several radial locations (up to 31.5 cm) for HEU core at 57.8 MW 86
Table A2 - 2 – Digitized experimental axial neutron flux profile data at several radial locations (from 35.5 to 83.5 cm) for HEU core at 57.8 MW 86
Table A2 - 3 – Calculated HEU core thermal neutron flux axial profile at several radial locations (up to 31.5 cm) at a power of 57.8 MW 87
Table A2 - 4 – Calculated HEU core thermal neutron flux axial profile at several radial locations (from 35.5 to 83.5 cm) at a power of 57.8 MW 88
Table A2 - 5 – Digitized experimental and calculated (at 57.8MW) neutron flux in midplane for HEU 89
Table A2 - 6 – HEU (52.8 MW) and LEU (57.8 MW) thermal neutron flux profile at a distance of 30 cm from the core center 92

Tables in appendix A3

Table A3 - 1 – digitized experimental data representing the ratio between stripe averaged power and average core power at several radial locations of the HEU core 94
Table A3 - 2 – digitized experimental data representing the ratio between local power and average core power at several radial locations of the HEU core 94
Table A3 - 3 – HEU fuel power density at BOC (core power at 57.8 MW) 95
Table A3 - 4 – HEU fuel power density at day 1 (core power at 57.8 MW) 96
Table A3 - 5 – HEU fuel power density at day 5 (core power at 57.8 MW) 97
Table A3 - 6 – HEU fuel power density at day 12 (core power at 57.8 MW) 98
Table A3 - 7 – HEU fuel power density at day 18 (core power at 57.8 MW) 99
Table A3 - 8 – HEU fuel power density at day 24 (core power at 57.8 MW) 100
Table A3 - 9 – HEU fuel power density at day 30 (core power at 57.8 MW) 101
Table A3 - 10 – HEU fuel power density at day 36 (core power at 57.8 MW) 102
Table A3 - 11 – HEU fuel power density at day 42 (core power at 57.8 MW) 103
Table A3 - 12 – HEU fuel power density at EOC, day 45.5 (core power at 57.8 MW) 104
Table A3 - 13 – LEU fuel power density at BOC (core power at 57.8 MW) 105
Table A3 - 14 – LEU fuel power density at day 1 (core power at 57.8 MW) 106
Table A3 - 15 – LEU fuel power density at day 5 (core power at 57.8 MW) 107
Table A3 - 16 – LEU fuel power density at day 12 (core power at 57.8 MW) 108
Table A3 - 17 – LEU fuel power density at day 18 (core power at 57.8 MW) 109
Table A3 - 18 – LEU fuel power density at day 24 (core power at 57.8 MW) 110
Table A3 - 19 – LEU fuel power density at day 30 (core power at 57.8 MW) 111
Table A3 - 20 – LEU fuel power density at day 36 (core power at 57.8 MW) 112
Table A3 - 21 – LEU fuel power density at day 42 (core power at 57.8 MW) 113
Table A3 - 22 – LEU fuel power density at EOC, day 48 (core power at 57.8 MW) 114
Table A3 - 23 – HEU and LEU power density evolution at location presenting at least once the peak value. When highlighted in yellow, values represent the peak. 115

Tables in appendix A4

Table A4 - 1 – Experimental device reactivity worth total and when flooded 116
Table A4 - 2 – Detailed reactivity effect of passage from room temperature to full power (57.8 MW) conditions 117
Table A4 - 3 – Control Element (CE) reactivity worth at BOC in cold conditions and during irradiation at full power condition . 118
Table A4 - 4 – Core reactivity change due to the insertion of the safety rods 119

List of Abbreviations

2D	*two dimensional*
3D	*three dimensional*
ANL	*Argonne National Laboratory*
BOC	*Beginning Of Cycle*
CE	*Control Element*
CEA	*Commissariat à l'Energie Atomique et aux énergies alternatives*
EOC	*End Of Cycle*
GTRI	*Global Threat Reduction Initiative*
HEU	*Highly Enriched Uranium*
HFIR	*High Flux Isotope Reactor*
ILL	*Institut Laue-Langevin*
IRSN	*Institut de Radioprotection et de Sûreté Nucléaire*
LANL	*Los Alamos National Laboratory*
LEU	*Low Enriched Uranium*
MCNP	*Monte Carlo N Particle*
ORNL	*Oak Ridge National Laboratory*
RERTR	*Reduced Enrichment for Research and Test Reactor*
RHF	*Réacteur à Haut Flux*
RJH	*Réacteur Jules Horowitz*
RSAR	*Review of the Safety Analysis Report*
SR	*Safety Rods*
T-H	*Thermal-Hydraulic*
U7Mo	*Uranium-Molybdenum fuel with 7wt% Mo dispersed in an aluminum matrix*

1. Introduction

The French High Flux Reactor (RHF) of the Laue-Langevin Institute (ILL) based in Grenoble, France, is a research reactor designed primarily for neutron scattering experiments supporting applied and fundamental science. It delivers one of the most intense neutron flux worldwide [ILL, 2008]. The reactor currently uses a Highly Enriched Uranium (HEU) fuel.

In the framework of its non-proliferation policies, the international community presently aims to minimize, and when possible eliminate, nuclear material that could be used for nuclear weapons or other non-desirable use. In this geopolitical context, most worldwide research and test reactors have already started a program of conversion to the use of Low Enriched Uranium (LEU) fuel [RERTR, 2014], [GTRI, 2014].

A new type of LEU fuel based on a mixture of uranium and molybdenum (7wt% Mo) dispersed in an aluminum matrix (later simply referred as U7Mo), currently in development, is expected to allow the conversion of compact high performance reactors like the RHF.

An ANL study carried out in 2010 has shown that it could be technically feasible to convert the RHF reactor to the use of U7Mo LEU fuel [ANL, 2010]. An acceptable U7Mo LEU design has emerged from this study which is still the reference design today.

Since that time, several improvements have been applied to the neutronics model. None of them are believed to challenge the 2010 conclusions regarding the technical feasibility of converting the RHF to LEU U7Mo fuel. However, providing an update of all calculated parameters published in the feasibility analyses has become necessary. In addition, from the recent preliminary Review of the Safety Analysis Report (RSAR) [ANL, 2014a], additional parameters to be evaluated for the production of a conversion safety analysis report have been identified.

The present report updates the main parameters studied during the feasibility report as well as new parameters identified in the RSAR. The report is organized as follows: Section 2 gives a brief overview of the RHF reactor, reference LEU design and the correspondent neutronics model. Section 3 describes the tools that have been used to perform the analysis. Section 4 presents the results obtained with the reference LEU design as well as comparisons with the HEU core currently in operation. When available, the HEU results are compared to experimental or benchmarked data in order to verify the accuracy of the neutronics models.

2. RHF Reactor and Neutronics Model

As described in [NEA, 2011] and [ILL, 2008], the Institut Laue-Langevin (ILL) is an international research center which operates one of the most intense neutron source in the world, the ILL High Flux Reactor (RHF), which has an unperturbed thermal neutron flux of 1.5×10^{15} n/cm²/s in the reflector. The reactor feeds intense beams of neutrons to a suite of 40 high-performance instruments. Research carried out in this institute focuses primarily on fundamental science in a variety of fields: condensed matter physics, chemistry, biology, nuclear physics and materials science. The neutrons are extracted from the reactor vessel by beam tubes that are able to transport neutrons up to 150 m away from the core.

2.1. Brief Reactor Description

The reactor has been designed to operate continuously for 45 days per cycle using one element per cycle at a thermal power of 58.3 MW (nuclear power of 57.8 MW). Originally, 9 elements were burned every two years (4.5 element / year). In order to reduce the operation costs, the power has been decreased few years ago to a thermal power of 53.3 MW (nuclear power of about 52.8 MW) so that the reactor can operate continuously for 49-50 day per cycle and burned 4 elements per year (about 200 days of operation per year).

The reactor is cooled, moderated and reflected by heavy water. It has only one fuel element similar to the Oak Ridge National Laboratory (ORNL) High Flux Isotope Reactor (HFIR) design. The heavy water tank containing the fuel element and the experimental devices has a diameter of 2.50 m and is about 3 m high. It is placed at the bottom of a larger light water pool which has a diameter of 6 m and a height of 14 m. This pool is placed at the center of a 60 m diameter cylindrical building. The reactor is mainly used for fundamental research, employing 13 horizontal and 3 inclined beam tubes which extract neutrons from the core. One graphite hot source and two deuterium-cooled cold neutron sources are also present in the heavy water tank (later referred to as the reflector). The beam tubes extend through the building's heavy concrete walls. A cross section and a top view of the heavy water tank are shown in Figure 2.1-1 and Figure 2.1-2 respectively.

The RHF has unique single annular fuel element made of 280 plates curved as involute, welded to two concentric aluminum tubes. The internal and external diameters of the element are 26.08 cm and 41.36 cm, respectively. Each fuel plate is bent into an involute shape with an originating radius of 13.681 cm. The advantage of the involute shape is to maintain a constant distance between each plate, simplifying the thermal-hydraulic cooling of such a compact core.

The constant distance between two fuel plates which defines the coolant channel thickness, is 1.8 mm. Each fuel plate has a total height of 90.3 cm. The height of the meat (fissile part of the plates made of dispersed UAl_x) is 80 cm. On each plate, 3 cm long borated zones are present at the upper and lower extremities of the fuel. The borated zones act as a reactivity reserve for the End-Of-Cycle (EOC) and to reduce the power peaking occurring on the edges of the plate, especially at the Beginning-Of-Cycle

(BOC). The total mass of ^{10}B in a fresh element is 5.77 g. The overall fuel plate thickness is 1.27 mm. Fuel and borated regions are 0.51 mm thick. The plate's cladding is made of the aluminum alloy AlFeNi which has a thickness of 0.38 mm on both sides of the plate The HEU UAlx powder is enriched at 93 wt% in ^{235}U. The powder is dispersed in the aluminum matrix to load 30.6 g of ^{235}U per plate (8568 g of ^{235}U / core). The fuel plate and element dimensions are shown in Figure 2.1-3 and Figure 2.1-4, respectively.

RHF has a single Control Element (CE) made of two structural aluminum tubes and two absorbing nickel tubes located in the central cavity formed by the annular shape of the fuel element. The RHF control element mechanisms are set up below the fuel element. During the cycle, the control element is progressively withdrawn toward the bottom of the vessel. At EOC, the top of the control element is below the bottom of the fuel.

Five Safety Rods (SR) surround the core to shut the reactor down at any time. The safety rods are tubes made of AIC alloy (Ag-In-Cd) filled with heavy water. Each safety rod has a specific angle and position around the core. When fully inserted, their bottoms are located 40 cm below the reactor median plane. When they are moved along their axes to the fully withdrawn position, their bottoms are located 120 cm higher, at 80 cm above the reactor median plane, with the same angle. The safety rods, labeled as BS1 to BS5, can be seen in Figure 2.1-2.

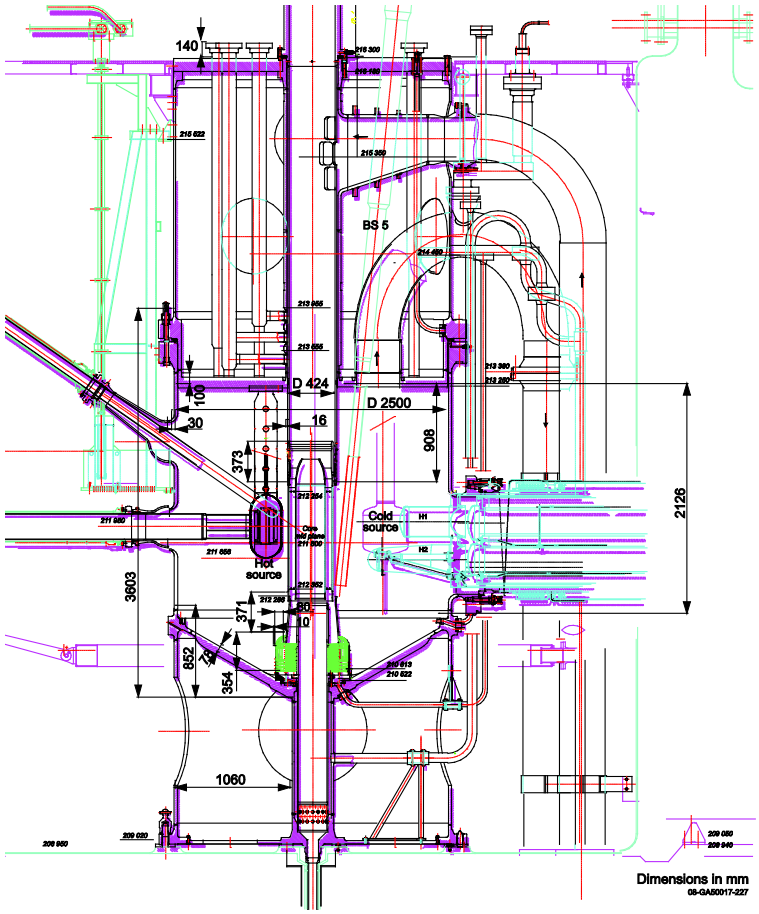

Figure 2.1-1 – Cross-section of the RHF reactor [NEA, 2011]

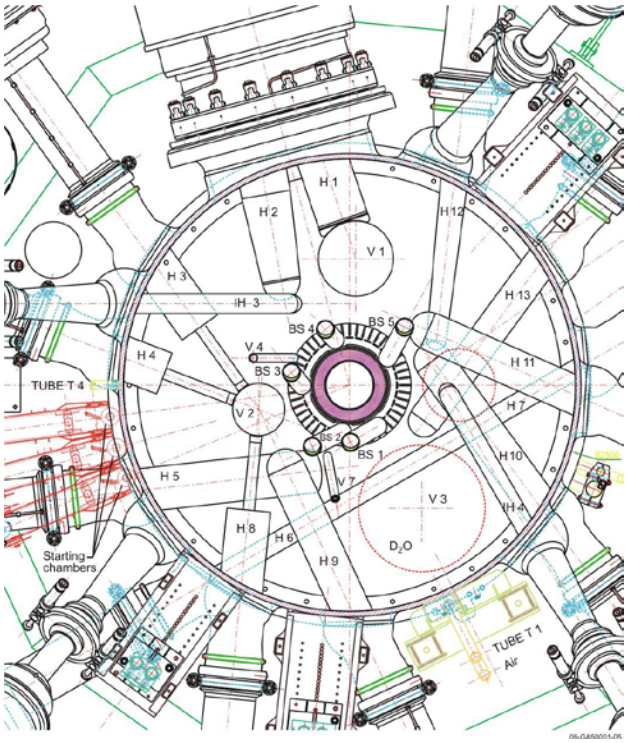

Figure 2.1-2 – Top view of the RHF reactor; the fuel element is colored in pink. [NEA, 2011]

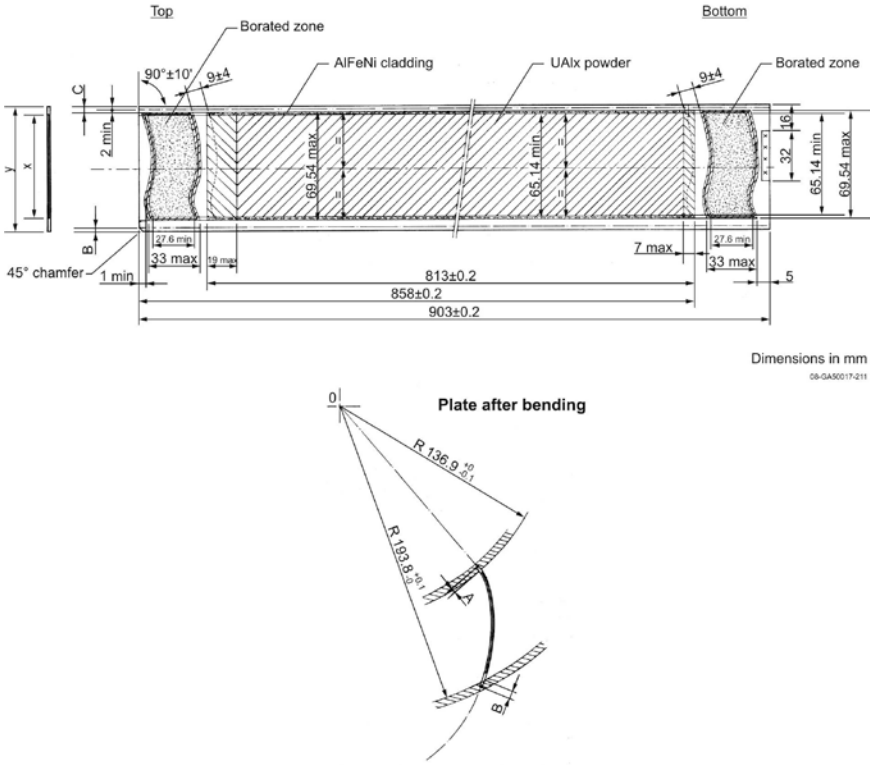

Figure 2.1-3 – Dimensions of the RHF HEU fuel plate [NEA, 2011]

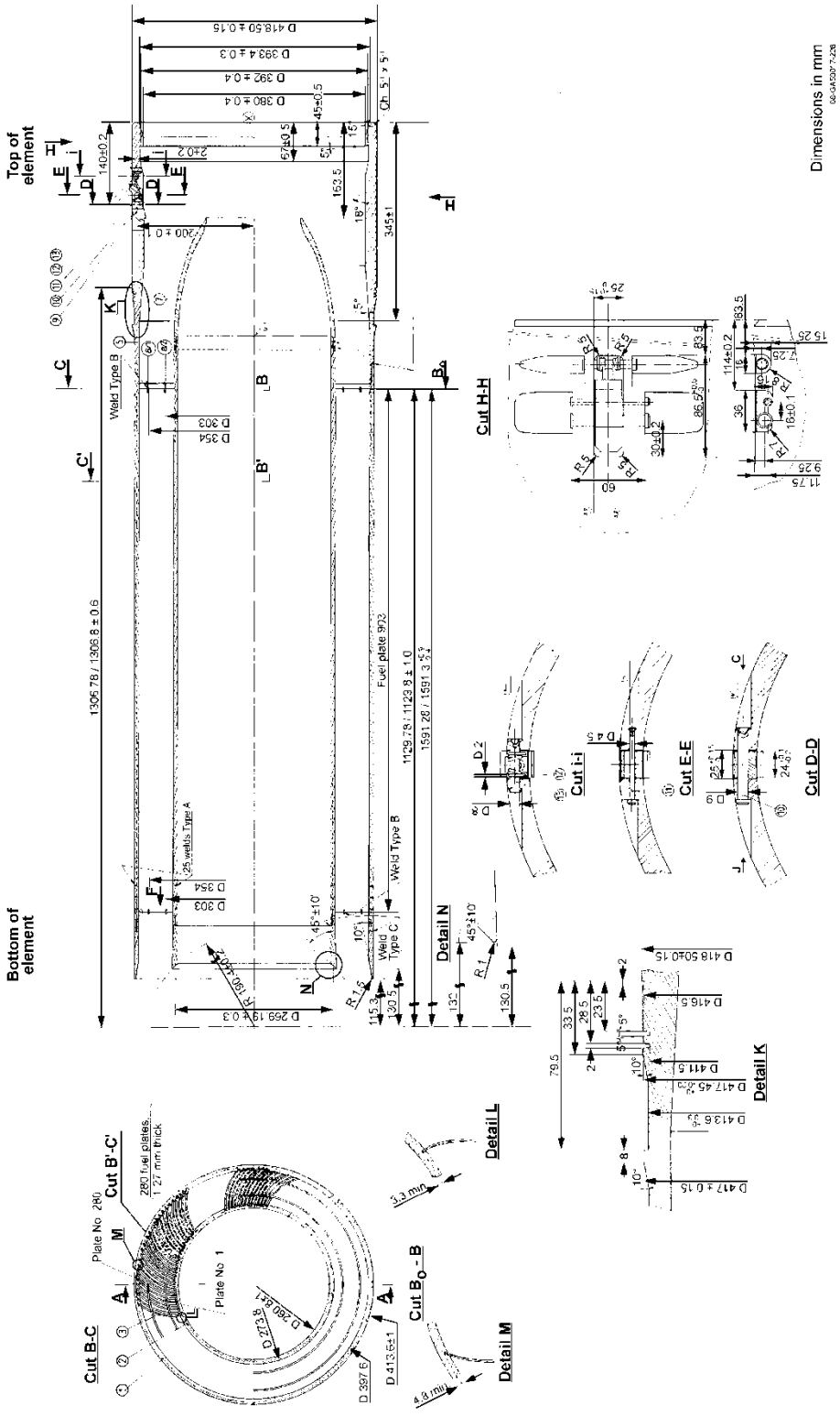

Figure 2.1-4 – Dimensions of the RHF HEU fuel element [NEA, 2011]

2.2. U7Mo LEU Reference Design

For RHF, performances are defined by the duration of the cycle (later called cycle length) as well as the magnitude of the neutron flux entering the beam tubes. Studies have shown that direct replacement of HEU by LEU U7Mo fuel would lead to an unacceptable loss of performance [ANL, 2010]. At similar power, compared to the HEU core, the cycle length would be considerably shortened (about 20%) and the magnitude of the flux would be decreased by about 10%.

In [ANL, 2010] it has been shown that the LEU cycle length could be increased substantially by increasing the height of the meat inside the plate (from 80 to 88 cm) while maintaining the same fuel thickness (0.051 cm) and the same fuel width (6.734 cm). The plates' cladding remains made of the aluminum alloy AlFeNi with a thickness of 0.38 mm. The ^{235}U loading per plate and per core is 47.75g and 13,370g, respectively. The uranium loading per plate and per core is 238.75g and 66,850g, respectively. At 57.8 MW nuclear (maximum nuclear power), the extended LEU fuel cycle length would be around 48 days compared to the 45 day of the HEU core at similar power.

ILL has recently decreased the power of the reactor by about 10% in order to increase the cycle length by about 4-5 days. Therefore, the 57.8 MW LEU core cycle length with the meat extended (~48 days) becomes reasonably close to the current HEU core cycle length (49-50 days). In addition, by decreasing the HEU core power by about 10% (from 57.8 to 52.8 MW nuclear), the neutron flux magnitude has also decreased by 10% which is about the same magnitude of the LEU core at 57.8 MW. In conclusion, the LEU core with the meat extended operated at 57.8 MW nuclear would lead to essentially the same performance of the current HEU core (52.8 MW).

However, the meat extension does not leave enough room to have borated regions on top and bottom of the fuel since the overall plate height remains unchanged (increasing the length of the plate has been suggested but has not been considered as a viable option by the conversion team so far). The absence of neutron absorber leads to strong power peaking, especially on the top outermost part of the plate (facing the reflector). The power density in this region would become higher than the current fuel qualification envelop. It does not mean that such power density values would necessarily be challenging for the fuel, many others parameters come into play when characterizing the fuel (e.g.: temperature, fission density, etc.).

In order to reduce the power peaking in the top outermost region, insertion of an annular-shaped burnable absorber (later called poison belt) located just above the fuel plates, along the fuel element outer tube (a.k.a. side plate) has been studied [ANL, 2010]. Among the different absorber materials investigated, boron dispersed in aluminum has been found to be the more suitable. It has been shown that a boron density in the poison belt four times larger than in the borated regions of the HEU core would reduce the power density (W/cm^3) significantly below the currently foreseen fuel qualification envelope.

After the release of the feasibility analyses, the RHF fuel manufacturer (CERCA) has issued a conceptual drawing of the poison belt including preliminary dimensions. A schematic comparing HEU borated regions with the proposed LEU core poison belt is provided in Figure 2.2-1.

In [ANL, 2010], it has been shown that the modifications to the original HEU core design described above would lead to an acceptable design not only in term of performance but also regarding shutdown margins and steady-state thermal-hydraulic (T-H) margins. The LEU element described above constitutes the reference LEU design.

However, it must be acknowledged that the poison belt design solution is not exempt of risks. Production of helium gas during irradiation of the absorber might lead to significant swelling [Anselmet, 2013]. The neutron flux magnitude received by the poison belt would not be dramatically different from the HEU core borated absorber, however, because the poison density increased by a factor of four, the helium density would also increase by the same magnitude. To date, it is not known if the manufacturer proposed poison belt design would retain its mechanical integrity under such conditions. In order to mitigate the risk related to this design solution, the following actions are ongoing or considered:

- Using the most advanced available U7Mo fuel behavior model, perform a sensitivity analyses on the fuel swelling, oxide formation, fuel temperature rise and interaction compounds formation when varying the density of boron in the poison belt. Preliminary conclusions showed that a reduction in poison density would not lead to substantial changes in the maximum fuel swelling or peak fuel temperature despite a higher power peaking.
- Engage discussions with the CEA (Commissariat à l'Energie Atomique et aux énergies alternatives) to understand how the failed réacteur Jules Horowitz (RJH) borated plate design [Anselmet, 2013] and the most recent RJH design compared to the RHF poison belt solution (e.g. in term of flux magnitude, helium production rate…). Discussions should indicate if the poison belt design is close to a “failed” design or a “successful” one.
- Perform mechanical analyses (stress, deformation) on the poison belt design, if deemed necessary.
- Perform alternative design studies, if deemed necessary.

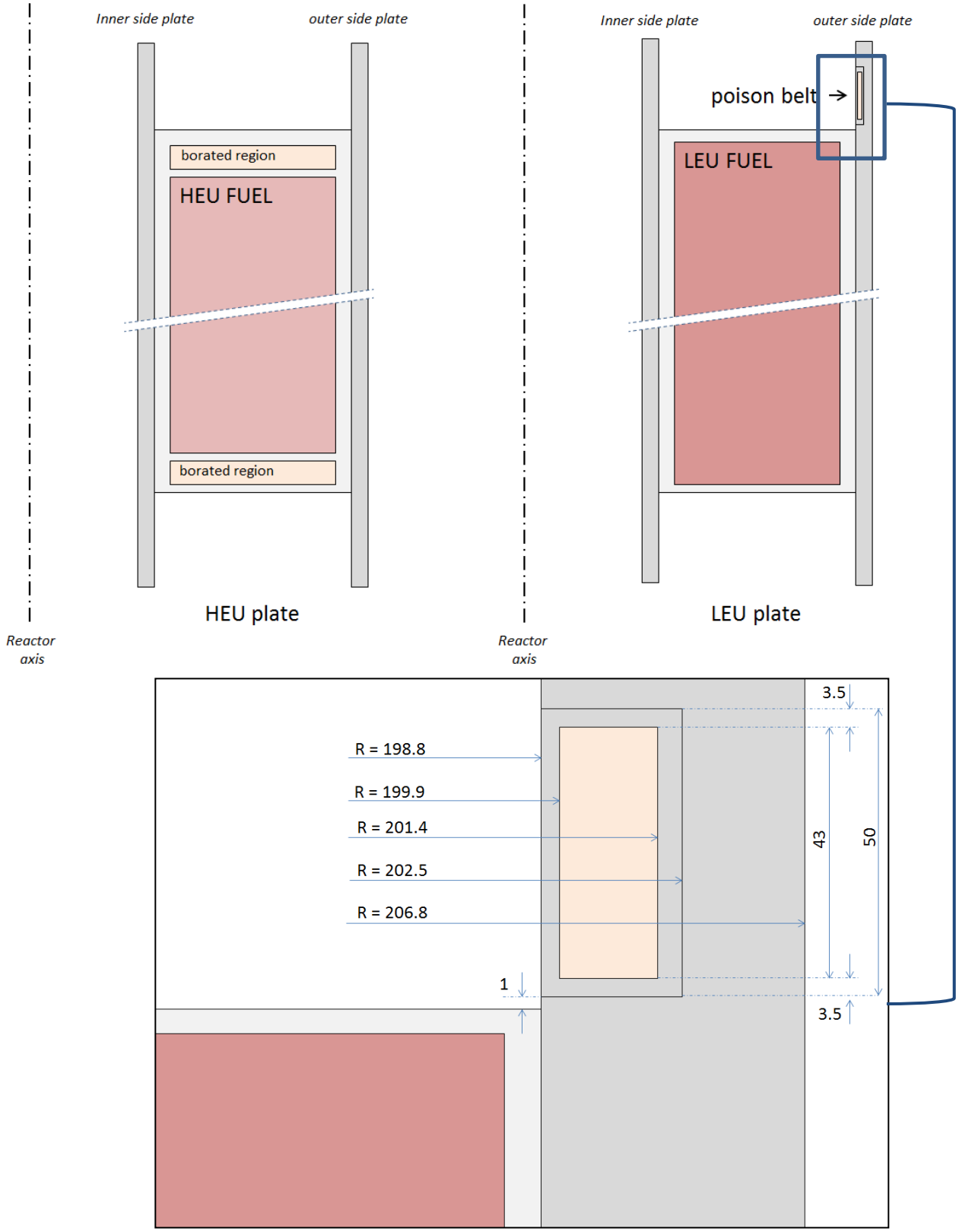

Figure 2.2-1 – Schematic of RHF HEU and LEU fuel plate and dimensions of the poison belt (mm)

2.3. Neutronics Models

ILL neutronics model of the RHF is very detailed, modeling accurately all in-core components up to the concrete walls that extend beyond the reactor vessel. ILL developed such model to cover their own analysis needs (e.g. dose calculations, etc…). All neutronics analysis and modifications made by the conversion team are based on this original ILL model. More details on the different aspects of the model can be found in [NEA, 2011] and [ANL, 2010].

As stated before, modifications have been applied to the model since the release of the feasibility report [ANL, 2010] and some other since the release of the OECD-NEA benchmark [NEA, 2011].
Since the release of the feasibility report, the following modifications to the model were made:

- Corrections in the fuel dimensions and compositions (one compensating the other, no change in reactivity was observed).
- More detailed description of the anti-turbulence grids at the exit of the element (relatively large difference of reactivity was obtained at EOC simulation which happens to improve the comparison to experimental data).
- Re-definition of the heavy water cells in the reflector (considerable improvement in memory use which accelerates calculation efficiency).
- Replacing old cold source design by new one (no change in reactivity was observed).
- Corrections to the definitions of beam tubes H3, H4, H8 (no change in reactivity was observed).
- Applying density and temperature (energy) information to the material definitions to reflect full power conditions (see Table 2.3-1, improved comparison to depletion experimental data).
- Complete redefinition of the fuel plates which were modeled as piece of arc instead of involute following the method described in [ANL, 2012] and [NEA, 2011] (no change in reactivity was observed but considerable acceleration of calculation time and possibility to apply exact same meshing as in 3D T-H analysis).

Additional modifications to the model were also made after the OECD-NEA benchmark report [NEA, 2011] was released:

- Corrections in orientation of very cold neutron extraction tubes inside the cold source (no change in reactivity was observed).
- Corrections of the involute orientation (no change in reactivity was observed).
- Generation of a set of cross section at specific temperature (corresponding at full power condition) for all material isotopes used in the model.

All the modifications mentioned above did not affect the good agreement between the HEU model and the experimental data. These modifications also didn't impact significantly the predictions of the model for the LEU core and therefore do not challenge the conclusions of the feasibility report. 3D views of the reflector obtained with a somewhat simplified version of this model are shown in Figure 2.3-1.

Screenshots of a top view of the fuel element and detailed of one plate are shown in Figure 2.3-2 and Figure 2.3-3. These figures have been obtained with the MCNP code Visual Editor [Vised, 2014].

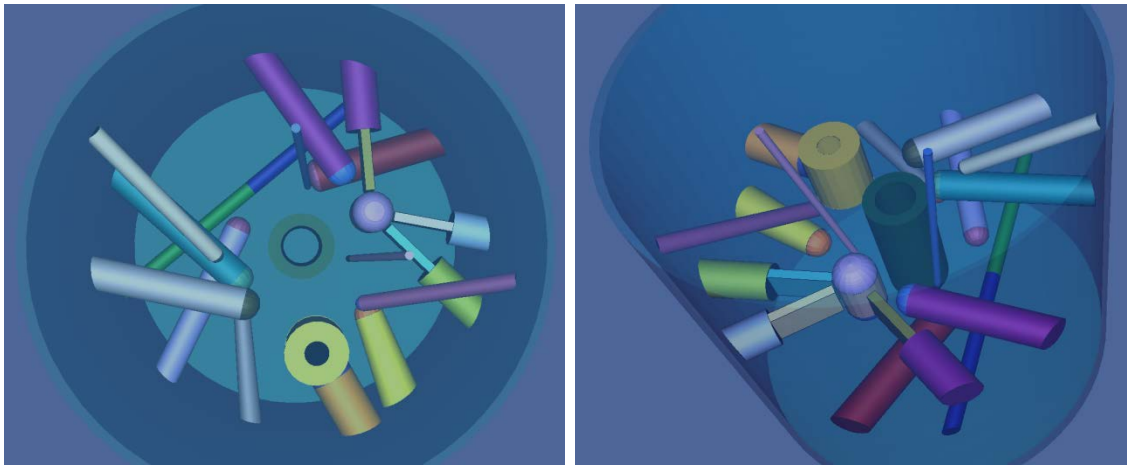

Figure 2.3-1 – 3D view of the RHF reflector obtained with a simplified neutronics model

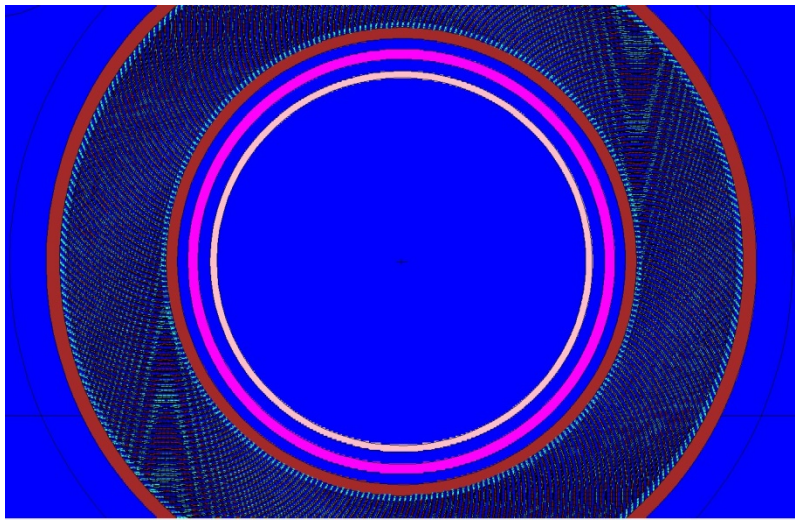

Figure 2.3-2 – Top view of the fuel element as modeled

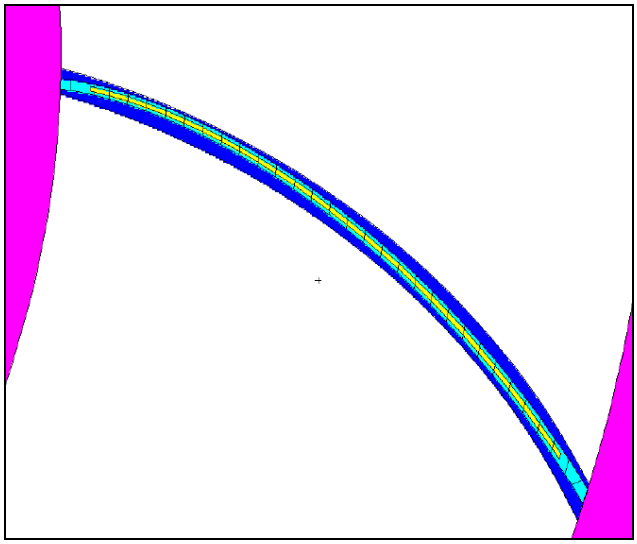

Figure 2.3-3 – Model details of unit cell (cladding is cyan, fuel is yellow, coolant channel is blue and side-plates are pink)

Depending on the reactor state being analyzed, the heavy water density and all material temperatures reflect either room temperature conditions (later called cold state) or full power conditions (later called hot state). The different pressures and temperatures used to model both the cold state and hot state are summarized in Table 2.3-1 provided below. Heavy water density data for a given set of temperature and pressure have been found on the NIST database [NIST, 2014a].

Table 2.3-1 – Materials temperature, pressure and density for the cold and hot states

	Temperature (K)		Pressure (bar)	Density (g/cc)	
	Cold	**Hot**	**Cold & hot**	**Cold**	**Hot**
Heavy water					
Reflector	293	323	4	1.1054765	1.0958499
Above fuel element	293	303	14.5	1.1060305	1.1039768
Below fuel element	293	323	4	1.1054765	1.0958499
Between the plates	293	313	9.25	1.1057537	1.0990054
Central cavity	293	303	14.5	1.1060305	1.1039768
Other structures					
Fuel	293	393			
Clad	293	393			
Borated region	293	293			
Beam tubes deuterium	24	24			
Graphite hot source	293	2400[SAR, 2004]			
Other structure	293	293			

For depletion and power distribution calculations, the fuel and borated regions need to be discretized in order to take into account the strong power gradients across those regions. To avoid numerical artifacts in the power distribution, it is preferable to use the same discretization for both the power distribution

and the depletion calculations. The selected mesh must therefore be fine enough to model properly both the burnup gradient (over the entire cycle) and the power gradient. The selected mesh for both the HEU and LEU fuel has 13 lateral and 46 axial divisions for a total of 598 regions.

For both the HEU and LEU, the size (width) of the 13 lateral stripes does not change, however, due to the different fuel height, the height of the axial divisions are not identical. The HEU core borated regions (located on top and bottom of the fuel) have the same lateral discretization as the fuel but are subdivided axially in three equal length (3 cm) zones. Due to the thin-annular shape of the poison belt, it is assumed that there is no need to discretize radially. However, the poison belt is divided in 4 unequal axial regions. A summary of the nodes dimensions used to discretize both fuel and borated regions is provided in Table 2.3-2, Table 2.3-3 and Table 2.3-4.

Table 2.3-2 – Axial discretization used for the HEU and LEU fuel (1 = top; 46 = bottom)

Axial node	Number of axial nodes	Node's height (cm)	
		HEU	LEU
1 to 15	15	0.3	0.3
16 to 35	20	3.6	4
36	1	0.5	0.5
37 to 46	10	0.3	0.3

Table 2.3-3 – Lateral discretization used for the HEU fuel, borated regions and LEU fuel (1 = inner side; 13 = outer side)

lateral node	Number of lateral nodes	Node's width (cm)
1 to 4	4	0.3
5	1	1
6	1	1.734
7	1	1
8 to 13	6	0.3

Table 2.3-4 – Axial discretization used for the HEU and LEU borated regions (1 = top; 3 or 4 = bottom)

Axial node	Number of axial nodes	Node's height (cm)	
		HEU borated regions	LEU poison belt
1 to 3	3	1	1
4	1	none	1.3

The fresh fuel and fresh borated compositions in the HEU and LEU cores are provided in Table 2.3-5 to Table 2.3-8. Molar masses have been obtained from [NIST, 2014b].

Table 2.3-5 – Comparison of the fresh HEU fuel as used in the neutronics model

Isotope	Molar mass (g/mol)	Atomic density (at/barn.cm)	Density (g/cc)	Atomic fraction	Weight fraction
^{234}U	2.34041E+02	3.12744E-05	1.21546E-02	5.60921E-04	3.41479E-03
^{235}U	2.35044E+02	2.85696E-03	1.11510E+00	5.12409E-02	3.13282E-01
^{236}U	2.36046E+02	3.39239E-06	1.32972E-03	6.08440E-05	3.73580E-04
^{238}U	2.38051E+02	1.77620E-04	7.02134E-02	3.18569E-03	1.97262E-02
^{27}Al	2.69815E+01	5.26863E-02	2.36061E+00	9.44952E-01	6.63203E-01
total =	-	5.57555E-02	3.55940E+00	1.00000E+00	1.00000E+00

Table 2.3-6 – Composition of the fresh borated regions in the HEU neutronics model

Isotope	Molar mass (g/mol)	Atomic density (at/barn.cm)	Density (g/cc)	Atomic fraction	Weight fraction
^{10}B	1.00129E+01	6.01466E-04	1.00007E-02	1.06441E-02	4.09282E-03
^{11}B	1.10093E+01	2.39400E-03	4.37667E-02	4.23667E-02	1.79116E-02
^{24}Mg	2.39850E+01	1.39637E-03	5.56162E-02	2.47116E-02	2.27611E-02
^{25}Mg	2.49858E+01	1.76779E-04	7.33472E-03	3.12846E-03	3.00175E-03
^{26}Mg	2.59826E+01	1.94634E-04	8.39769E-03	3.44443E-03	3.43677E-03
^{27}Al	2.69815E+01	5.17435E-02	2.31836E+00	9.15705E-01	9.48796E-01
total =	-	5.65067E-02	2.44348E+00	1.00000E+00	1.00000E+00

Table 2.3-7 – Composition of the LEU fuel as used in the neutronics model

Isotope	Molar mass (g/mol)	Atomic density (at/barn.cm)	Density (g/cc)	Atomic fraction	Weight fraction
^{27}Al	2.69815E+01	2.92267E-02	1.30950E+00	5.39570E-01	1.31577E-01
^{28}Si	2.79769E+01	8.00912E-04	3.72087E-02	1.47861E-02	3.73869E-03
^{29}Si	2.89765E+01	4.06685E-05	1.95688E-03	7.50803E-04	1.96625E-04
^{30}Si	2.99738E+01	2.68089E-05	1.33438E-03	4.94934E-04	1.34077E-04
^{92}Mo	9.19068E+01	5.61113E-04	8.56362E-02	1.03590E-02	8.60465E-03
^{94}Mo	93.9050883	3.49750E-04	5.45389E-02	6.45692E-03	5.48002E-03
^{95}Mo	94.9058421	6.01948E-04	9.48661E-02	1.11129E-02	9.53206E-03
^{96}Mo	95.9046795	6.30685E-04	1.00441E-01	1.16434E-02	1.00922E-02
^{97}Mo	96.9060215	3.61094E-04	5.81072E-02	6.66635E-03	5.83856E-03
^{98}Mo	97.9054082	9.12376E-04	1.48334E-01	1.68439E-02	1.49044E-02
^{100}Mo	99.907477	3.64119E-04	6.04089E-02	6.72220E-03	6.06983E-03
^{234}U	2.34041E+02	5.35195E-05	2.08000E-02	9.88052E-04	2.08996E-03
^{235}U	2.35044E+02	4.04808E-03	1.58000E+00	7.47338E-02	1.58757E-01
^{236}U	2.36046E+02	9.38842E-05	3.68000E-02	1.73325E-03	3.69763E-03
^{238}U	2.38051E+02	1.60950E-02	6.36238E+00	2.97139E-01	6.39287E-01
total =	-	5.41667E-02	9.95232E+00	1.00000E+00	1.00000E+00

Table 2.3-8 – Composition of the fresh poison belt as used in the LEU neutronics model

Isotope	Molar mass (g/mol)	Atomic density (at/barn.cm)	Density (g/cc)	Atomic fraction	Weight fraction
^{10}B	1.00129E+01	2.40589E-03	4.00034E-02	3.90335E-02	1.64490E-02
^{11}B	1.10093E+01	9.57611E-03	1.75069E-01	1.55364E-01	7.19867E-02
^{24}Mg	2.39850E+01	1.39639E-03	5.56169E-02	2.26552E-02	2.28692E-02
^{25}Mg	2.49858E+01	1.94636E-04	8.07563E-03	3.15780E-03	3.32063E-03
^{26}Mg	2.59826E+01	1.76781E-04	7.62741E-03	2.86812E-03	3.13633E-03
^{27}Al	2.69815E+01	4.78868E-02	2.14557E+00	7.76921E-01	8.82238E-01
total =	-	6.16366E-02	2.43196E+00	1.00000E+00	1.00000E+00

3. Tools and Methods

The tools and methods described below have been selected to perform the neutronics analysis. They are identical to the ones used in [ANL, 2012] to perform the review of the neutronics calculations carried out for the HFIR.

3.1. Tools

3.1.1. Steady-state Neutronics Calculations – MCNP

The Monte Carlo N Particles (MCNP) computer code has been selected to perform the steady-state calculations. This software package is developed by Los Alamos National Laboratory (LANL) [LANL, 2008a], [LANL, 2008b]. It is used primarily for the simulation of nuclear processes and particle interactions such as neutrons, photons and electrons. Its range of application is very large and covers, among other things, medical physics, fission and fusion reactor design, criticality and radiation protection. The MCNP code has a large base of users worldwide and has often been benchmarked against experiments. Its ability to model complex geometries in three-dimensions (3D) and calculate a wide variety of parameters (eigenvalues, neutron flux, spectrum…) make the code an excellent tool for the study of complex systems such as RHF. However, MCNP is not able to model a surface curved along an involute. In late 2010, ANL developed a methodology to model an approximation of the involute almost as accurately as desired (see [NEA, 2011] or [ANL, 2012]). The version MCNP5 1.6 of the code has been used for the study (simply referred to MCNP through the rest of the report).

3.1.2. Depletion Calculations - ORIGEN

ORIGEN is a versatile tool that has been designed for calculating the buildup, decay and processing of radioactive materials [ORNL, 2002]. It has been developed by ORNL. ORIGEN uses the matrix exponential method to solve a large system of coupled, linear differential equations. ORIGEN v2.2 has been used as the depletion module for the RHF analyses through the Monte-Carlo depletion code VESTA with couples it to MCNP.

3.1.3. Monte-Carlo-Depletion - VESTA

Studying the isotopic evolution of a complex reactor like RHF requires having a detailed time-discretization and, consequently, performing multi-step depletion calculations. In order to reduce the computational time and the risk of error, a so-called “Monte-Carlo depletion” code has been used to couple the steady state calculation (performed by MCNP) with the depletion module (performed by ORIGEN). The code VESTA, developed by the Institut de Radioprotection et de Sûreté Nucléaire (IRSN) has been selected for these analyses [IRSN, 2008].

3.1.4. Nuclear Library

The nuclear library used is ENDF/B-VII.0. The point-wise pre-generated cross-sections (43,000 groups) used by VESTA are also based on this library. ORIGEN uses its own fission yield and decay library. The one group cross-sections used by ORIGEN are obtained from the VESTA calculation.

3.2. Methods

3.2.1. Critical Search

Due to the buildup of fission products and the consumption of fuel during irradiation, the reactivity of the core decreases over time. To maintain the reactor critical, control elements are gradually withdrawn to compensate this reduction in reactivity. Once the control elements have reached their limit position (fully withdrawn), the cycle is over because criticality cannot be achieved any longer. Thus, calculation of the critical control element positions during the cycle can be used to estimate the cycle length of the core. This work uses a simple but robust method to calculate the critical position of the control elements. The problem that a critical search algorithm has to solve is to predict by how much the control elements have to be moved to achieve criticality. The methodology used here is based on the evaluation of a very simple parameter which is the average reactivity worth of the control elements. It is calculated between two extreme points: control elements fully inserted and fully withdrawn. The variation of reactivity obtained between them is then divided by the distance between these two points. This calculation gives an average reactivity worth per unit distance. If, at the end of the steady state calculation, criticality is not achieved, the missing or excess reactivity is calculated and divided by the average worth of the control elements which provides a guess for the critical position. The process is repeated until criticality (plus or minus the uncertainties of the steady state calculation) is achieved. This method is simple, works with different systems, can certainly be improved but has been judged efficient enough for the type of calculations carried out for this work. Depletion calculation scheme including critical search is presented in Figure 3.2-1.

3.2.2. Generating MCNP Cards for Discrete Involute Modeling

As stated earlier, despite the fact that MCNP can handle complex geometries, it does not have a standard option to model a surface curved along an involute. Many possibilities exist to get around this difficulty: One can homogenize the fuel element or approximate the shape by using another geometric shape (arc segments were previously used to model RHF [ANL, 2010]). However, an approximate modeling of the fuel elements will always introduce a systemic bias on the physics of the model which needs to be assessed (via benchmarking for instance). In order to reduce the geometric bias to the lowest level possible, ANL has developed a methodology based on discretization of the involute (see [NEA, 2011] or [ANL, 2012]). Once “sliced” in several parts, the pieces of the involute plate can be modeled by simple geometric objects such as polyhedrons. The magnitude of the geometric bias is thus directly correlated to the degree of discretization: The finer the discretization, the lower the bias introduced by the approximation in the geometry. Cell, geometric and data cards used in the MCNP inputs to model the discrete involute are generated externally.

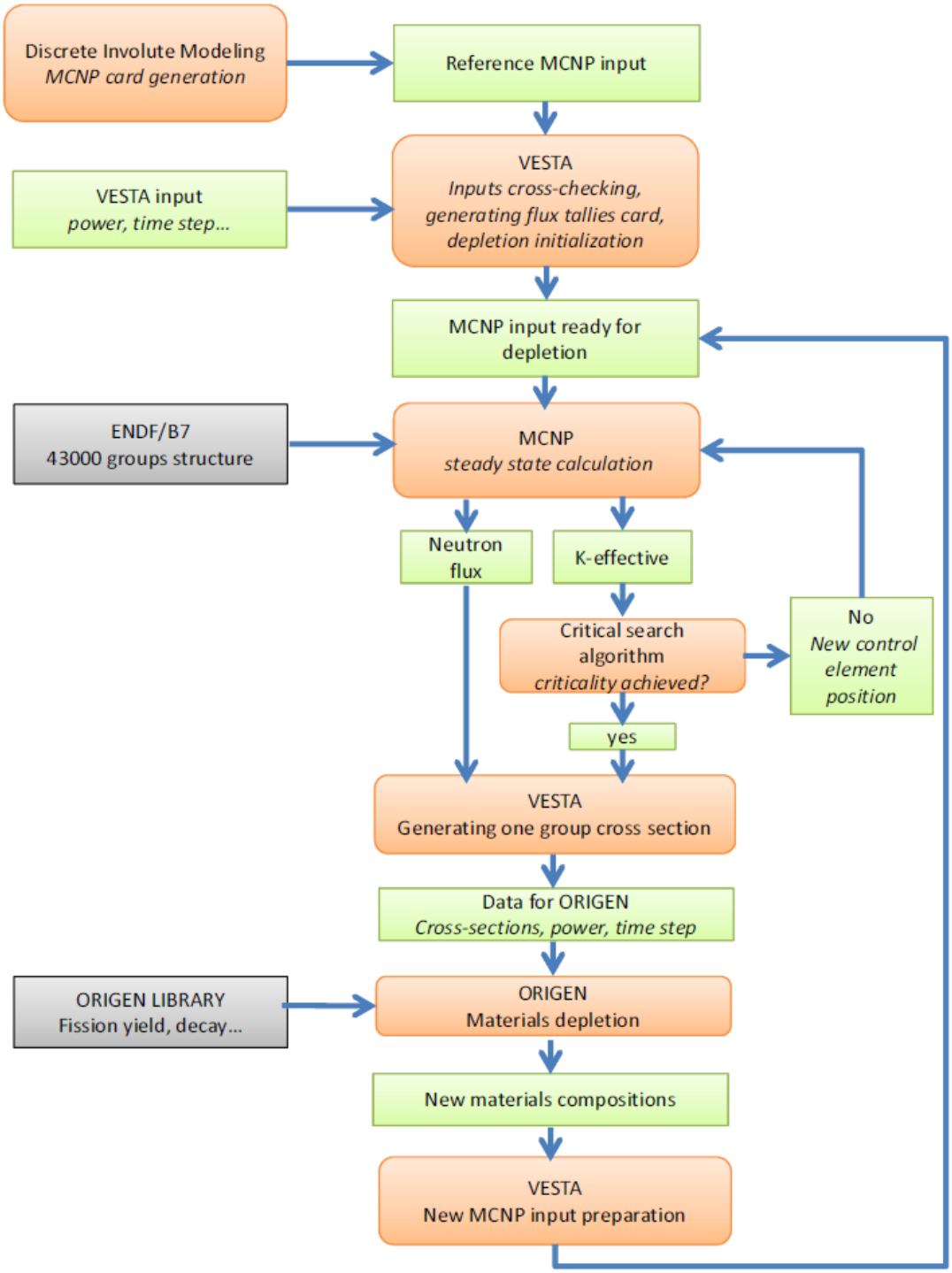

Figure 3.2-1 – Depletion scheme including critical search used for this study

3.2.3. Power Distribution Normalization in MCNP

The total energy released by the fission of heavy nuclei in a nuclear reactor comes from several contributions: kinetic energy of the fission products, prompt and delayed neutrons, prompt and delayed gammas, beta energy, gammas from capture and anti-neutrinos. Except for the anti-neutrinos which can be neglected (non-recoverable), all the above contributions must be accounted for an accurate representation of the energy distribution released during the fission process.

The code MCNP does not model all phenomena cited above and for the ones it calculates, does not calculate the magnitude either, only the distribution. Therefore, one has to introduce some hypotheses and externally normalize the calculated results to obtain the parameter of interests. The different contributions considered relevant to the evaluation of the total power as well as the method to calculate them are summarized in Table 3.2-1. The method is largely inspired from [Villele, 2008].

Table 3.2-1 – Individual contribution to the nuclear power and methods to evaluate them

contribution	evaluation	MCNP tallies or values
Kinetic energy of fission fragments	Calculated by MCNP	F6:n
Kinetic energy of fission neutrons	Calculated by MCNP	F6:n
Gamma energy from capture (prompt)	Calculated by MCNP	F6:n,p
Prompt gamma energy from fission	Calculated by MCNP	F6:p
Beta decay energy	assumed deposited in fuel only and to have same distribution as fission distribution	Relative fraction of core total 6.5MeV/fission ^{235}U scaled base on the local fission distribution
Delayed gamma energy	assumed to have prompt gamma distribution	Relative fraction of core total 6.33MeV/fission ^{235}U scaled base on the prompt gamma distribution (used of the PIKMT card)

All of the calculated contributions are based on the MCNP heating tally, “F6”. The beta decay energy is assumed to be deposited only in the fuel, worth 6.5 MeV/fission of ^{235}U and its distribution is assumed to be the same as the fission one (obtained using “F6 mode n” tally).

The evaluation of the delayed gamma energy is more complicated. Its magnitude is assumed to worth 6.33 MeV/fission of ^{235}U. Its distribution is not calculated by MCNP and it is assumed that the distribution is the same as the prompt gamma one. Unfortunately, by default, there is no distinction between the capture and prompt gamma energy using a F6 tally. However, it is possible to disable the

capture reaction in MCNP thanks to the card PIKMT, and thus to obtain the prompt gamma distribution. Using this approach, two MCNP calculations, with and without the use of the PIKMT card, are required.

The total effective recoverable energy per fission, *Q,* is the sum of the different contributions described in Table 3.2-1. The MCNP score of a F6 tally is expressed in MeV/MCNP-neutron-source-particle. One has to multiply this score by the number of neutrons per second, ν (also calculated by MCNP), to obtain the energy per fission. Thus, by tallying the entire core and normalizing the number by ν one can deduce *Q*:

$$Q = Q_1 + Q_2 + Q_3 + Q_4 + Q_5 + Q_6$$

$$s_{MCNP} = (Q_1 + Q_2 + Q_3 + Q_4).\upsilon$$

$$Q = s_{MCNP} + Q_5 + Q_6 = s_{MCNP} + 6.5 + 6.33 = s_{MCNP} + 12.83$$

where

- *Q* (MeV/fission): total effective recoverable energy per fission.
- Q_1, Q_2, Q_3, Q_4 (MeV/fission): total recoverable energy per fission due to the fission fragments, kinetic energy of the neutrons, gamma capture and prompt gamma, respectively.
- Q_5, Q_6 (MeV/fission): total recoverable energy due to beta decay and delayed gamma, respectively.
- S_{MCNP} (MeV/neutron-source): F6 tally score when applied to the entire reactor.
- ν: number of neutrons created per fission.

Once Q is known, the number of fissions created per second, α, in the reactor is deduced from the total nuclear power, P, via the relation:

$$\alpha = \frac{P}{Q \cdot e}$$

where:

- *α* (fissions/second): number of fissions created per second in the reactor
- *P* (MW): total nuclear power
- *Q* (MeV/fission): total effective recoverable energy per fission
- *e* (MJ/MeV): constant, from 1eV = 1.602×10^{-19} J.

One can then deduce the power deposited in a region of the reactor, P_{region}, by summing the six contributions obtained from the method describe above, normalizing the results to have the local energy deposited per fission, Q_{region} (MeV/fission), and multiplying the result by the product, α·e:

$$P_{region} = Q_{region} . \alpha \cdot e$$

where:

- α (fissions/second): number of fissions created per second in the reactor
- P_{region} (MW): nuclear power deposited in the region
- Q_{region} (MeV/fission): recoverable energy per fission in the region
- e (MJ/MeV): constant, from 1 eV = 1.602×10^{-19} J.

4. Neutronics Analysis

The following section summarizes the results obtained from the neutronics analyses of the HEU core and the LEU reference core design. When possible, credibility of the neutronics model is also demonstrated by comparing the HEU results against experimental data. A significant number of experimental data have been found in [SAR, 2004]. The origin of these sets of data is not explained in detail. The authors suspect that at least some of them come from measurements made in the critical experiment FOEHN [ILL, 1969]. The critical experiment FOEHN was a full size mockup of the current RHF core with some small differences in geometry. From a neutronics standpoint, the FOEHN design is thought to be sufficiently close to RHF to perform a direct comparison in this work.

In this section, most results are presented graphically but for each plot, the corresponding tabulated values can be found in Appendix A1 to A4.

4.1. Depletion

The cycle length is one of the key performance parameter of the RHF. Cycle length is an output of the depletion calculations. This type of calculation is also used to characterize the irradiation conditions (e.g.: fission density and fission rate, inventory of nuclei, etc…). The following section describes the results of the depletion calculations.

The overall uncertainty (statistical uncertainty and systematic bias) on the cycle length is not provided by the calculations presented in this report. Considering the good quality of the HEU benchmark (see Section 4.1.1 below), it is assumed to be plus or minus one day. The statistical uncertainty provided for some parameters (e.g.: fission rate, fission density, flux, etc…) at each time do not take into account the accumulation of errors from the previous time steps. Calculation of time-dependent uncertainty is challenging due to the interplay between one quantity and all the others.

4.1.1. Model Credibility

There is no destructive or non-destructive Post-Irradiation Examination (PIE) data available to validate the RHF depletion models. However, the complete cycle histories (power level and control element position) of a few cycles are available. They can be used to perform a validation of the predicted integral effect of depletion by comparing calculated and measured time-dependent critical control element positions during these cycles. This type of comparison cannot guarantee that the predicted local fuel consumption match experimental values.

The cycle 143 history data [ILL, 2009] is often used as a reference because it is relatively easy to model: a fresh control element was used and the power level did not fluctuate much over the entire cycle. Depletion calculations modeling this cycle were carried out assuming a total nuclear power of 57.8 MW. A critical search algorithm (see Section 3.2.1) was used to determine the control element position that

would lead to criticality. These critical positions are presented in Figure 4.1-1 and compared to the experimental ones. On this figure, the solid line represents the calculations results and the dotted line represents the experimental ones. It can be seen that a good agreement is obtained from the beginning to the end of the cycle. Even though local fuel consumption data is not available, the good agreement between experimental and calculated CE position enhances the credibility of the approach and indicates that both models and methods are unlikely to contain major errors.

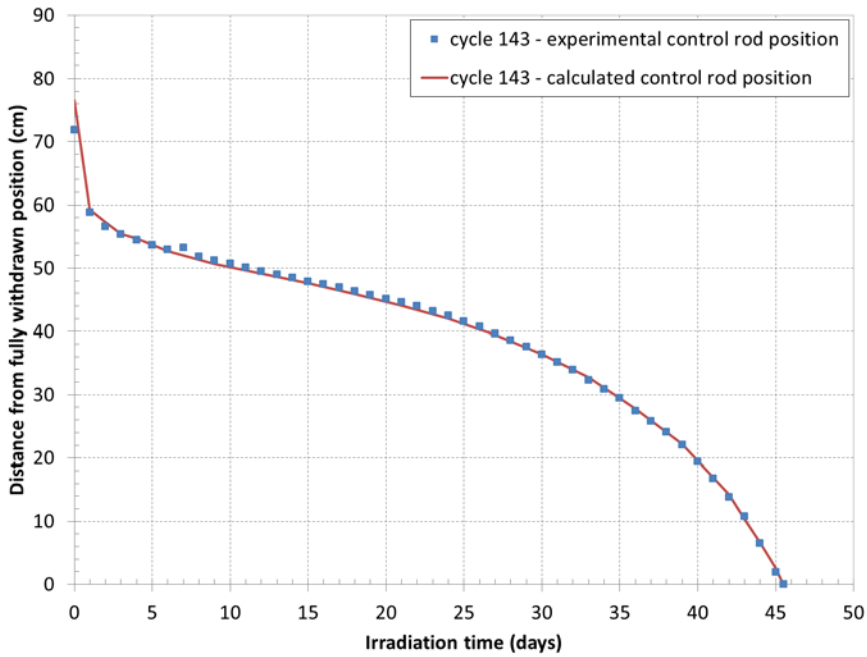

Figure 4.1-1 – Comparison of calculated versus measured control element position of cycle 143; relative error on cycle length is estimated at one day

4.1.2. HEU vs. LEU Cycle Length

The cycle length of a RHF core is defined by the time interval necessary for the control element to go from the fully inserted to fully withdrawn position. To deduce the HEU and LEU cores cycle length using the critical search algorithm described in Section 3.2.1, one has to check when the critical control element position has reached the fully withdrawn position.

Models used to compare the HEU and LEU cycle lengths do not contain the inclined beam tubes IH4 since it has been removed from the core few years ago. It should be noted that this beam was present in cycle 143 and therefore in the HEU cycle 143 model used for the analysis presented in Section 4.1.1.). The HEU and LEU cores have been depleted at full nuclear power (57.8 MW) until the control element reached its fully withdrawn position. The evolution of the control element critical position is presented for both cores in Figure 4.1-2. It can be seen that the LEU core cycle length is longer than the HEU one, 48 days instead of 45.5 days, at 57.8 MW.

Today, RHF is operated at a lower power (around 52.8 MW). At this power, the HEU core cycle length is around 49-50 days. Therefore, the LEU core operated at 57.8 MW should provide a cycle length very close to the one currently obtained with the HEU core.

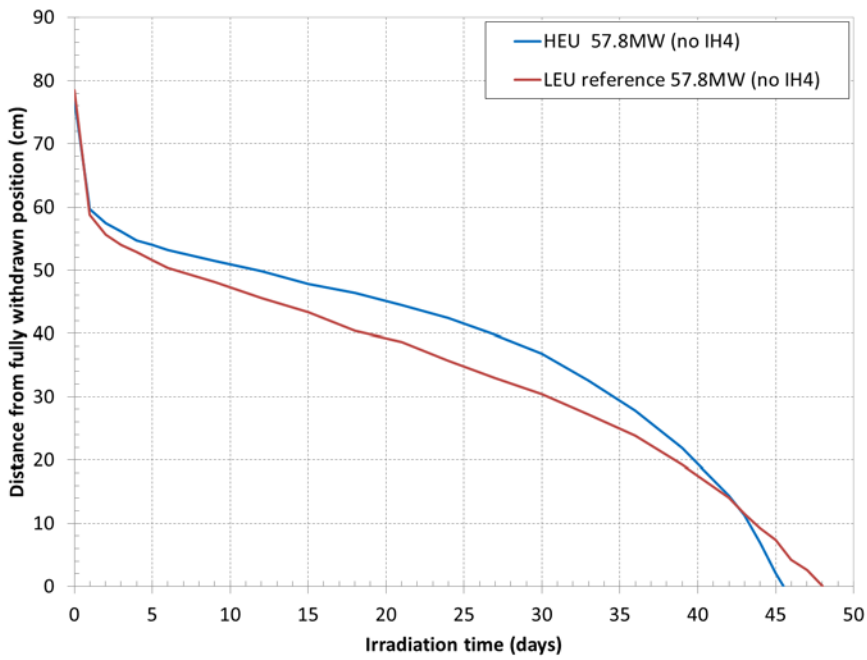

Figure 4.1-2 – Control element position evolution of the HEU and LEU cores depleted at a constant nuclear power of 57.8 MW; relative error on cycle length is estimated at one day

4.1.3. Fission Rate and Fission Density

Fission rate (fission/cm^3.s) and fission density (fission/cm^3, integral of the fission rate over the irradiation period) are two key parameters characterizing the fuel behavior under irradiation. Y.S Kim showed that the UMo fuel kernel swelling is well correlated with fission density and that the buildup of the interaction compounds between the aluminum matrix and the UMo fuel kernel is correlated to the fission rate and the fuel temperature [Kim, 2011], [Kim, 2013].

At each time step, identification of the maximum value of these parameters allow the construction of an envelope which can be used by experiment designers to ensure that fuel qualification tests envelop the expected conditions of irradiation of the RHF.

The fission rate envelopes for both HEU and LEU cores are presented below in Figure 4.1-3. For both cores, the peak occurs after one day of irradiation. It can be observed that the peak HEU value is very close to the LEU one. The fission rate decreases non-monotanically during the cycle. This is explained by the change of location of the peak value. For the LEU core, the peak fission rate is first located in the outer edge of the plate, around the core midplane. Close to mid cycle, the peak is located on the same edge but at the very top of the plate, when the boron of the poison belt is sufficently depleted. The

fission rate envelope profile of the HEU core is more complicated and reflects the fact that the peak value changes location multiple times during the cycle. As expected, the fission rate peak envelope is vey similar in shape to the peak power density (W/cm^3) envelope since the latter is derived from the former. The peak power density envelope is presented in Section 4.3.

On Figure 4.1-3, the average fission rate of the HEU and LEU cores are also presented. Despite the fact that the power at which both cores have been depleted is identical, the average fission rate of the LEU core is lower than the HEU one. This is simply due to the larger volume of LEU fuel which decreases the average value. It can also been observed that the ratio between peak and average is relatively large at BOC (around 2.5) for the HEU and LEU cores. This ratio decreases afterwards (close to 1.5 at EOC). This illustrates the significant gradient of power that exists between the outer edge of the plate (facing the reflector) and the rest of the fuel plate.

Also presented in Figure 4.1-3 is the ^{235}U fission rate for both the core average and peak envelope. From BOC to EOC, the ^{235}U fission rate of the HEU core represents almost 100% of the total fission rate. For the LEU core, due to the buildup of ^{239}Pu, it can be seen clearly that the contribution of ^{235}U to the total fission rate is decreasing.

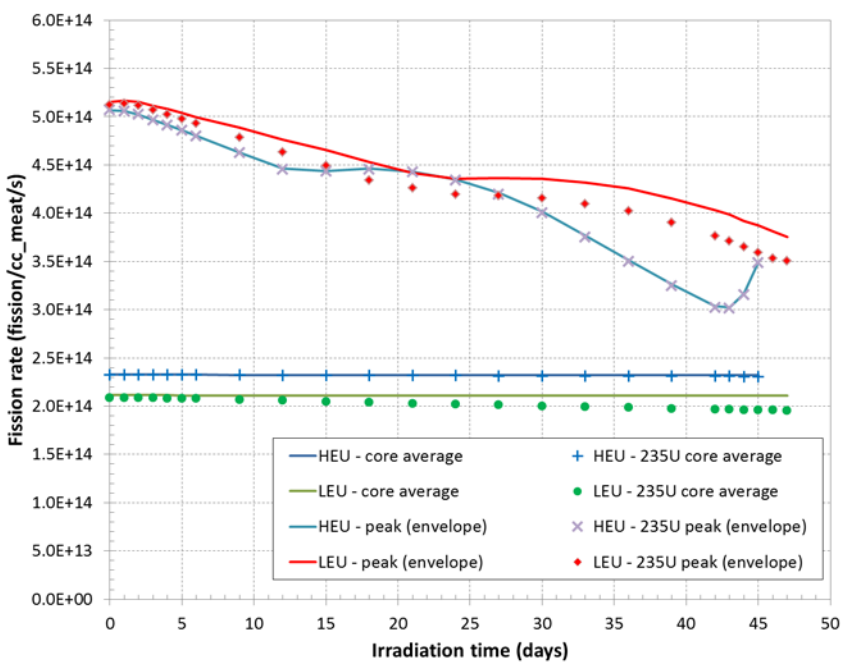

Figure 4.1-3 – Evolution of the average and maximum fission rate for HEU and LEU cores.; relative error is estimated at 10%

The evolution of the average and peak fission densities are presented in Figure 4.1-4. The LEU peak fission density envelope is relatively similar to the HEU one for most of the cycle but becomes larger towards the end of the cycle. This is explained by the fact that the LEU core power remained more peak than the HEU core and also because the LEU cycle length is longer. At EOC, the peak value of the HEU

and LEU cores is about 1.6×10^{21} and 1.8×10^{21} fission/cm^3_{meat}, respectively. Assuming a fuel volume fraction of 50%, the LEU peak fission density in the fuel kernel is 3.6×10^{21} fission/cm^3_{fuel}.

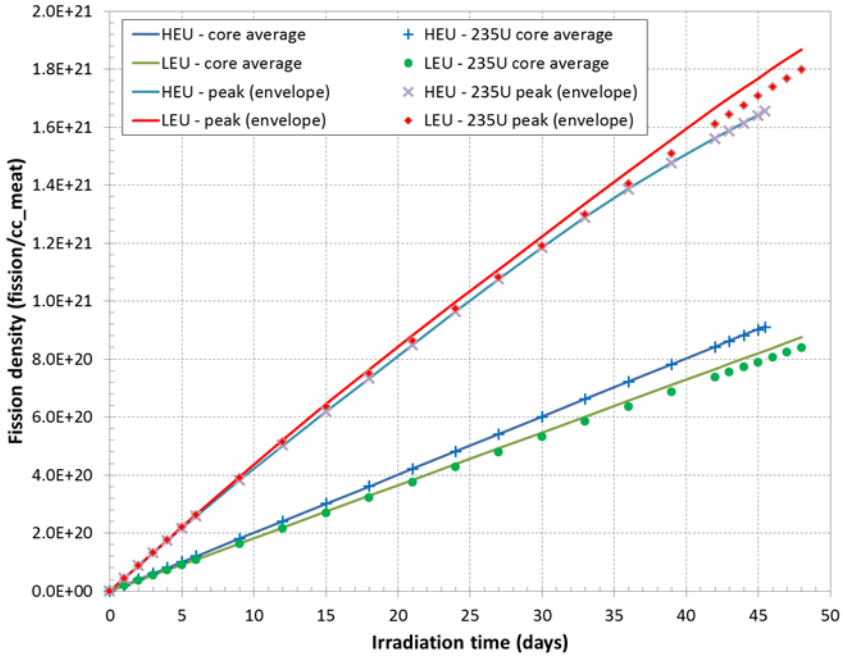

Figure 4.1-4 – Evolution of the average and maximum fission density for HEU and LEU cores; relative error is estimated at 10%

The total ^{235}U consumption (a.k.a. ^{235}U burnup) is often used to describe the irradiation of a given test or fuel design. In Figure 4.1-5 presents the evolution of the peak and average ^{235}U consumption for the HEU and LEU cores.

The average and peak HEU core ^{235}U consumption are 39% and 65%, repsectively. Since the ^{235}U mass in the LEU core is about 50% larger than in the HEU core, it is expected that the average LEU core ^{235}U consumption should be about half for the same cycle length and the same power (same number of fissions). At EOC, the average and peak LEU ^{235}U consumption are 25% and 50%, respectively.

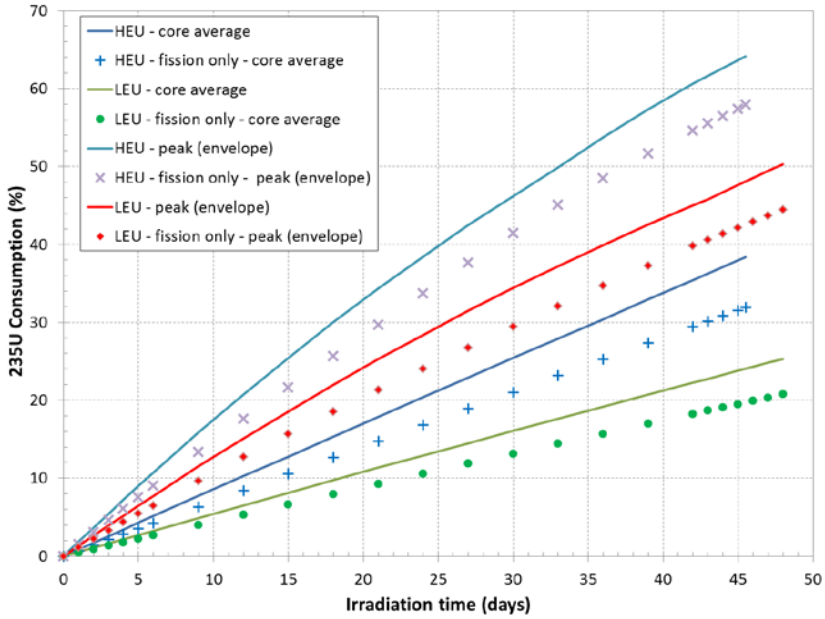

Figure 4.1-5 – Evolution of the average and maximum ^{235}U consumption for HEU and LEU cores; relative error is estimated at 10%

On Figure 4.1-5, the ^{235}U consumption due to all reactions as well as only to fission-only is also indicated. The distinction between total and due-to-fission-only ^{235}U consumption shows clearly that there is a significant difference between them. This is due to the (n,g) reaction which account for about 15 to 20% of the total ^{235}U consumption. As illustrated in Figure 4.1-6 below, when the total ^{235}U consumption is compared to the total fission density, the former appears to be clearly higher than the latter. A practical consequence is that the total ^{235}U consumption can be used as a simple and easy way to extract a conservative estimate of the total fission density.

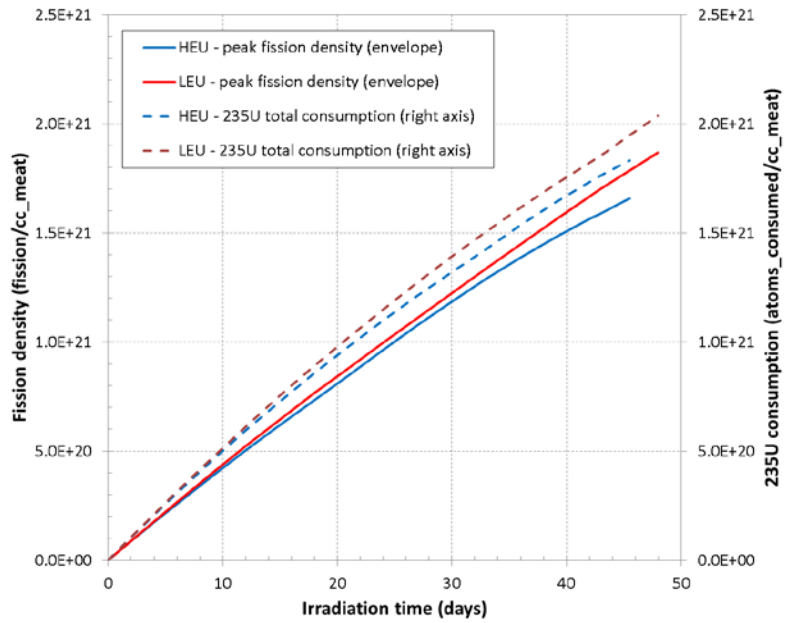

Figure 4.1-6 – Comparison between peak fission density and peak ^{235}U consumption; relative error is estimated at 10%

4.1.4. Heavy Isotopes Inventory

The inventory of heavy nuclei has been evaluated for both HEU and LEU cores. Depletion calculations have been set up to include in the material compositions the isotopes that contribute to 99.95% of the total absorption. This choice is considered to be a reasonable approximation and allows for a considerable speed up of the calculation compared to a case that includes all the isotopes modeled in ORIGEN.

As a consequence, the only heavy isotopes present in the material composition are uranium, neptunium and plutonium. The inventory of key isotopes of these elements is presented in Table 4.1-1. Due to the significant increase in ^{238}U mass, the plutonium produced in the LEU core is significantly larger than in the HEU core. Nonetheless, it remains a modest fraction of the total heavy nuclei inventory.

Table 4.1-1 – Inventory of Uranium, Neptunium and Plutonium isotopes at BOC and EOC; relative error is estimated at 10%

Element	Isotope	HEU		LEU	
		Mass BOC (g)	Mass EOC (g)	Mass BOC (g)	Mass EOC (g)
Uranium	**235**	8578	5287	13370	9983
	238	541	512	53836	53339
Neptunium	**237**	0	13	0	20
	239	0	3	0	34
Plutonium	**239**	0	15	0	296
	240	0	3	0	34
	241	0	2	0	13
	242	0	0.2	0	1

4.1.5. Helium Production in Borated Zone

As stated in Section 2.2, the large boron density in the poison belt of the LEU reference design can potentially lead to a large He-induced swelling (He is a byprodyct of the n-γ reaction in the B_4C). It must be determined if this large He-induced swelling can lead to a failure of the poison belt.

Several actions are ongoing and/or planned in order to mitigate the risk to a successful LEU fuel design associated with th high boron loading of the poison belt. Such risk mitigation strategies required a detailed characterization of the boron and helium evolution in the poison belt.

Figure 4.1-7 presents some of these important features. It is shown the evolution of the neutron flux, the ^{10}B density and the ^{4}He density for both the HEU and LEU burnable absorber regions. Figure 4.1-7 presents the results corresponding to the region which has the sharpest ^{10}B depletion rate based on the discretisation described in Section 2.3. It correpsonds to the top of the poison belt in the LEU core and the top outer edge of the upper borated regions in the HEU core.

Since the borated regions are close to the fuel in the HEU core, they are exposed to a larger neutron flux than the poison belt design used in the LEU core. Consequently, the ^{10}B consumption rate is larger and the borated regions in the HEU core are almost completely depleted at mid-cycle. In the LEU core, it takes almost the entire cycle to deplete completely the ^{10}B.

As expected, the ^{4}He density at EOC is four times larger in the LEU core's poison belt than in the HEU core's borated regions since the initial density of ^{10}B in the LEU design is four times larger and the ^{10}B is completely depleted. It will have to be demonstrated that the resulting helium-induced pressure will not be challenging for the poison belt cladding and its overall integrity.

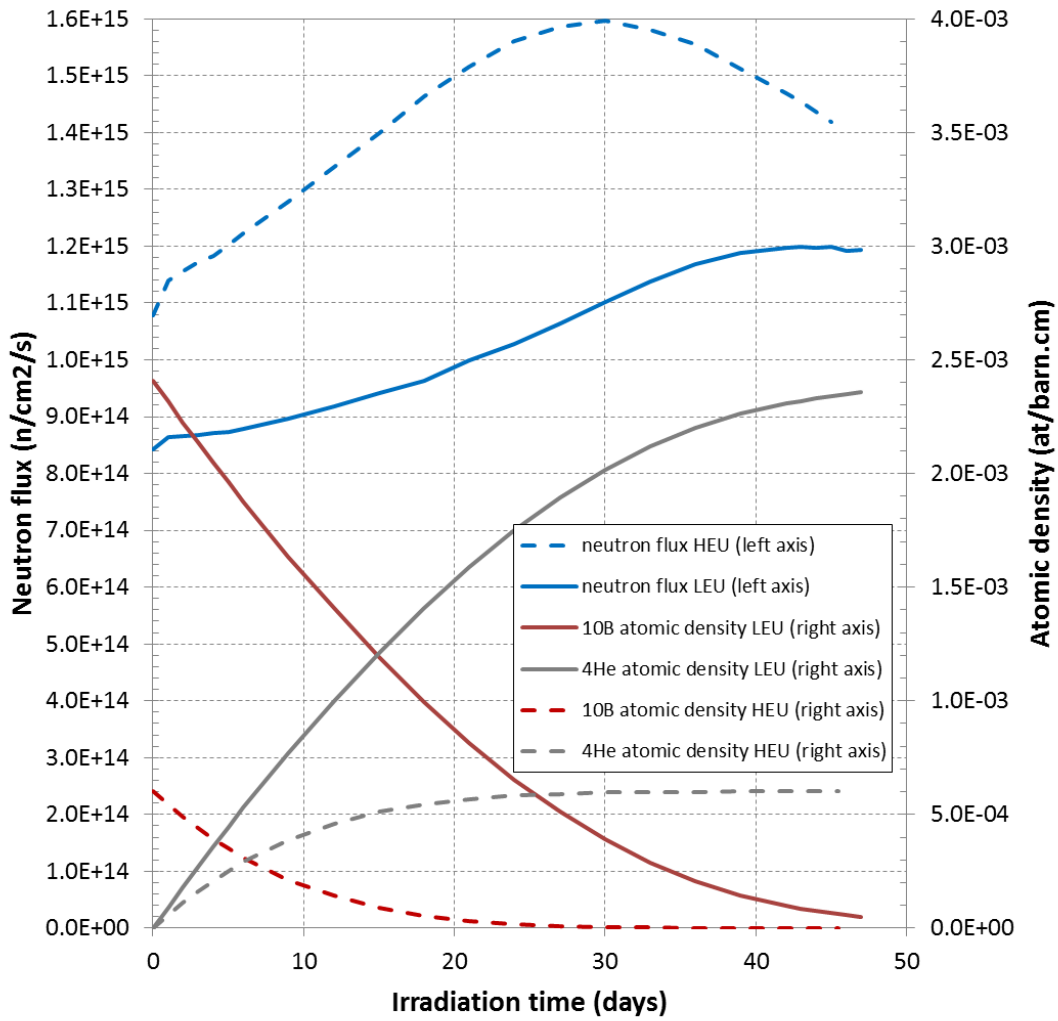

Figure 4.1-7 – Evolution of the neutron flux magnitude and ^{10}B, ^{4}He composition in the borated region; relative error is estimated at 10%

4.1.6. Kinetic Parameters Evolution

The delayed neutron fraction (a.k.a. beta-effective, β_{eff}) and prompt neutron lifetime (ℓ) have been calculated at each time step. MCNP calculates them using the adjoint-weighted tallies method. Some benchmarks and comparison to experimental data have been published in the literrature and seems to demonstrate the validity of this method [LANL, 2011]. In [SAR, 2004], a β_{eff} of 650 pcm and a ℓ of 650 µs are reported. It is unclear whether these values come from measurements, best estimate calculations or are conservative estimations. The evolution of the β_{eff} and ℓ of both the HEU and LEU cores is presented in Figure 4.1-8 and Figure 4.1-9, respectively.

At BOC, the calculated β_{eff} of the HEU and LEU cores are almost identical and worth about 675 pcm. For the HEU core, it is slightly higher (but reasonably close) to the value reported in the SAR (650 pcm) and remains relatively constant during the cycle. For the LEU core, we can observe a declining trend. This

can be explained by the buildup of the plutonium which has a lower delayed neutron fraction than uranium. However the effect is relatively small since, at EOC (48 days), the β_{eff} of the LEU core has decreased by about 25 pcm.

The prompt neutron lifetimes at BOC are relatively similar for both the HEU and LEU cores (about 740 µs). This value is significantly higher than the one reported in the SAR (650 µs). Since the origin of this number in the SAR is not explained, it is difficult to draw a conclusion on this apparent discrepancy.

The prompt neutron lifetimes decrease sharply in the first days of operation probably due to the xenon buildup until they reach 700 µs and 680 µs after 5 days, for HEU and LEU cores respectivelely. For the rest of the cycle, the prompt neutron lifetimes increase at a relatively constant rate probably due to the progressive withdrawing of the control element and the depletion of the borated regions. At EOC, the prompt neutron lifetimes are 800 µs and 725 µs, for HEU and LEU cores respectivelely.

The discrepancy at BOC between the values in SAR and HEU model must be further investigated. Other methods exist to calculate this parameter with MCNP [ANL, 1997], [Hanson, 2006] so comparisons between the different evaluation methods could be performed.

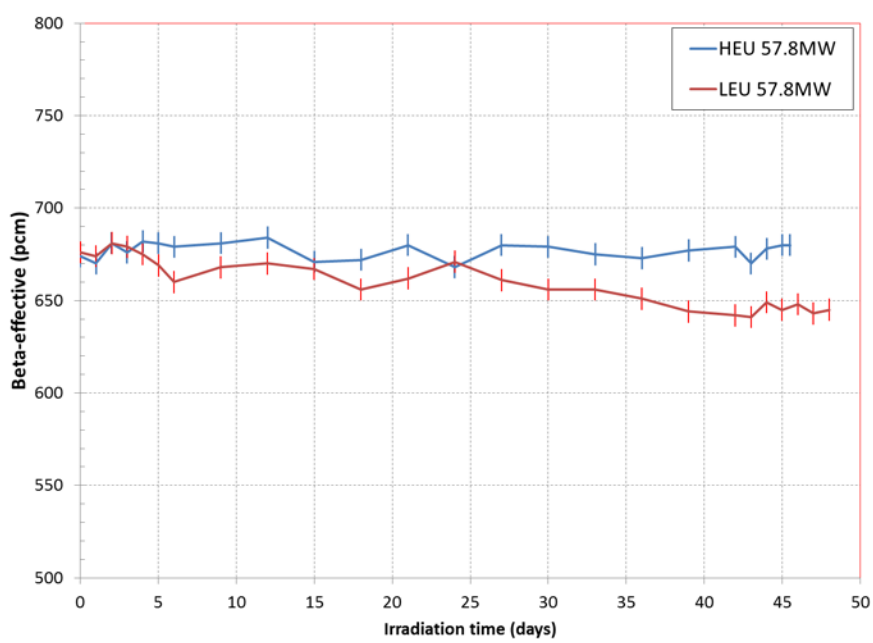

Figure 4.1-8 – Evolution of the β_{eff} for the HEU and LEU cores; steady state uncertainty is 6 pcm at one standard deviation; relative error including effect of depletion calculation estimated at 10%

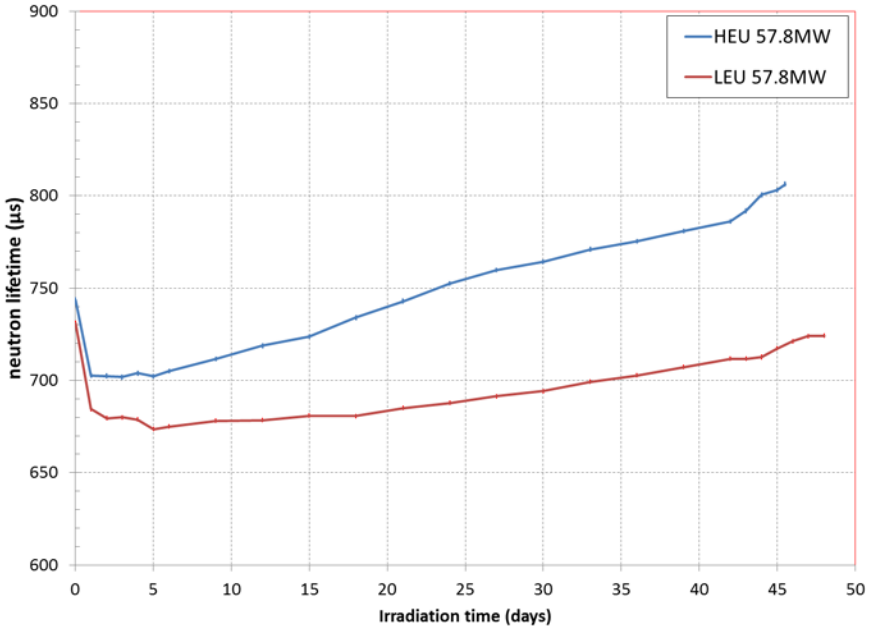

Figure 4.1-9 – Evolution of the neutron lifetime for the HEU and LEU cores; steady state uncertainty is 1.3 µs at one standard deviation; relative error including effect of depletion calculation estimated at 10%

4.2. Neutron flux

The following section presents the neutron flux values obtained at different reactor locations. These neutron fluxes are calculated with the MCNP tally "F4".

4.2.1. Model Credibility

Plots showing the measured axial distribution of the flux at different radial location are provided in Figure 27.3 of the current SAR [SAR, 2004]. Tabulated values were not available but it was possible to digitize the plots using the digitizer software Engauge [Engauge, 2014]. Error bars on the plots were not provided and the overall measurement uncertainty is unknown. The energy range is not specified either but, from the context, it is likely to correspond to the thermal range (E < 0.625 eV). It is specified in Section 272.2 of [SAR, 2004] that the measurements were made in an unperturbed core (no experimental devices). The measurements were likely to be made in cold conditions (reactor close to room temperature) with a fresh fuel, probably close to critical conditions.

Despite all these limitations, a comparison of the calculated versus measured values has been carried out. Calculations (axial/radial node size of 2cm and 0.25cm, respectively) , however, assumed hot (full power) conditions and all in-core devices were present. The results are presented in Figure 4.2-1 and Figure 4.2-2. It can be seen on these plots that a good agreement is obtained not only for the distribution but also for the magnitude of the flux. Some discrepancies appear (10% maximum) when the radial distance is in the range of 35.5 to 51.5 cm. The presence of the experimental devices in the simulations is likely to be the predominant source for these discrepancies. The experimental devices are located – at the closest – at 30 cm from the core center.

A plot showing the calculated radial distribution of the flux in the median plane (axial/radial node size of 2cm and 0.25cm, respectively) of the reactor is provided in Figure 27.2 of the current SAR [SAR, 2004]. Like previously, tabulated values were not available but the plot could be digitized. The calculations presented in the SAR were also carried out using an unperturbed core model. A plot showing the comparison between the ANL and SAR calculated values is presented in Figure 4.2-3. For the four energy range presented, the agreement between the two sets of calculations is reasonably good. Like previously some discrepancies exist. The difference between perturbed/unperturbed cores is believed to be the main driver for these discrepancies.

Overall, the agreement between the measurements and calculated values is sufficiently good to assume that the codes and models are able to calculate the neutron flux magnitude and distribution correctly and are adapted for the type of calculations presented in this study.

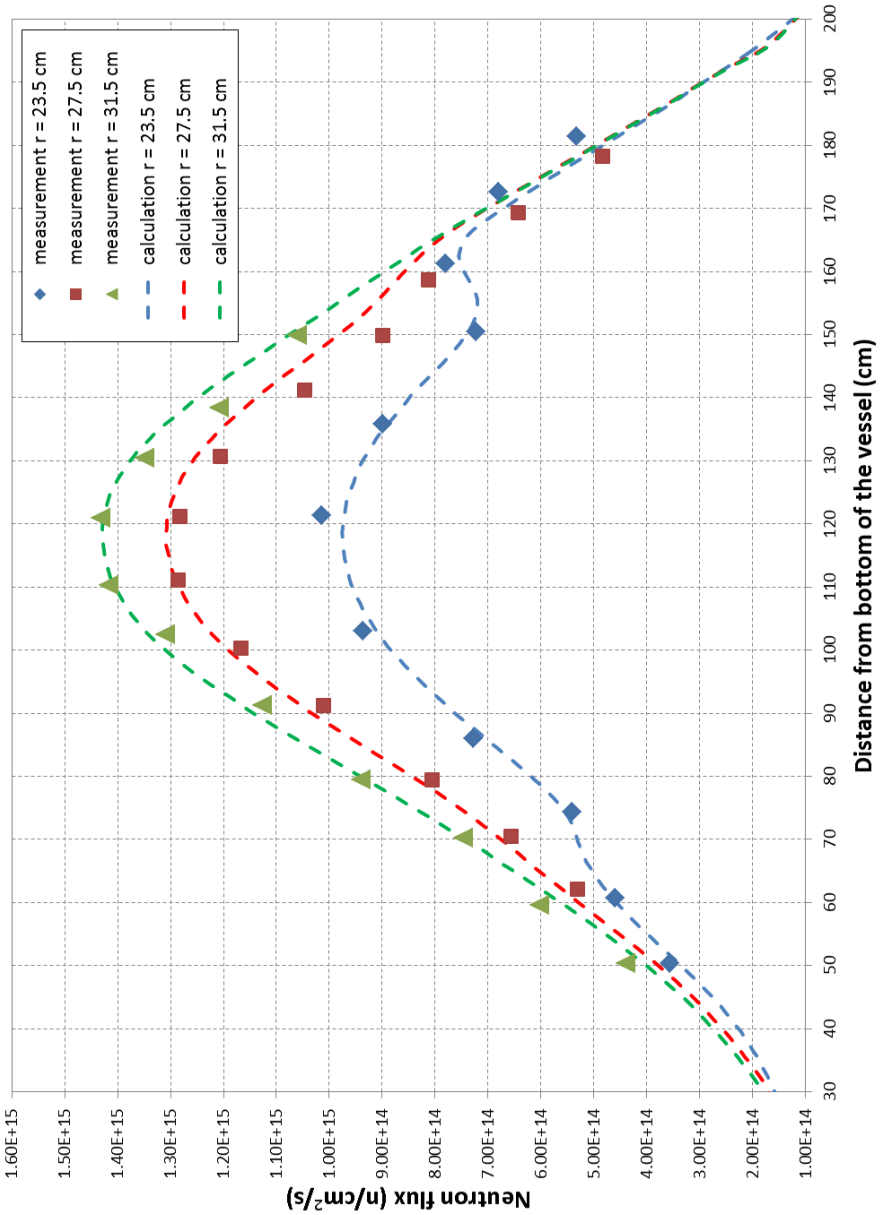

Figure 4.2-1 – Calculated versus measured axial thermal flux profile at a distance of 23.5, 27.5 and 31.5 cm from the core center; relative error is less than 2% at one standard deviation

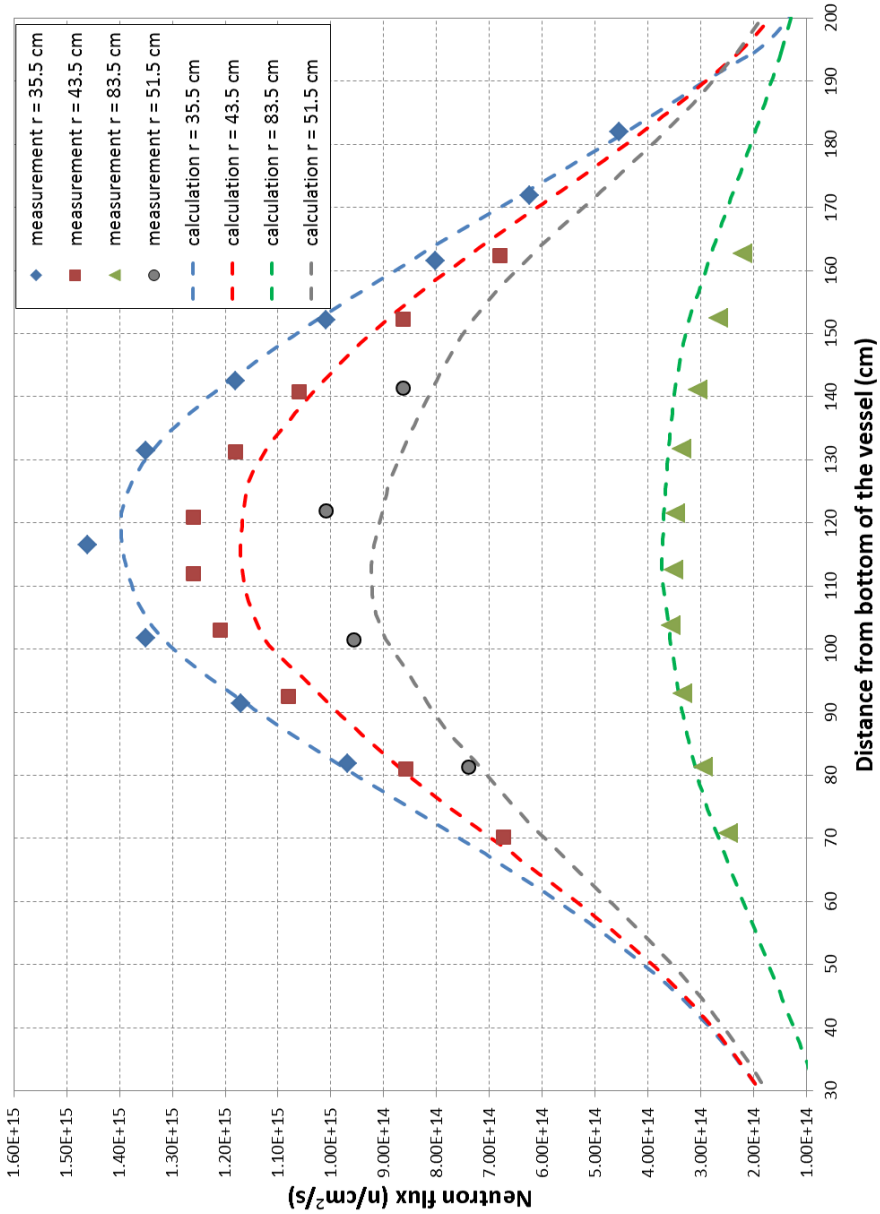

Figure 4.2-2 – Calculated versus measured axial thermal flux profile at a distance of 35.5, 43.5, 51.5 and 83.5 cm from the core center; relative error is less than 2% at one standard deviation

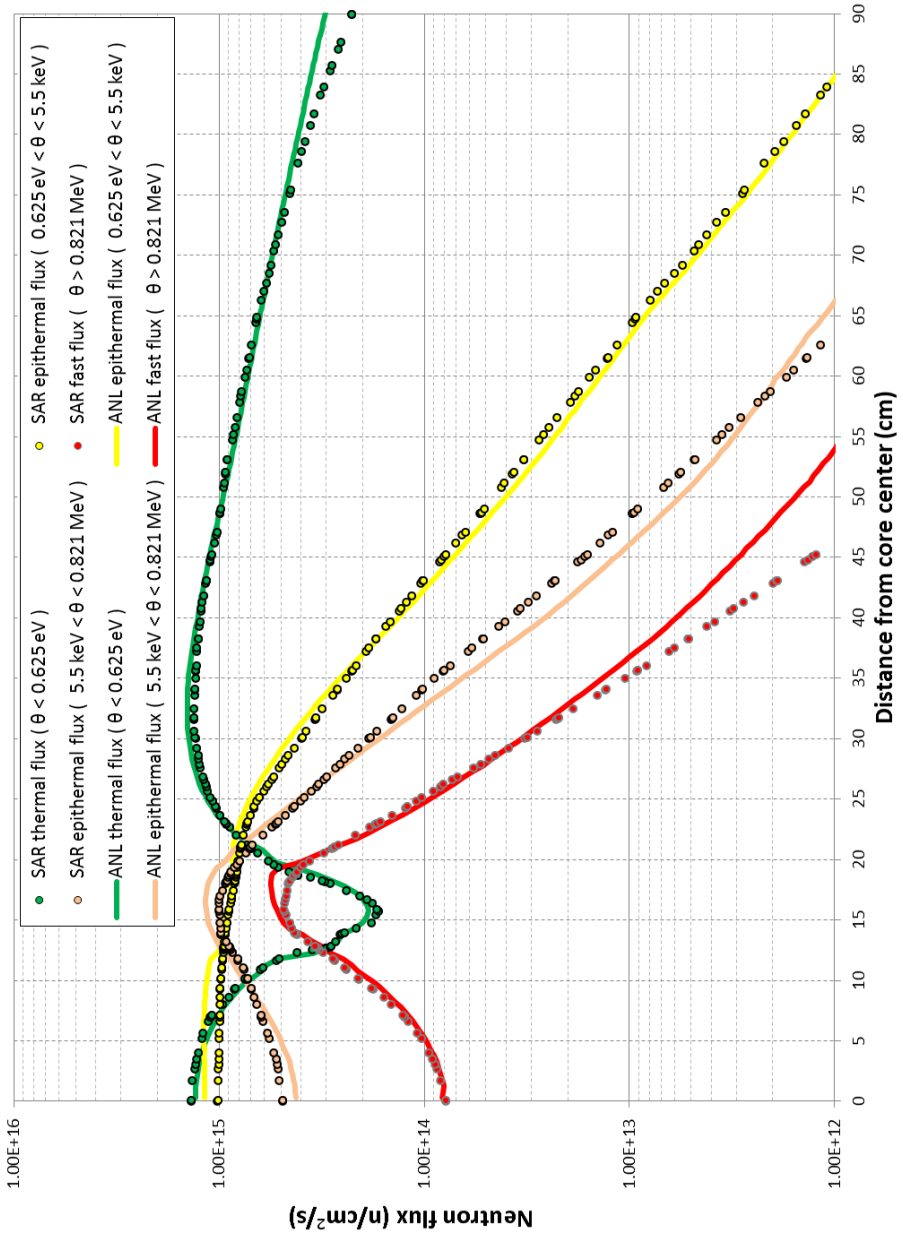

Figure 4.2-3 – ANL versus SAR calculated radial flux distribution in the median plane of the reactor; relative error is less than 2% at one standard deviation

4.2.2. Neutron Flux at the Beam Tube Entrances

The magnitude of the neutron flux entering the beam tubes (which transport neutrons to the experimental hall located outside the reactor building) is one of the two parameters defining the performance of the reactor. The other one is the cycle length which determines the length of time the neutron flux can be maintained without interruption.

The RHF core contained 13 horizontal, 1 inclined and 2 vertical beam tubes. One beam tube can feed one or more instruments. Before entering the beam tube, the neutron spectrum might be modified by the presence of a cold or hot source. Sources are volumes that are cooled at very low temperature (typically 25K) or heated up at very high temperature (2400K). These volumes lower or increase the energy of the neutron that crosses them. Table 4.2-1 lists the different sources present in the core and which beam tubes they perturbed.

Table 4.2-1 – Categories of beam tubes defined by the presence or absence of cold/hot sources

Source	Influenced beam tubes
Hot	H3, H4, H8
Cold vertical	H1, H2
Cold horizontal	H5
None	H6, H7, H9, H10, H11, H12, H13, IH3, VX4, VX7

The neutron flux at the entrance of the beam tubes has been calculated for both the HEU and LEU cores at “full power” conditions for several time steps. To ensure a good statistical convergence of the results within a reasonable calculation time, relatively large volumes (covering relatively large distance) have been used. Because this study focuses on the comparison between the HEU and LEU cores, this is not an issue since the neutron flux ratio between the two cores is the metric of interest. Since the same volumes' normalization has been used to tally the flux, the comparison is relevant.

Table 4.2-2 provides the ratio between the LEU and HEU core peak thermal neutron flux at each beam tube entrance. The ratio is provided at BOC and EOC for two combinations of HEU and LEU reactor powers: 1) HEU and LEU cores are operated at 52.8 MW, and 2) the HEU core is operated at 52.8 MW and the LEU core is operated at 57.8 MW. Recall that the former corresponds to a case for which the HEU cycle length is shorter by about three days compared to the LEU core, and the latter corresponds to a case for which the cycle length is about the same between the two cores (see Section 4.1.2).

For the reactor power combinations discussed above, it can be seen in Table 4.2-2 that the neutron flux differences between the two cores is more pronounced at EOC than at BOC. The neutron flux magnitude tends to increase over time to compensate the fission products poisoning (more neutrons are necessary to keep the power at a constant level). The neutron flux increase over time is more pronounced for the HEU core than for the LEU. In addition, due to the progressive withdrawal of the control element during irradiation, the center of the axial flux distribution shifts downward from the core median plane, as

illustrated in Figure 4.2-4. Again, the variation is not completely identical between the two cores. The HEU core being shorter, the power and consequently the flux is less spread which favors higher flux at the beam tube inlet. Both phenomena explain why the flux variation is higher at EOC than at BOC and why the variation differs from one beam tube to the other (see Table 4.2-3). Overall, assuming that all beam tubes have the same importance, the average variation between HEU and LEU cores would be a little bit less than 3% compared to today's performance, for a cycle length essentially similar.

Table 4.2-2 – Ratio LEU/HEU core peak neutron flux at BOC, EOC and at different power; relative error is less than 1% at BOC and estimated at 10% at EOC

source	beam tubes	beam tubes elevation* (cm)	Ratio LEU/HEU peak neutron flux (%)			
			LEU/HEU both at 57.8MW		LEU at 57.8MW /HEU at 52.8 MW	
			BOC	EOC	BOC	EOC
no source	**H6-7**	-35.0	-8.9%	-14.0%	1.2%	-4.4%
	H9	15.0	-12.3%	-14.3%	-2.6%	-4.8%
	H10	0.0	-13.0%	-16.4%	-3.3%	-7.1%
	H11	25.0	-11.9%	-14.0%	-2.1%	-4.4%
	H12	-25.0	-10.7%	-14.9%	-0.7%	-5.4%
	H13	-25.0	-11.0%	-15.4%	-1.1%	-6.0%
	IH3	-5.0	-10.5%	-13.9%	-0.5%	-4.3%
	VX4	-5.0	-11.3%	-13.7%	-1.4%	-4.1%
	VX7	-5.0	-10.4%	-12.3%	-0.4%	-2.5%
hot	**H3**	15.0	-11.0%	-13.5%	-1.1%	-3.9%
	H4	15.0	-11.9%	-13.1%	-2.0%	-3.4%
	H8	15.0	-11.2%	-14.6%	-1.3%	-5.1%
cold vertical	**H1**	17.5	-11.2%	-13.5%	-1.3%	-3.8%
	H2	-17.5	-9.9%	-14.4%	0.1%	-4.8%
cold horizontal	**H5**	-25.0	-10.0%	-14.8%	0.0%	-5.3%
average			**-11.0%**	**-14.2%**	**-1.1%**	**-4.6%**
core lifetime average			**-12.6%**		**-2.9%**	

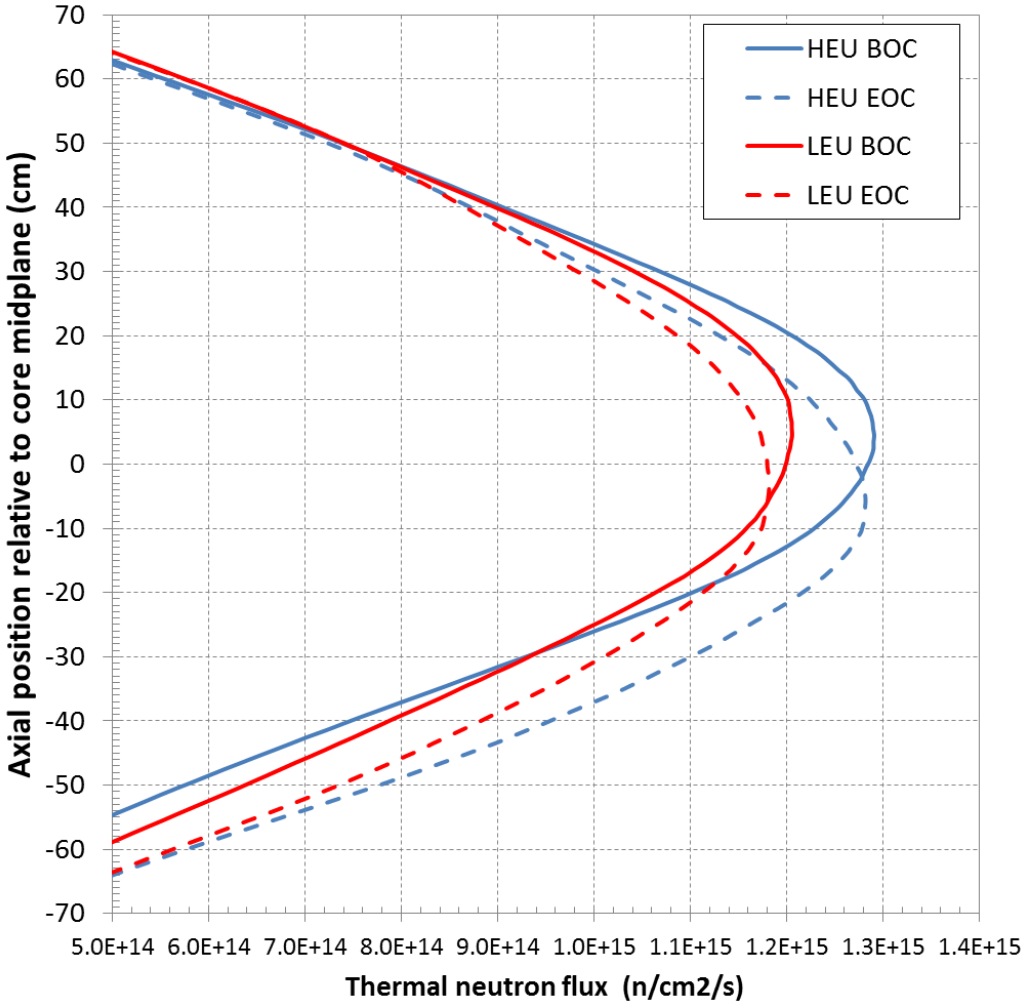

Figure 4.2-4 – HEU (52.8 MW) and LEU (57.8 MW) axial profile of the thermal neutron flux at a radial distance of 30 cm (typical distance from beam tube inlet) from the core center; relative error is less than 0.1% at one standard deviation at BOC and estimated at 10% at EOC

Table 4.2-3 – Ratio BOC/EOC peak neutron flux of HEU and LEU cores; relative error estimated at 10%.

source	beam tubes	beam tubes elevation* (cm)	EOC/BOC peak neutron flux variation (%)	
			HEU	LEU
no source	**H6-7**	-35.0	10.2%	4.1%
	H9	15.0	0.2%	-2.1%
	H10	0.0	3.3%	-0.8%
	H11	25.0	-0.4%	-2.7%
	H12	-25.0	10.1%	4.9%
	H13	-25.0	9.9%	4.4%
	IH3	-5.0	-0.1%	-3.9%
	VX4	-5.0	0.0%	-2.7%
	VX7	-5.0	-0.6%	-2.7%
hot	**H3**	15.0	1.0%	-1.8%
	H4	15.0	0.9%	-0.5%
	H8	15.0	2.5%	-1.4%
cold vertical	**H1**	17.5	1.5%	-1.1%
	H2	-17.5	6.9%	1.7%
cold horizontal	**H5**	-25.0	9.2%	3.4%

4.3. Power Distribution

Power distribution calculations provide inputs for the Thermal-Hydraulic (TH) models which are used to determine if the core can be properly and safely cooled at any time. The method used to calculate and normalize the MCNP tallies is explained in Section 3.2.3. This section starts with a comparison to experimental data which is intended to demonstrate the consistency of both the neutronics model and the power normalization method. Then, the distribution of power in the core and inside a fuel plate is described.

4.3.1. Model Credibility

A graph showing the ratio between the stripe-based, axially average power density and the plate average power density measured at different radial location is provided in Figure 27.4 of the current SAR [SAR, 2004]. Tabulated values were not available but it was possible to digitize the plot using digitizer software [Engauge, 2014]. Error bars on the plots are not provided and the overall measurement uncertainty is unknown. The measurements were likely made at cold conditions (reactor near room temperature) with a fresh fuel, probably near critical conditions. However, on the original figure, the control element position indicated is surprisingly low (few centimeters above the midplane). The typical control element position at BOC is much higher, about 25 cm above the midplane. It is unclear if the control element position indicated on the figure is correct or not.

The good agreement between the measured and calculated values can be seen in Figure 4.3-1. The calculated power peaking on the edges, especially the inner edge, is however slightly underestimated. If the control element position set in the model is really higher than it was during the measurement, it could explain the discrepancy seen on the inner and outer edge.

A graph showing the measured ratio between the local power and the average power is presented in Figure 27.5 of the SAR. Measurements are provided at different axial and radial location. A comparison between the measured and calculated values is presented in Figure 4.3-2. It can be seen that the calculated values are very consistent with the measured ones.

For both comparisons, the fuel discretization used in the neutronics model was not intended to match the precise location of the measurements. In most cases, the calculated values are likely to cover a larger region than the measured ones. Consequently, it is expected that the calculated values might represent slightly larger values in the middle of the plate and slightly lower values on the edge. Overall the comparisons to the measured values are satisfying.

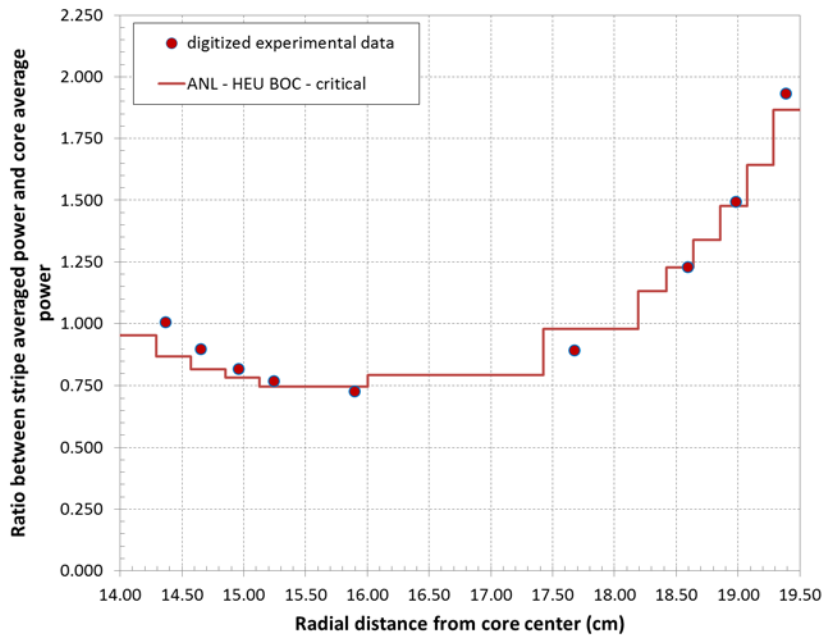

Figure 4.3-1 – Comparison between measured and calculated axially averaged radial power profile; calculation relative error is less than 0.25%

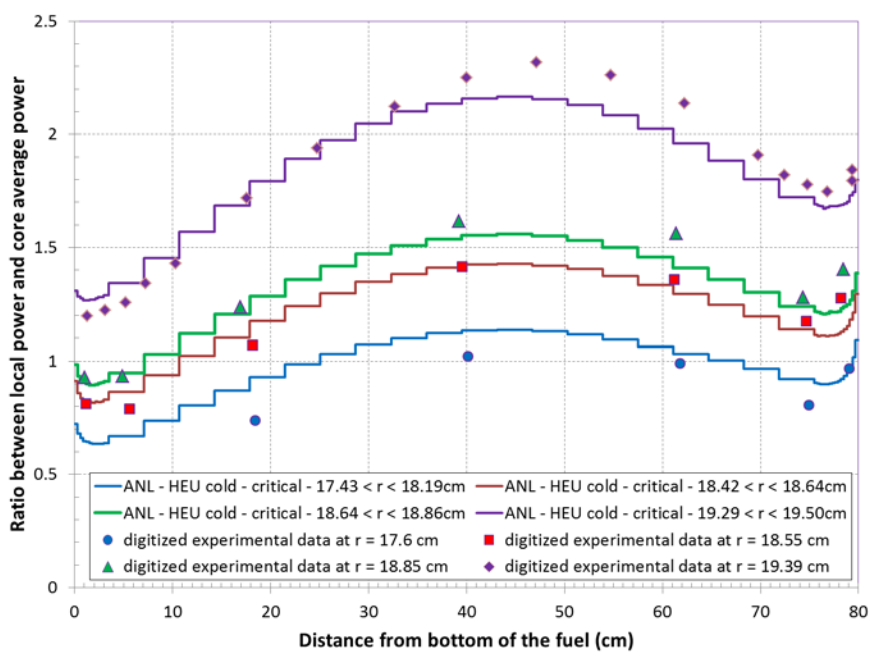

Figure 4.3-2 – Comparison between measured and calculated ratio between local and average power; calculation relative error is less than 0.25%

4.3.2. Power Deposition in the Core

As shown in Table 4.3-1, the distribution of power deposited in the core is relatively similar between the HEU and LEU cores. The largest differences are seen in the power deposited in the fuel meat and the reflector. At full power (nuclear power of 57.8 MW), the power deposited in the LEU fuel meat is about 1.1 MW higher than in the HEU fuel meat. The power deposited in the rest of the fuel element and the reflector is however lower (0.4 and 0.5 MW, respectively).

The distribution of power remains relatively constant during the cycle. The only noticeable difference comes from the control element which is highly absorbing but progressively withdrawn during irradiation. The control element power deposited in the control element (about 0.4 MW) is partially redistributed in the heavy water of the central cavity.

Table 4.3-1 – Distribution of power at BOC and EOC for both the HEU and LEU cores; calculated relative error is less than 1% at BOC and estimated at 10% at EOC

Power (MW) deposited in	HEU		LEU	
	BOC	EOC	BOC	EOC
entire reactor	57.81	57.81	57.81	57.81
fuel element	53.043	53.185	53.723	53.890
- outer side plate	*0.235*	*0.234*	*0.177*	*0.172*
- inner side plate	*0.143*	*0.162*	*0.111*	*0.123*
- coolant between plates	*0.978*	*1.011*	*0.843*	*0.865*
- plate's cladding	*0.583*	*0.614*	*0.427*	*0.442*
- top borated region	*0.048*	*0.004*	*0.034*	*0.002*
- bottom borated region	*0.027*	*0.012*	-	-
- fuel	*51.028*	*51.149*	*52.132*	*52.285*
light water pool	0.356	0.369	0.321	0.326
vessel	0.230	0.244	0.215	0.221
reflector	3.024	3.054	2.552	2.544
heavy water central cavity	0.607	0.780	0.532	0.669
control element	0.462	0.069	0.376	0.055
- long Ni rod	*0.366*	*0.060*	*0.285*	*0.048*
- long Al tube	*0.047*	*0.007*	*0.038*	*0.005*
- short Ni rod	*0.043*	*0.002*	*0.047*	*0.001*
- short Al rod	*0.006*	*0.000*	*0.006*	*0.000*

4.3.3. Power Distribution in the Fuel

Two-dimensional (2D) maps representing the volumetric heat generation rate (sometimes referred as power density) of the HEU and LEU cores at BOC and EOC is presented in Figure 4.3-3. That figure shows clearly that, for the HEU and LEU core, the significant gradient in the power between the outer edge (facing the reflector) and the rest of the plate. From BOC to EOC, one can see the sharp decrease of power in the outer edge which is redistributed towards the middle of the plate and the inner edge. The evolution of the axial power profiles in the inner and outer edge is presented on Figure 4.3-4 and Figure 4.3-5. Each figure presents the axial power profile of the HEU and LEU cores at BOC, day 24 (about mid cycle) and EOC.

On the inner edge (Figure 4.3-4), it can be seen that the power profile is relatively identical for both HEU and LEU cores, except at the top and bottom of the fuel element. The larger power increase at the axial edges in the LEU core is due to the absence of burnable absorber on top and bottom. Also visible on this figure is the significant impact of the control element on the power shape; far less power is generated in the fraction of the fuel element located below the tip of the control element. This explains the step in the power distribution at 24 days.

On the outer edge (Figure 4.3-5), at BOC, the HEU and LEU power profiles are similar except at the top and bottom where a larger increase in power is observed in the LEU core (similar to the inner edge). Nonetheless, the peak power occurs for both cores at 5 to 10 cm above the mid-plane. Without the poison belt, the power peak in the LEU core would occur at the very top of the fuel as shown in [ANL, 2010]. At mid-cycle and EOC, it can be observed that the axial power in the HEU fuel tends to be lower than the LEU towards the middle of the fuel element.

The HEU and LEU cores peak power envelopes are presented in Figure 4.3-6 and Figure 4.3-7, respectively. In Figure 4.3-6, the HEU peak power envelopes as well as the evolution of the local spots values that allow the construction of the envelope are presented. It can be seen that the peak value is first encountered on the outer edge mid-plane but become dominated by the power on the outer edge top afterwards. Towards the end of cycle, the location of the peak power changes between the bottom outer edge and bottom inner edge.

The LEU peak power envelope is presented in Figure 4.3-7. It can be seen that the peak power is located on the outer edge mid-plane from BOC to about mid-cycle. Afterwards, the peak power value is located on the same edge but at the very top of the fuel once the boron of the poison belt is sufficiently depleted.

The peak power envelopes of the HEU and LEU cores are compared in Figure 4.3-8. It can be seen that despite some local change in shape, both profiles are relatively similar. For both cores, the maximum value is obtained at day 1 and worth 14.4 and 14.8 W/mm^3 for the HEU and LEU cores, respectively.

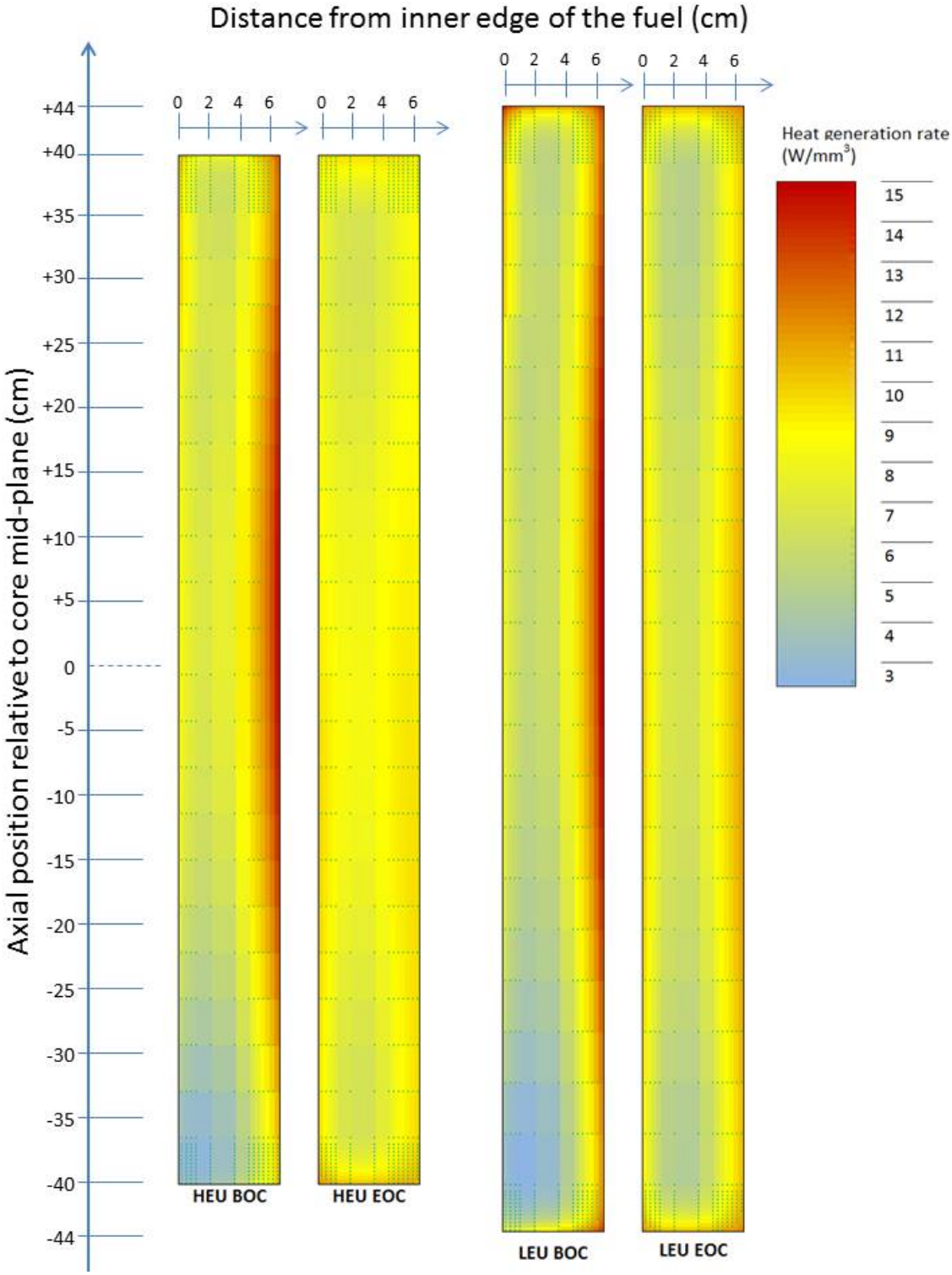

Figure 4.3-3 – 2D representation of the power density in the fuel; from left to right, HEU BOC, HEU EOC, LEU BOC and LEU EOC; calculated relative error is less than 0.25% at BOC and estimated at 10% at EOC

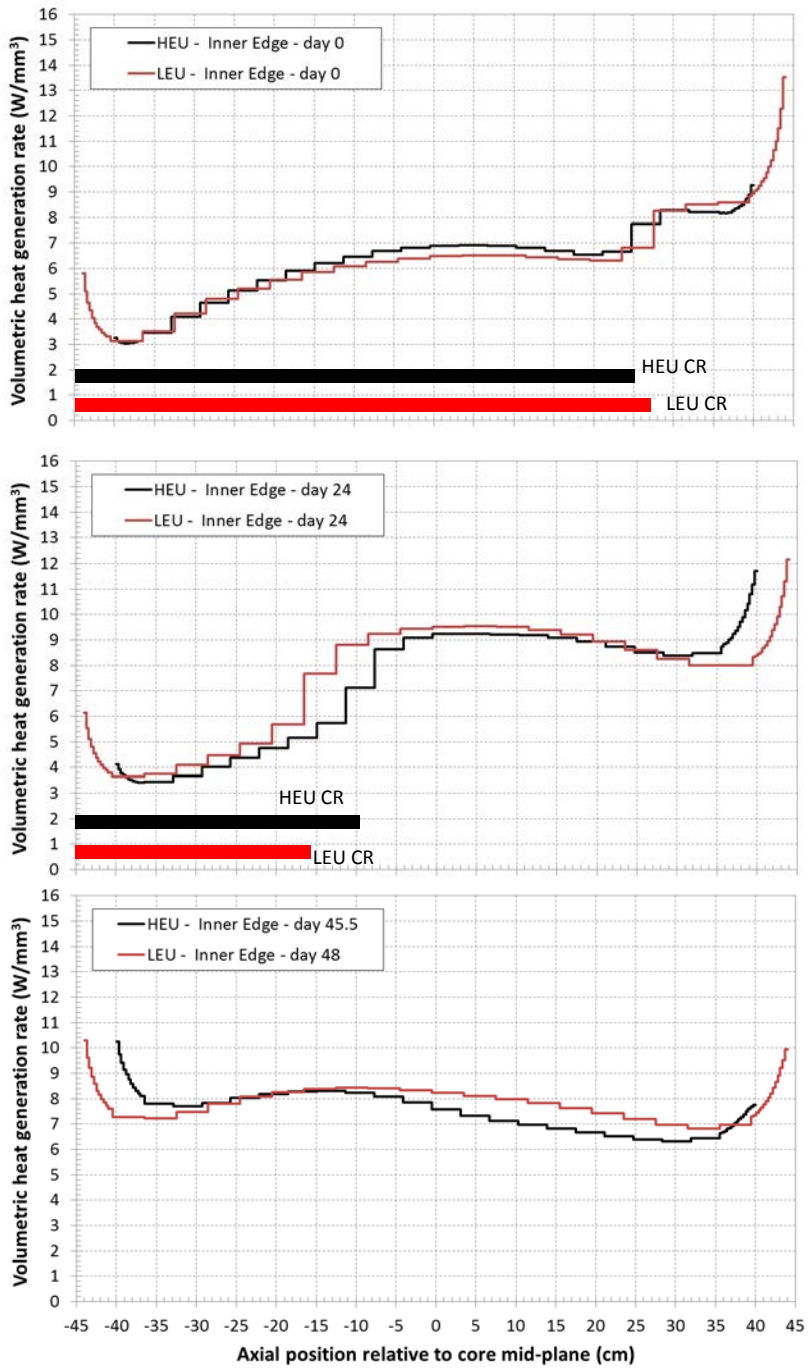

Figure 4.3-4 – Power density axial profile in the inner edge of the fuel element; from top to bottom: at BOC, at day 24 and at EOC; calculated relative error is less than 0.25% at BOC and estimated at 10% otherwise. Position of the HEU and LEU core control rod is represented with a black and red rectangle, respectively.

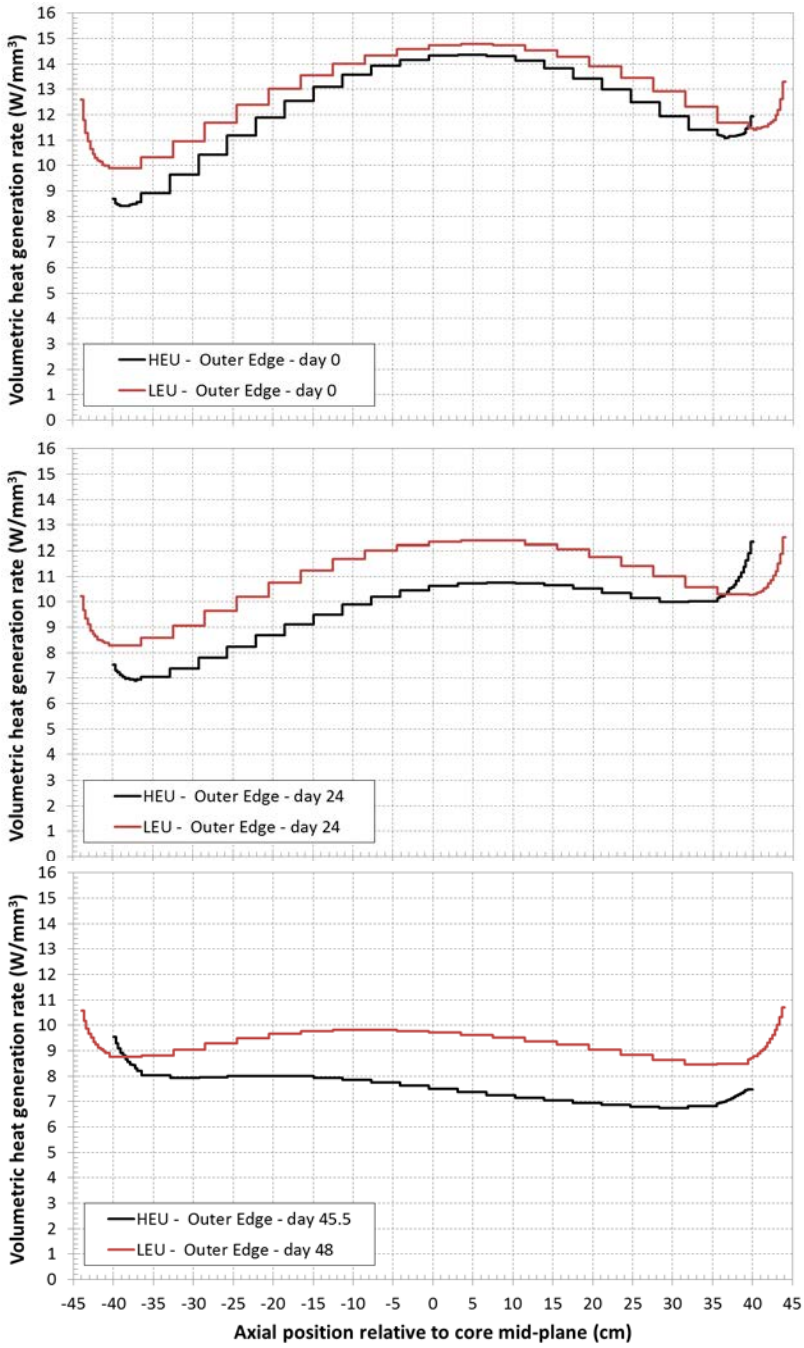

Figure 4.3-5 – Power density axial profile in the outer edge of the fuel element; from top to bottom: at BOC, at day 24 and at EOC; calculated relative error is less than 0.25% at BOC and estimated at 10% otherwise

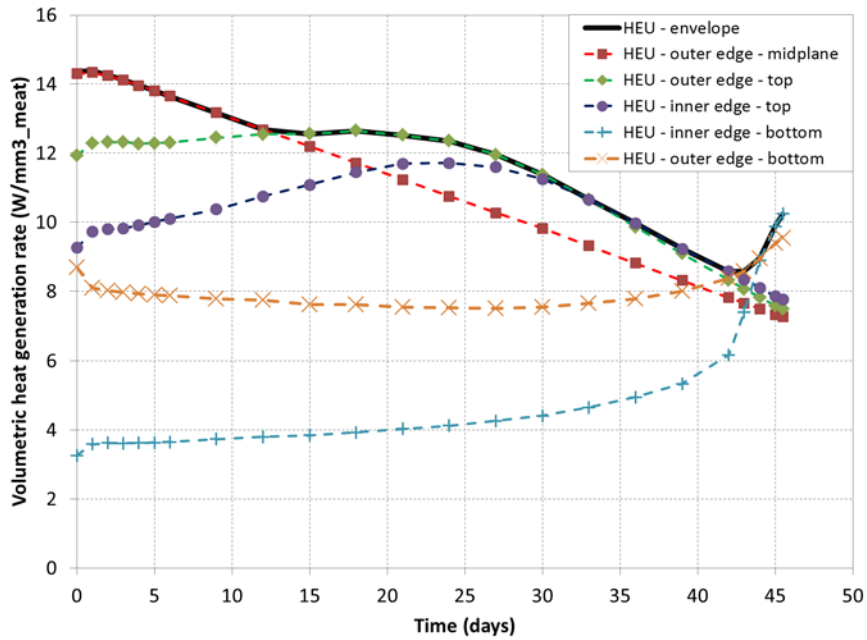

Figure 4.3-6 – Evolution of the power density at different location and resulting power density envelope in HEU core; calculated relative error is less than 0.25% at BOC and estimated at 10% otherwise

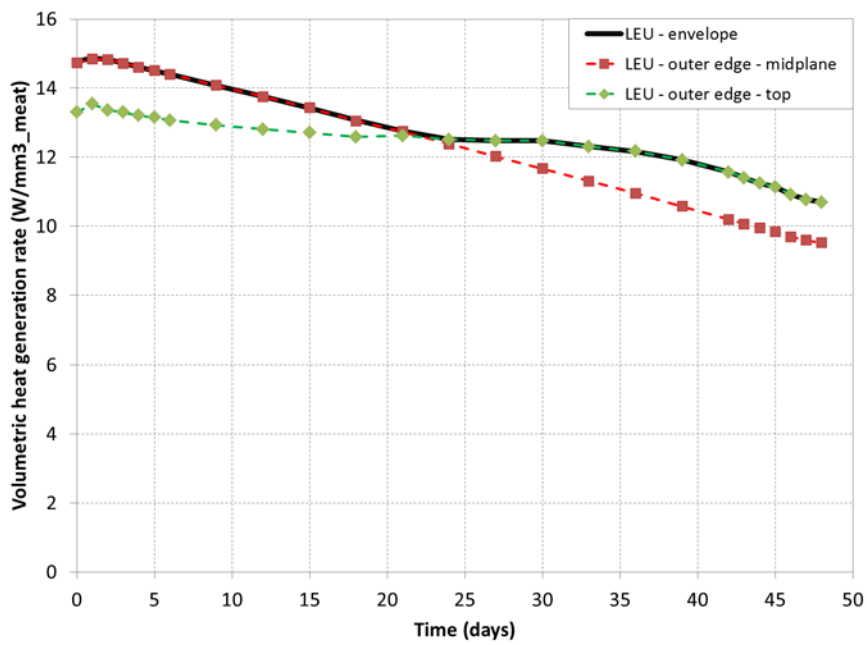

Figure 4.3-7 – Evolution of the power density at different location and resulting power density envelope in LEU core; calculated relative error is less than 0.25% at BOC and estimated at 10% otherwise

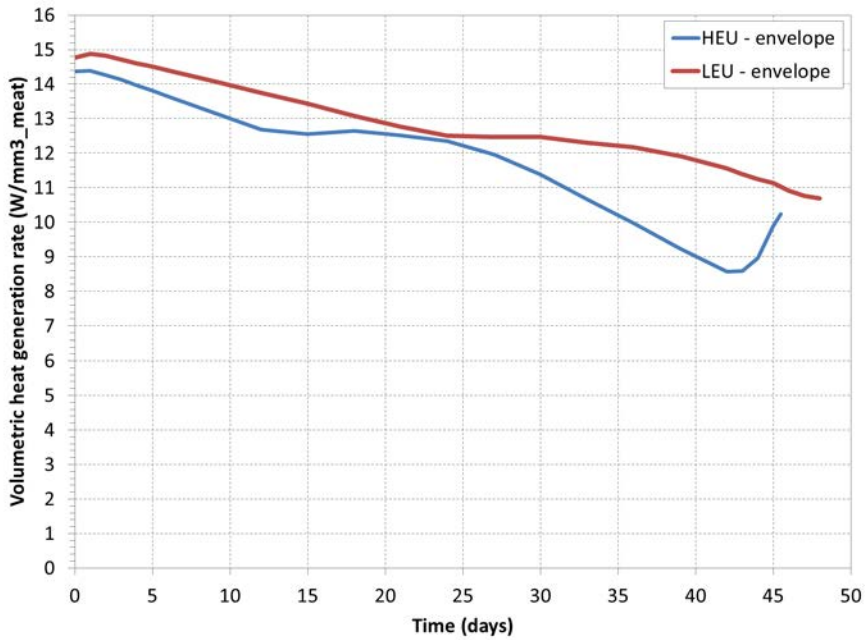

Figure 4.3-8 – Power density envelope for HEU and LEU cores; calculated relative error is less than 0.25% at BOC and estimated at 10% otherwise

4.4. In-Pile Reactivity Worth & Feedback Coefficient

The following section provides the reactivity worth of the different in-pile components. Table 4.4-1 below summarizes the most important values and the following sub-sections described in more detailed the reactivity worth of the sources and beam tubes, the evaluation of the power defect, the reactivity of the control element worth and the shutdown margins.

In Table 4.4-1 it can be seen that at BOC, when the control element (CE) is completely inserted, the reserve of negative reactivity for both cores is above 3000 pcm and thus largely exceed the required 2000 pcm. The overall core reactivity worth is about 13000 pcm for the HEU core and about 1500 pcm less for the LEU core. Despite the larger mass of ^{235}U in the LEU core, the presence of larger fraction of ^{238}U explains the difference. The worth of the control element is evaluated at 16850 pcm for the HEU core which is slightly less than the 17200 pcm reported in [SAR, 2004]. The origin of the discrepancy is not understood but small enough to be ignored for the present study. For the LEU core, the control element reactivity worth is about 1700 pcm less. The worth of the borated poison belt is about half the worth of the HEU borated regions. The difference is first explained by the difference of mass: there is only 3.25 g of ^{10}B in the LEU poison belt whereas there is 5.77 g of ^{10}B in the HEU core borated regions. Moreover, the LEU core poison belt is located further away from the fuel region than the HEU core borated regions. The void coefficient is negative for both the HEU and LEU cores but its magnitude is reduced significantly in the LEU core. For both the HEU and LEU cores, the temperature coefficients are negative everywhere except in the central cavity where it is slightly positive (about +1 pcm/K).

Table 4.4-1 – Reactivity worth of in-pile components and temperature and void coefficient; relative error is less than 1% at one standard deviation

parameter	HEU	LEU
Reactivity at BOC when CE fully inserted, all SR fully withdrawn (cold)	-3546	-3290
Core reactivity at BOC (no CE, cold)	13029	11592
Control element worth at BOC (cold)	16852	15119
Borated zone worth at BOC (cold)	3874	1998
All experimental devices BOC (cold) [a]	5477	5120
Power defect (from cold to full power conditions) [b]	-240	-252
Void coefficient (pcm/cm^3/%void) [c]		
- Heavy water fuel element	-0.00232	-0.00118
- Heavy water reflector	-0.00034	-0.00025
- Heavy water entire reactor	-0.00144	-0.00086
Temperature coefficient (pcm/K)		
- Reflector (average value between 293 and 323K)	-8.3	-5
- Heavy water fuel element (average value between 293 and 323K)	-1.6	-2.4
- Chimney + central cavity (average value between 293 and 303K)	+1.3	+1.2
- Fuel (average value between 293 and 393K)	-0.4	-1.9

[a] Individual experimental device worth is presented below

[b] More details are provided below

[c] Void coefficient have been calculated assuming a heavy water volume of 51.5cm^3 in the fuel element, 10.3m^3 in the reflector and 11.0m^3 total replaced entirely by void.

4.4.1. Experimental Device Worth

The experimental device worth (beam tubes and hot/cold sources) has been calculated for both the HEU an LEU core in cold conditions.

The temperature effect on the device reactivity has been calculated for the HEU core only and is presented in Figure 4.4-1 below. The calculation has been carried out in "cold" conditions (reactor at room temperature) and at full power (hot) conditions. It can be seen on the figure that for most of the experimental devices, the difference between "cold" and "hot" is small. The only noticeable variation is for the hot source (about 100 pcm). This is explained by the very large difference of temperature that the passage of full power implies for this device; at full power the hot source temperature is at 2400 K which is about 2100 K above the temperature in "cold" condition. For all the other devices, the passage from "cold" to "hot" condition does not lead to a change in temperature except for their environment (reflector, fuel element…) which experiences a modest temperature increase of about 30 K.

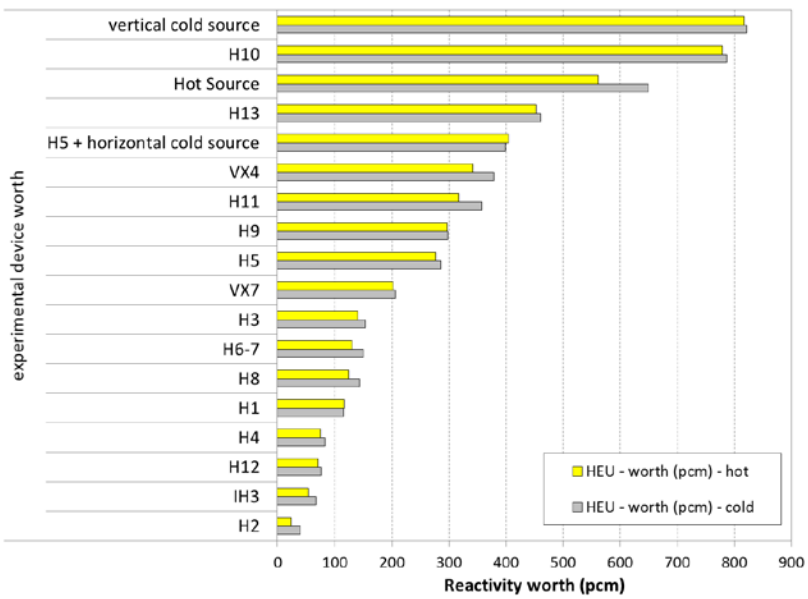

Figure 4.4-1 – Reactivity worth of the HEU core in-pile experimental devices in cold and hot conditions; relative error is less than 15 pcm at one standard deviation

The comparison between HEU and LEU has been carried out in "cold" condition since this is the state that leads to the higher reactivity worth. The comparison between the HEU and LEU experimental device reactivity worth is presented on Figure 4.4-2. In all cases, it can be seen that the LEU reactivity worths are slightly lower than for the HEU. The variation is almost negligible for most of them. The biggest variation is found for the beam tube H10 (about 70 pcm).

A guillotine type rupture of the beam tube is not considered plausible in the safety analysis. Only the beam tube flooding is considered possible. The scenario considers that a break appears in a beam tube (reflector side) which leads to its filling by heavy water (the beam tube structure is still in place). The reactivity worth of the beam tubes in these conditions has been calculated. The results are presented in

Figure 4.4-3 below. It can be seen that the reactivity worth reduction in the HEU core is significant whereas it is relatively modest in the LEU core. Nonetheless, the maximum reactivity worth (beam tube H10 flooded) is less than one dollar (even when the contribution of the photofission, estimated at 33 pcm, is not included).

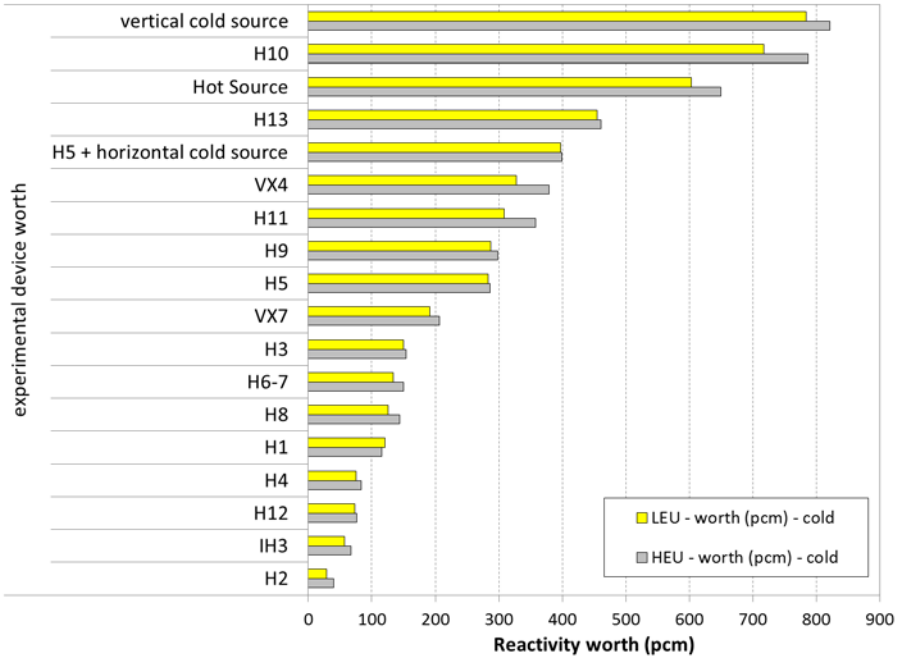

Figure 4.4-2 – Reactivity worth of the HEU and LEU cores in-pile experimental devices in cold conditions; relative error is less than 15 pcm at one standard deviation

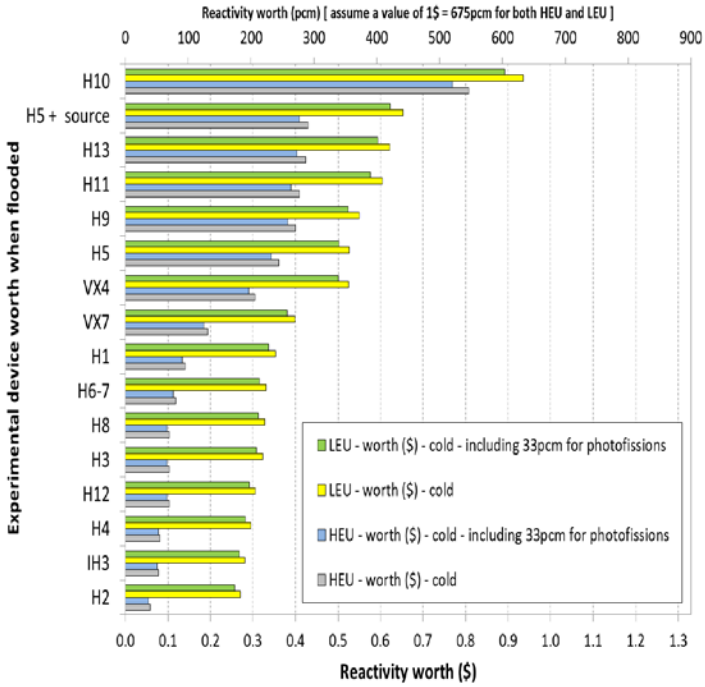

Figure 4.4-3 - Reactivity worth of the HEU and LEU cores flooded beam tubes in cold conditions; relative error is less than 15 pcm at one standard deviation

4.4.2. Power Defect

The effect on the core reactivity of going from room teperature to full power condition has been analysed in detail. The results are presented in Figure 4.4-4 presented below. The effect has been studied at different location for the coolant and for the different type of in-pile components. For each category, the temperature effect on the material density (later simply referred as density), the temperature effect on cross-sections and S(α,β) (later simply referred as cross-section and S(α,β)) and elastic scattering cross section (later simply referred as elastic) is studied separately and in combination. To study the doppler effect, specific sets of isotope cross-section and S(α,β) have been generated using the software makxsf [LANL, 2006] that correpsonds to the specific set of temperature found in the reactor at full power (described in Section 2.3).

Regarding the heavy water, for both HEU and LEU, the cross-section and S(α,β) combined effect is always positive. Except in the heavy water of the LEU fuel element, the elastic one is also positive. The magnitude of both effect is however relatively small compared to the density effect which is strongly negative in the reflector and in the fuel element. It is however relatively small in the central cavity. As a result, the combined effect for all the in-pile heavy water is strongly negative (density strongly negative, elastic and cross-section and S(α,β) positive). There is a relatively large difference between the HEU and LEU cores which worth -260 and -165 pcm, repsectively.

For the structures, it is assumed that the temperature increase does not lead to a change of the material density. For both the HEU and LEU cores, the elastic effect is slightly positive and the cross-section and S(α,β) negative. The cross-section and S(α,β) of the LEU core is significantly larger (-150 pcm) than for the HEU one (-32 pcm). For both cores, the combined effect is largely negative. The significant temperature increase in the hot source (about 2100 K) makes this relatively large volume considerably less absorbing which increases the core reactivity noticeably. It is not surprising to see that the cross-section and S(α,β) effect contribution is largely positive: +140 pcm for the HEU core and +65 for the LEU one. The combined effect for the others structures (e.g. beam tubes), for which the temperature increase is very modest (about 30 K) is completely negligible.

Overall, considering the entire reactor, the combined effect is negative: -240 pcm for the HEU core and -250 pcm for the LEU one. The density effect in the heavy water reflector plays without any doubt the major contribution to the overall negative reactivity. For the LEU core, both the elastic and cross-section and S(α,β) effect are negative. The HEU core sees a small positive elastic effect and a modest negative effect due to the cross-section and S(α,β) change.

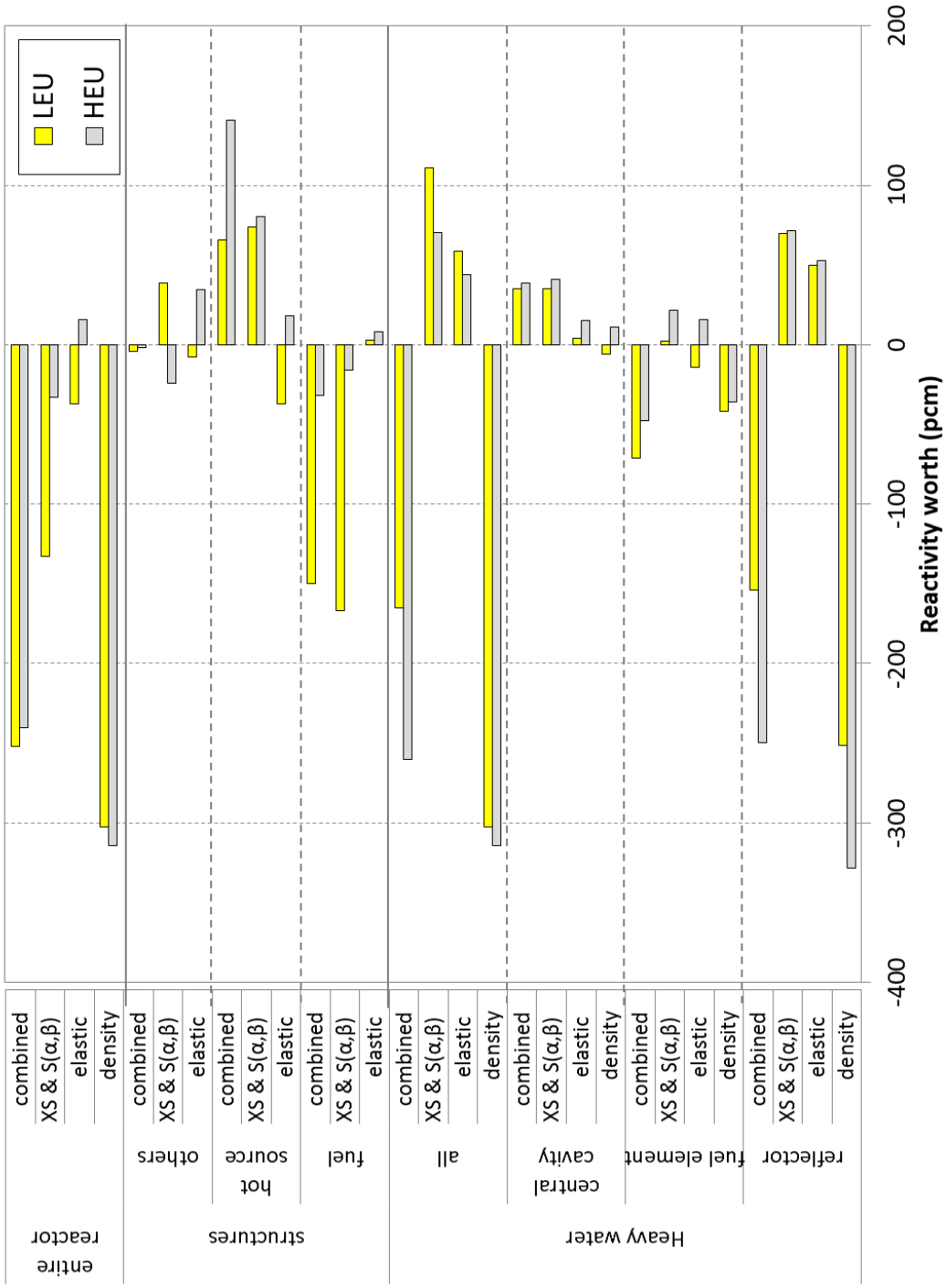

Figure 4.4-4 – Reactivity change due to passage from cold to full power conditions; relative error is less than 15 pcm at one standard deviation

4.4.3. Control Element Differential Worth

The differential worth of the control element (CE) has been calculated for both cores at BOC and also during irradiation to include the effect of the depletion of the core. Results are presented on Figure 4.4-5 below.

For both cores, the shape of the differential worth is similar: it starts to increase when the control element is withdrawn, peaks when the CE is about 35-50 cm withdrawn and starts to decrease afterwards. HEU and LEU cores CE differential worth is relatively identical except in the peak region where the HEU one is about 50 pcm/cm higher than the LEU one. For both cores, the effect of the core depletion is relatively modest. It tends to increase the control element worth by about 25 pcm/cm. Close to the fully withdrawn position (101.5 cm), the LEU core CE differential worth is higher than in the HEU core due to the fuel length extension. In the HEU core, at this position, the CE is already far away from the fuel and relatively inefficient.

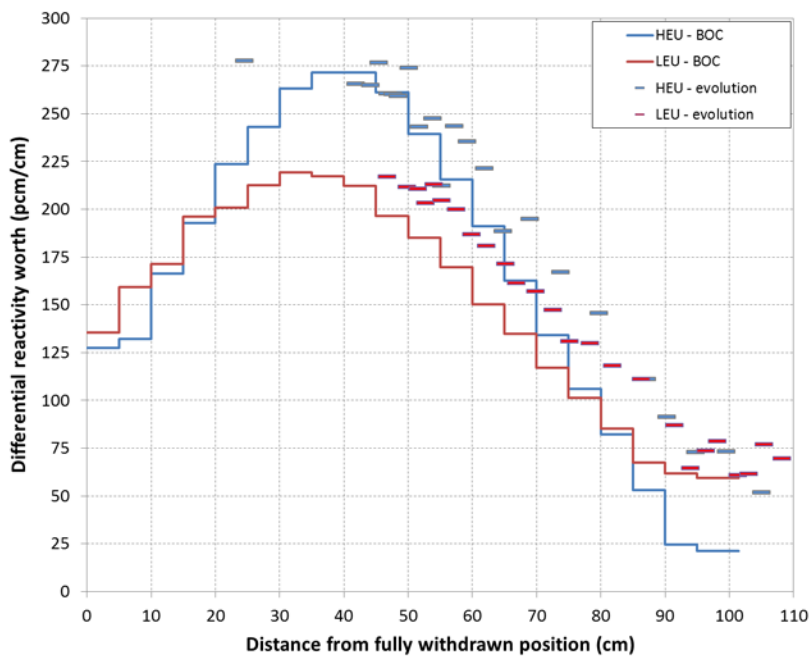

Figure 4.4-5 – Differential worth of the control element; relative error is less than 15 pcm at one standard deviation

4.4.4. Safety Rods Worth & Shutdown Margins

Five safety rods surrounds the fuel element. During normal operation, they are located above the fuel element. When a SCRAM is initiated, the five safety rods fall and encircle very closely the fuel element. All accident scenario studied in the safety analysis consider that the most efficient rod stay stuck in its fully withdrawn position during the SCRAM.

4.4.4.1. Model Credibility

Prior to the start of cycle 143, nine critical configurations were tested with at least one safety rod fully inserted. Starting at the fully inserted position, the control rod was then progressively withdrawn until criticality was achieved, followed by stabilization of the power at few kilowatts. The nine configurations are described in Table 4.4-2 provided below. An extensive uncertainty propagation analysis has been carried out for this experiment and results have been published in [NEA, 2011]. It has been concluded that, for these configurations, the uncertainties were relatively small and well understood and this experiment could be accepted as benchmark data. For each configuration, the combination of all calculated uncertainties (materials, geometry, and temperature) was estimated at +234/-231 pcm at one standard deviation (1σ).

In order to verify that the modifications made to the neutronics model did not introduce significant errors, each experimental configuration has been modeled. K-effective results are presented in Table 4.4-3. All results are in good agreement with the benchmark which indicates that the safety rod modeling is credible.

Table 4.4-2 - Critical configurations tested prior to cycle 143

case number	configuration	measured critical control rod position (cm withdrawn)
1	All safety rods (SR) up	24.92 ± 0.2
2	SR1 inserted	52.06 ± 0.2
3	SR2 inserted	48.20 ± 0.2
4	SR3 inserted	48.88 ± 0.2
5	SR4 inserted	49.93 ± 0.2
6	SR5 inserted	45.73 ± 0.2
7	SR1 + SR2 inserted	67.95 ± 0.2
8	SR1 + SR5 inserted	87.05 ± 0.2
9	SR1 + SR4 inserted	No criticality

Table 4.4-3 - Results of the modeling of the critical configurations tested prior to cycle 143

case number	configuration	calculated k-effective	Benchmark k-effective	(C-E)/E (pcm)
1	All safety rods up	1.00259 ± 7 pcm	1.00000 (+234/-231 pcm)	259
2	SR1 inserted	1.00221 ± 7 pcm	1.00000 (+234/-231 pcm)	221
3	SR2 inserted	1.00033 ± 7 pcm	1.00000 (+234/-231 pcm)	33
4	SR3 inserted	1.00056 ± 7 pcm	1.00000 (+234/-231 pcm)	56
5	SR4 inserted	1.00290 ± 7 pcm	1.00000 (+234/-231 pcm)	290
6	SR5 inserted	1.00139 ± 7 pcm	1.00000 (+234/-231 pcm)	139
7	SR1 + SR2 inserted	1.00263 ± 7 pcm	1.00000 (+234/-231 pcm)	263
8	SR1 + SR5 inserted	1.00171 ± 7 pcm	1.00000 (+234/-231 pcm)	171
9	SR1 + SR4 inserted	0.93295 ± 7 pcm	no criticality	does not apply

4.4.4.2. Reactivity Worth of the Four Less Efficient Safety Rods

Figure 4.4-6 below presents the evolution of the core reactivity with the distance of insertion of the four less efficient safety rods. The calculations have been carried out at BOC, the control element at critical position and “cold” conditions. It can be seen that the HEU and LEU cores reactivity evolution profile is very similar. The only noticeable difference is at the fully inserted position, for which the worth of the safety rods in the LEU core is smaller than for the HEU core. This is probably explained by the larger fuel length of the LEU core. It can be seen that once 34 cm inserted (which takes 0.116 s), the core reactivity is already reduce by more than 1500 pcm. Once 70 cm inserted (which takes less than 0.2 s), the core reactivity drop is about the same order of magnitude than the the initial core reactivity (about 13000 pcm for HEU and 11500 pcm for LEU).

For safety analysis, the worst case must be considered. The currently selected configuration considers than the most reactive beam tube (H10, see Section 4.4.1) is flooded. The above calculations have been repeated considering H10 completely flooded. On Figure 4.4-6 the results are shown as dots. It can be seen that the flooding of H10 leads to essentially the same results than before and does not have a meaningful impact. This is explained by the efficient configuration of the safety rods which encircle very closely the core and screen significantly the fuel element from the reflector.

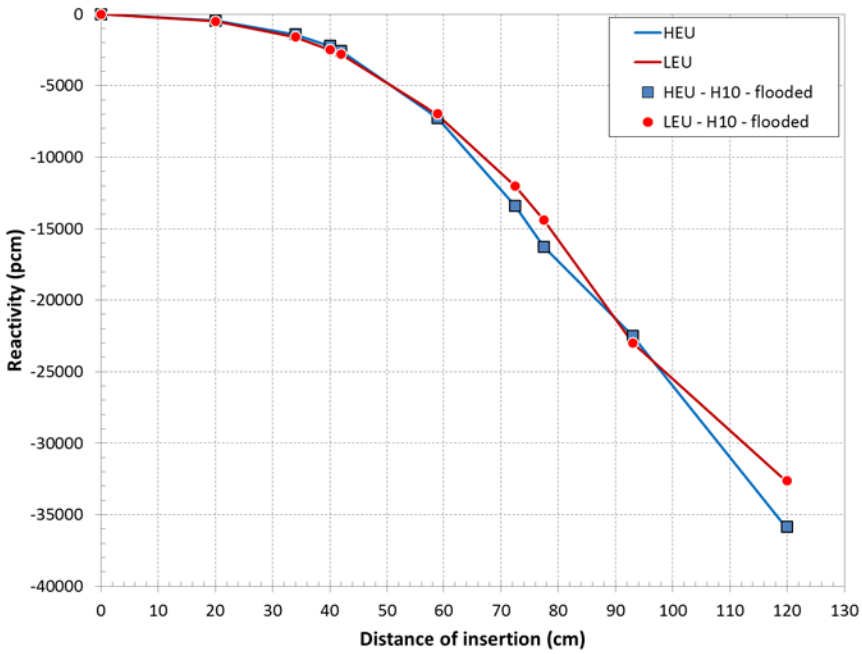

Figure 4.4-6 – Reactivity change due to the insertion of the four less efficient safety rods; relative error is less than 40 pcm at one standard deviation

5. Conclusions

The present report was intended to provide a description of the ILL RHF neutronics results obtained with the MCNP model of the U7Mo LEU reference design element that has been established in 2010 during the feasibility analysis. The motivation to produce these analyses came from the fact that the neutronics model has been improved significantly since 2010 and the release of the feasibility report. Since then, neutronics description of the LEU design has been established but never published in a complete and concise manner.

The changes applied to the neutronics model lead to better comparison with experimental data or improved the calculation efficiency but do not challenge the conclusion of the feasibility analysis. If the U7Mo fuel is commercially available, not cost prohibitive, a back-end solution is established and if it is possible to manufacture the proposed element, neutronics analyses show that the performance of the reactor would not be challenged by the conversion to LEU fuel.

The use of MCNP to perform the neutronics analysis is a significant change in the codes and methodologies used so far to perform neutronics calculations. Demonstrate the credibility of the MCNP neutronics model is a key mission for the conversion project of the RHF. In this report, credibility of the model has been tested whenever it was possible. Except for the neutron lifetime which is predicted to be 20% higher than the reference value reported in the SAR, all other compared parameters have been found to be in relative good agreement with the experimental data. Nonetheless, the sources of information used to build the comparisons are relatively poor in details. However a lot of details are provided on the critical experiment FOEHN which was an almost identical full size mockup of the RHF core. In order to strengthen the neutronics model credibility and mitigate the regulatory risk related to the introduction of new codes and methodologies, the authors recommend in future work modeling the FOEHN experiment and benchmark the calculated results to the large and well detailed sets of experimental data available.

The reference design requires the insertion of an annular borated region located almost immediately above the fuel plates. Its purpose is to reduce the power peaking on the outer edge of the fuel (facing the reflector) and to provide additional reactivity margin at BOC. To remain under the expected qualification limit, the density of ^{10}B in the so-called poison belt must be increased by a factor of four compared to the current HEU core borated region. Because the consumption of ^{10}B can lead to significant swelling and because the poison belt design has not been tested in-pile, it cannot be guaranteed, to date, that the reference absorber design would not lead to unacceptable swelling/failure. One way to reduce the risk is to find credible alternative design solutions. Future work is expected to focus on this topic.

References

[ANL, 1997] M. M. Bretscher: *"Perturbation-Independent Methods For Calculating Research Reactor Kinetic Parameters"*, Argonne National Laboratory, ANL/RERTR/TM-30, 1997.

[ANL, 2010] A. Bergeron, A. Tentner, J.G. Stevens: "*Feasibility Analyses for HEU to LEU Fuel Conversion of the Laue-Langevin Institute (ILL) High Flux Reactor (RHF)*", Argonne National Laboratory, ANL/RERTR/TM-10-21, 2010.

[ANL, 2012] A. Bergeron: "*Review of the Oak Ridge National Laboratory (ORNL) Neutronic Calculations Regarding the Conversion of the High Flux Reactor (HFIR) to the Use of Low Enriched Uranium (LEU) Fuel*", Argonne National Laboratory, ANL/RERTR/TM-12-49, 2012.

[ANL, 2014a] A. Bergeron, B. Dionne, J. Licht, Y. Calzavara, F. Thomas, H. Guyon, V. Caillot: *"Review of the Safety Analysis Report (RSAR) of the RHF for Establishing Conversion Analysis Scope*", Argonne National Laboratory, ANL/GTRI/TM-14/9.

[Anselmet, 2013] M-C. Anselmet, M. Ripert, P. Lemoine, E. Koonen, W. Claes, F. Geens, S. Van Den Berghe: *"Qualification of the JHR Fuel Element Under JHR Operating Conditions",* Proceedings of the European Research Reactor Conference (RRFM), 2014, St-Petersburg, Russia.

[Engauge, 2014] Engauge Digitizer – Digitizing Software website: http://digitizer.sourceforge.net/

[GTRI, 2014] Global Threat Reduction Initiative (GTRI) website: http://nnsa.energy.gov/aboutus/ourprograms/dnn/gtri

[Hanson, 2006] A. L. Hanson, Hans Ludewig, David J. Diamond: *"Calculation of the Prompt Neutron Lifetime in the NBSR"*, Nuclear Science and Engineering, vol. 153, pp. 26-32, 2006.

[ILL, undated] K. Scharmer, G. Eckert: "FOEHN L'expérience critique pour le réacteur Franco-Allemand", Institut Laue-Langevin, report reference and publication date unknown.

[ILL, 2008] Institut Laue-Langevin (ILL): *"The Yellow Book: Guide to the Neutron Research Facilities"*, 2008. http://www.ill.eu/fr/instruments-support/instruments-groups/yellowbook/

[ILL, 2009] Y. Calzavara: private communication (2009)

[IRSN, 2008] W. Haeck: *"Vesta User's Manual Version 2.0.0"*, Institut de Radioprotection et de Sûreté Nucléaire, DSU/SEC/T/2008-331 – Index A, 2008.

[Kim, 2011] Y. S. Kim, G. L. Hofman: *"Fission products induced swelling of U-Mo allow fuel"*, Journal of Nuclear Materials, vol. 419, 2011.

[Kim, 2013] Y. S. Kim, G. L. Hofman, H. J. Ryu, J. M. Park, A. B. Robinson, D. M. Wachs: *"Modeling of interaction layer growth between U-Mo particles and Al matrix"*, Nuclear Engineering and Technology, vol. 45 no7, pp. 827-838, 12/2013.

[LANL, 2006] F. B. Brown: "The makxsf Code with Doppler Broadening", Los Alamos National Laboratory, LA-UR-06-7002, 2006.

[LANL, 2008a] X-5 Monte Carlo Team: *"MCNP – A General Monte Carlo N-Particle Transport Code, Version 5 Volume II: User's Guide"*, Los Alamos National Laboratory, LA-CP-03-0245, 2/1/2008 revision.

[LANL, 2008b] X-5 Monte Carlo Team: *"MCNP – A General Monte Carlo N-Particle Transport Code, Version 5 Volume I: Overview and Theory"*, Los Alamos National Laboratory, LA-CP-03-1987, 2/1/2008 revision.

[LANL, 2011] B. C. Kiedrowski: *"Adjoint Weighting Methods Applied to Monte Carlo Simulations of Applications and Experiments in Nuclear Criticality"*, Los Alamos National Laboratory, LA-UR-14-21608, 3/11/2014, intended for University of Michigan seminar.

[NEA, 2011] Y. Calzavara, S. Fuard, A. Bergeron: *"Evaluation of Measurements Performed on the French High Flux Reactor (RHF)"*, OECD-NEA report, NEA/NSC/DOC(2006)1, rev. 3, 2011.

[NIST, 2014a] National Institute of Standards and technology (NIST), thermophysical properties of fluid systems website: http://webbook.nist.gov/chemistry/fluid/

[NIST, 2014b] National Institute of Standards and technology (NIST), atomic weights and isotopic composition website: http://www.nist.gov/pml/data/comp.cfm

[ORNL, 2012] A. G. Croff, S. Ludwig: *"RSICC Computer Code Collection - Origen 2.2 – Isotope Generation and Depletion Code Matrix exponential Method"*, Oak Ridge National Laboratory, CCC-371/ORIGEN 2.2, 06/2002.

[RERTR, 2014] Reduced Enrichment for Research and Test Reactors (RERTR) website: http://www.rertr.anl.gov/

[SAR, 2004] Institut Laue-Langevin: "*Réacteur à Haut Flux – INB n°67 – Rapport de Sûreté*", 03/2004.

[Villele, 2008] E. de Villele, J. C. Lee, G. Yesilyurt, W. Ji : *"Estimation of the Spatial Distribution of Fission Energy Deposition in a VHTR with (only) MCNP5 - How to perform fission energy deposition calculations with standard MCNP tallies with application to a full core VHTR configuration",* PHYSOR 2008 Monte Carlo workshop, Interlaken, Switzerland, 09/2008. Published by Los Alamos National Laboratory under reference LA-UR-08-05891.

[Vised, 2014] MCNP Visual Editor website: http://www.mcnpvised.com/

Appendices

A1. Tabulated Values of Section 4.1

Table A1 - 1 – Cycle 143 experimental and calculated critical control element position

Cycle 143 experimental data		Cycle 143 - calculated results			
time (days)	CE distance from fully withdrawn position (cm)	time (days)	CE distance from fully withdrawn position (cm)	k-effective	k-effective uncertainty (pcm, 1σ)
0	71.86	**0**	76.58	1.00060	20
1	58.83	**1**	59.35	1.00128	20
2	56.59	**2**	57.28	0.99951	21
3	55.38	**3**	55.49	1.00133	18
4	54.48	**4**	54.70	1.00019	20
5	53.65	**5**	53.73	1.00045	20
6	52.91	**6**	52.74	1.00111	18
7	53.29	**9**	50.72	1.00085	18
8	51.88	**12**	49.15	1.00040	19
9	51.27	**15**	47.64	1.00007	19
10	50.71	**18**	45.85	1.00050	19
11	50.15	**21**	44.02	0.99994	19
12	49.55	**24**	42.01	1.00015	19
14	48.51	**27**	39.48	0.99989	20
16	47.47	**30**	36.41	0.99929	20
18	46.36	**33**	32.82	0.99864	18
20	45.16	**36**	27.79	0.99904	21
22	43.98	**39**	22.17	0.99868	19
24	42.46	**42**	14.29	0.99872	18
26	40.71	**43**	10.36	0.99927	20
28	38.66	**44**	6.56	0.99855	17
30	36.39	**45**	2.59	0.99852	19
32	33.95	**46**	-2.75	0.99876	18
34	30.92				
36	27.48				
38	24.06				
40	19.39				
42	13.8				
43	10.75				
44	6.54				
45	1.88				
45.5	0.01				

Table A1 - 2 – Calculated critical control rod position for HEU and LEU reference design core depleted at a constant power of 57.8 MW and without beam tube IH4

HEU full power (57.8MW) - no IH4				LEU full power (57.8MW) - no IH4			
time (days)	**CE distance from fully withdrawn position (cm)**	**k-effective**	**k-effective uncertainty (pcm, 1σ)**	**time (days)**	**CE distance from fully withdrawn position (cm)**	**k-effective**	**k-effective uncertainty (pcm, 1σ)**
0	77.12	0.99976	6	**0**	78.56	1.00071	5
1	59.70	1.00078	6	**1**	58.84	0.99981	5
2	57.44	0.99968	6	**2**	55.70	0.99963	5
3	56.17	0.99966	5	**3**	54.01	0.99991	5
4	54.77	1.00064	5	**4**	52.86	0.99947	5
5	53.99	1.00032	5	**5**	51.57	0.99979	5
6	53.19	1.00022	6	**6**	50.38	1.00002	5
9	51.51	0.99954	6	**9**	48.10	0.99935	5
12	49.87	0.99944	5	**12**	45.63	0.99921	5
15	47.79	1.00061	5	**15**	43.35	0.99902	5
18	46.37	0.99999	5	**18**	40.38	1.00003	5
21	44.42	1.00031	6	**21**	38.67	0.99887	5
24	42.40	0.99999	5	**24**	35.72	0.99951	5
27	39.76	0.99996	5	**27**	32.98	0.99967	5
30	36.83	0.99931	5	**30**	30.42	0.99918	5
33	32.60	0.99981	5	**33**	27.21	0.9993	5
36	27.82	0.99983	5	**36**	23.79	0.99914	5
39	21.89	0.99977	5	**39**	19.28	0.99927	5
42	14.39	0.99935	5	**42**	14.08	0.99916	5
43	11.29	0.99905	5	**43**	11.56	0.99928	5
44	6.86	0.99915	5	**44**	9.20	0.9993	5
45	2.10	0.99936	5	**45**	7.38	0.99902	5
45.5	0.00	0.99890	5	**46**	4.25	0.99965	5
				47	2.57	0.9991	5
				48	0.00	0.99769	5

Table A1 - 3 – Calculated fission rate for HEU and LEU reference design core depleted at a constant power of 57.8 MW and without beam tube IH4

HEU core fission rate (fission/cc_meat/s)					LEU reference design core fission rate (fission/cc_meat/s)				
time (days)	core average	^{235}U core average	peak (envelope)	^{235}U peak (envelope)	time (days)	core average	^{235}U core average	peak (envelope)	^{235}U peak (envelope)
0	2.32E+14	2.32E+14	5.07E+14	5.07E+14	**0**	2.11E+14	2.09E+14	5.15E+14	5.12E+14
1	2.32E+14	2.32E+14	5.06E+14	5.06E+14	**1**	2.11E+14	2.09E+14	5.17E+14	5.14E+14
2	2.32E+14	2.32E+14	5.02E+14	5.02E+14	**2**	2.11E+14	2.09E+14	5.15E+14	5.11E+14
3	2.32E+14	2.32E+14	4.96E+14	4.96E+14	**3**	2.11E+14	2.08E+14	5.11E+14	5.07E+14
4	2.32E+14	2.32E+14	4.91E+14	4.91E+14	**4**	2.11E+14	2.08E+14	5.08E+14	5.03E+14
5	2.32E+14	2.32E+14	4.86E+14	4.86E+14	**5**	2.11E+14	2.08E+14	5.04E+14	4.98E+14
6	2.32E+14	2.32E+14	4.80E+14	4.80E+14	**6**	2.11E+14	2.08E+14	5.00E+14	4.93E+14
9	2.32E+14	2.32E+14	4.63E+14	4.62E+14	**9**	2.11E+14	2.07E+14	4.89E+14	4.79E+14
12	2.32E+14	2.32E+14	4.46E+14	4.45E+14	**12**	2.11E+14	2.06E+14	4.76E+14	4.63E+14
15	2.32E+14	2.32E+14	4.44E+14	4.43E+14	**15**	2.11E+14	2.05E+14	4.65E+14	4.49E+14
18	2.32E+14	2.32E+14	4.46E+14	4.45E+14	**18**	2.11E+14	2.04E+14	4.53E+14	4.34E+14
21	2.32E+14	2.32E+14	4.43E+14	4.42E+14	**21**	2.11E+14	2.03E+14	4.42E+14	4.26E+14
24	2.32E+14	2.32E+14	4.35E+14	4.34E+14	**24**	2.11E+14	2.02E+14	4.36E+14	4.20E+14
27	2.32E+14	2.31E+14	4.21E+14	4.20E+14	**27**	2.11E+14	2.01E+14	4.36E+14	4.18E+14
30	2.32E+14	2.31E+14	4.02E+14	4.00E+14	**30**	2.11E+14	2.00E+14	4.36E+14	4.16E+14
33	2.32E+14	2.31E+14	3.76E+14	3.75E+14	**33**	2.11E+14	1.99E+14	4.31E+14	4.09E+14
36	2.32E+14	2.31E+14	3.52E+14	3.50E+14	**36**	2.11E+14	1.98E+14	4.26E+14	4.02E+14
39	2.32E+14	2.31E+14	3.26E+14	3.24E+14	**39**	2.11E+14	1.98E+14	4.15E+14	3.90E+14
42	2.32E+14	2.31E+14	3.03E+14	3.02E+14	**42**	2.11E+14	1.97E+14	4.03E+14	3.76E+14
43	2.32E+14	2.31E+14	3.02E+14	3.01E+14	**43**	2.11E+14	1.97E+14	3.98E+14	3.71E+14
44	2.32E+14	2.31E+14	3.16E+14	3.15E+14	**44**	2.11E+14	1.96E+14	3.92E+14	3.65E+14
45	2.32E+14	2.31E+14	3.50E+14	3.48E+14	**45**	2.11E+14	1.96E+14	3.87E+14	3.59E+14
					46	2.11E+14	1.96E+14	3.81E+14	3.53E+14
					47	2.11E+14	1.95E+14	3.75E+14	3.51E+14

Table A1 - 4 – Calculated fission density for HEU and LEU reference design core depleted at a constant power of 57.8 MW and without beam tube IH4

HEU core fission density (fission/cc_meat)					LEU reference design core fission density (fission/cc_meat)				
time (days)	**core average**	**^{235}U core average**	**peak (envelope)**	**^{235}U peak (envelope)**	**time (days)**	**core average**	**^{235}U core average**	**peak (envelope)**	**^{235}U peak (envelope)**
0	0.00E+00	0.00E+00	0.00E+00	0.00E+00	**0**	0.00E+00	0.00E+00	0.00E+00	0.00E+00
1	2.01E+19	2.01E+19	4.38E+19	4.38E+19	**1**	1.83E+19	1.80E+19	4.45E+19	4.43E+19
2	4.02E+19	4.02E+19	8.75E+19	8.75E+19	**2**	3.65E+19	3.61E+19	8.91E+19	8.86E+19
3	6.03E+19	6.02E+19	1.31E+20	1.31E+20	**3**	5.48E+19	5.41E+19	1.34E+20	1.33E+20
4	8.03E+19	8.03E+19	1.74E+20	1.74E+20	**4**	7.30E+19	7.21E+19	1.78E+20	1.77E+20
5	1.00E+20	1.00E+20	2.16E+20	2.16E+20	**5**	9.13E+19	9.01E+19	2.22E+20	2.20E+20
6	1.21E+20	1.20E+20	2.58E+20	2.58E+20	**6**	1.10E+20	1.08E+20	2.65E+20	2.63E+20
9	1.81E+20	1.81E+20	3.83E+20	3.82E+20	**9**	1.64E+20	1.62E+20	3.95E+20	3.91E+20
12	2.41E+20	2.41E+20	5.03E+20	5.02E+20	**12**	2.19E+20	2.16E+20	5.21E+20	5.15E+20
15	3.01E+20	3.01E+20	6.18E+20	6.18E+20	**15**	2.74E+20	2.69E+20	6.45E+20	6.35E+20
18	3.61E+20	3.61E+20	7.33E+20	7.33E+20	**18**	3.28E+20	3.22E+20	7.65E+20	7.51E+20
21	4.22E+20	4.21E+20	8.49E+20	8.48E+20	**21**	3.83E+20	3.75E+20	8.83E+20	8.64E+20
24	4.82E+20	4.81E+20	9.64E+20	9.63E+20	**24**	4.38E+20	4.27E+20	9.97E+20	9.74E+20
27	5.42E+20	5.41E+20	1.08E+21	1.08E+21	**27**	4.92E+20	4.80E+20	1.11E+21	1.08E+21
30	6.02E+20	6.01E+20	1.19E+21	1.18E+21	**30**	5.47E+20	5.32E+20	1.22E+21	1.19E+21
33	6.63E+20	6.61E+20	1.29E+21	1.29E+21	**33**	6.02E+20	5.84E+20	1.34E+21	1.30E+21
36	7.23E+20	7.21E+20	1.39E+21	1.38E+21	**36**	6.56E+20	6.35E+20	1.45E+21	1.41E+21
39	7.83E+20	7.81E+20	1.48E+21	1.48E+21	**39**	7.11E+20	6.87E+20	1.56E+21	1.51E+21
42	8.43E+20	8.41E+20	1.56E+21	1.56E+21	**42**	7.66E+20	7.38E+20	1.67E+21	1.61E+21
43	8.63E+20	8.61E+20	1.59E+21	1.59E+21	**43**	7.84E+20	7.55E+20	1.70E+21	1.64E+21
44	8.83E+20	8.81E+20	1.62E+21	1.61E+21	**44**	8.02E+20	7.72E+20	1.74E+21	1.67E+21
45	9.03E+20	9.01E+20	1.64E+21	1.64E+21	**45**	8.20E+20	7.89E+20	1.77E+21	1.71E+21
45.5	9.13E+20	9.11E+20	1.66E+21	1.65E+21	**46**	8.38E+20	8.06E+20	1.80E+21	1.74E+21
					47	8.57E+20	8.23E+20	1.84E+21	1.77E+21
					48	8.75E+20	8.40E+20	1.87E+21	1.80E+21

Table A1 - 5 – Calculated ^{235}U consumption for HEU and LEU reference design core depleted at a constant power of 57.8 MW and without beam tube IH4

HEU core ^{235}U consumption (%)					LEU reference design core ^{235}U consumption (%)				
time (days)	**core average**	**core average - fission only**	**peak (envelope)**	**peak (envelope) - fission only**	**time (days)**	**core average**	**core average - fission only**	**peak (envelope)**	**peak (envelope) - fission only**
0	0.00	0.00	0.00	0.00	**0**	0.00	0.00	0.00	0.00
1	0.86	0.70	1.83	1.53	**1**	0.55	0.45	1.31	1.09
2	1.72	1.41	3.65	3.06	**2**	1.10	0.89	2.61	2.19
3	2.58	2.11	5.46	4.58	**3**	1.65	1.34	3.92	3.28
4	3.44	2.81	7.25	6.08	**4**	2.20	1.78	5.22	4.36
5	4.30	3.51	9.02	7.57	**5**	2.74	2.23	6.50	5.43
6	5.16	4.22	10.77	9.03	**6**	3.29	2.67	7.77	6.50
9	7.72	6.32	15.87	13.39	**9**	4.92	4.00	11.50	9.65
12	10.26	8.43	20.77	17.58	**12**	6.54	5.32	15.11	12.72
15	12.80	10.54	25.48	21.62	**15**	8.15	6.64	18.61	15.68
18	15.34	12.64	30.00	25.64	**18**	9.75	7.95	22.00	18.56
21	17.87	14.74	34.33	29.68	**21**	11.34	9.26	25.27	21.33
24	20.39	16.84	38.48	33.70	**24**	12.93	10.56	28.42	24.06
27	22.91	18.95	42.43	37.63	**27**	14.50	11.85	31.46	26.75
30	25.43	21.05	46.20	41.44	**30**	16.07	13.14	34.39	29.43
33	27.93	23.14	49.91	45.07	**33**	17.63	14.42	37.21	32.09
36	30.44	25.24	53.78	48.48	**36**	19.18	15.70	39.91	34.71
39	32.93	27.34	57.36	51.65	**39**	20.73	16.97	42.52	37.28
42	35.43	29.43	60.64	54.60	**42**	22.27	18.23	45.01	39.78
43	36.27	30.13	61.67	55.51	**43**	22.78	18.65	45.82	40.58
44	37.11	30.83	62.67	56.42	**44**	23.29	19.07	46.71	41.37
45	37.95	31.53	63.63	57.37	**45**	23.81	19.49	47.62	42.15
45.5	38.37	31.88	64.10	57.90	**46**	24.32	19.91	48.52	42.92
					47	24.83	20.33	49.40	43.67
					48	25.34	20.74	50.27	44.42

Table A1 - 6 – Calculated neutron flux, ^{10}B and ^{4}He density evolution in most limiting boated region for HEU and LEU reference design core depleted at a constant power of 57.8 MW and without beam tube IH4

HEU core				LEU reference design core			
time (days)	neutron flux ($n/cm^2/s$)	^{10}B atomic density (at/barn.cm)	^{4}He atomic density (at/barn.cm)	time (days)	neutron flux ($n/cm^2/s$)	^{10}B atomic density (at/barn.cm)	^{4}He atomic density (at/barn.cm)
0	1.077E+15	6.015E-04	0.000E+00	**0**	8.426E+14	2.406E-03	0.000E+00
1	1.139E+15	5.452E-04	5.626E-05	**1**	8.648E+14	2.316E-03	8.972E-05
2	1.155E+15	4.904E-04	1.111E-04	**2**	8.659E+14	2.225E-03	1.808E-04
3	1.171E+15	4.395E-04	1.619E-04	**3**	8.671E+14	2.136E-03	2.703E-04
4	1.183E+15	3.926E-04	2.089E-04	**4**	8.713E+14	2.047E-03	3.585E-04
5	1.203E+15	3.494E-04	2.520E-04	**5**	8.729E+14	1.960E-03	4.455E-04
6	1.222E+15	3.098E-04	2.916E-04	**6**	8.786E+14	1.875E-03	5.309E-04
9	1.278E+15	2.133E-04	3.882E-04	**9**	8.967E+14	1.634E-03	7.713E-04
12	1.339E+15	1.416E-04	4.599E-04	**12**	9.173E+14	1.407E-03	9.990E-04
15	1.399E+15	9.032E-05	5.111E-04	**15**	9.417E+14	1.194E-03	1.212E-03
18	1.463E+15	5.531E-05	5.461E-04	**18**	9.631E+14	9.959E-04	1.410E-03
21	1.516E+15	3.248E-05	5.690E-04	**21**	9.999E+14	8.159E-04	1.590E-03
24	1.561E+15	1.836E-05	5.831E-04	**24**	1.027E+15	6.533E-04	1.752E-03
27	1.586E+15	1.004E-05	5.914E-04	**27**	1.063E+15	5.111E-04	1.895E-03
30	1.596E+15	5.365E-06	5.961E-04	**30**	1.102E+15	3.891E-04	2.017E-03
33	1.581E+15	2.819E-06	5.986E-04	**33**	1.137E+15	2.878E-04	2.118E-03
36	1.555E+15	1.478E-06	6.000E-04	**36**	1.167E+15	2.066E-04	2.199E-03
39	1.512E+15	7.766E-07	6.007E-04	**39**	1.187E+15	1.442E-04	2.261E-03
42	1.470E+15	4.127E-07	6.011E-04	**42**	1.197E+15	9.828E-05	2.307E-03
43	1.455E+15	3.356E-07	6.012E-04	**43**	1.199E+15	8.595E-05	2.320E-03
44	1.436E+15	2.732E-07	6.012E-04	**44**	1.197E+15	7.504E-05	2.331E-03
45	1.419E+15	2.229E-07	6.013E-04	**45**	1.198E+15	6.545E-05	2.340E-03
				46	1.192E+15	5.700E-05	2.349E-03
				47	1.193E+15	4.962E-05	2.356E-03

Table A1 - 7 – Calculated kinetic parameters evolution for HEU and LEU reference design core depleted at a constant power of 57.8 MW and without beam tube IH4

HEU core kinetic parameters					LEU reference design core kinetic parameters				
time (days)	**beta effective (pcm)**	**beta effective uncertainty (pcm)**	**neutron lifetime (μs)**	**neutron lifetime uncertainty (μs)**	**time (days)**	**beta effective (pcm)**	**beta effective uncertainty (pcm)**	**neutron lifetime (μs)**	**neutron lifetime uncertainty (μs)**
0	674	6	743.5	1.3	**0**	676	6	731.1	1.3
1	670	6	702.6	1.3	**1**	674	6	684.4	1.3
2	681	6	702.4	1.3	**2**	681	6	679.5	1.3
3	676	6	701.8	1.3	**3**	679	6	679.9	1.3
4	682	6	703.8	1.3	**4**	675	6	678.8	1.3
5	681	6	702.2	1.3	**5**	669	6	673.6	1.2
6	679	6	705.0	1.3	**6**	660	6	675.0	1.2
9	681	6	711.6	1.3	**9**	668	6	678.1	1.3
12	684	6	718.7	1.3	**12**	670	6	678.5	1.3
15	671	6	723.6	1.3	**15**	667	6	680.8	1.2
18	672	6	734.0	1.3	**18**	656	6	680.7	1.3
21	680	6	742.9	1.3	**21**	662	6	685.1	1.3
24	668	6	752.4	1.3	**24**	671	6	687.8	1.3
27	680	6	759.7	1.3	**27**	661	6	691.5	1.3
30	679	6	764.2	1.3	**30**	656	6	694.2	1.3
33	675	6	770.9	1.3	**33**	656	6	699.2	1.3
36	673	6	775.3	1.3	**36**	651	6	702.8	1.3
39	677	6	780.9	1.3	**39**	644	6	707.2	1.3
42	679	6	786.1	1.3	**42**	642	6	711.7	1.3
43	670	6	791.9	1.3	**43**	641	6	711.8	1.3
44	678	6	800.5	1.3	**44**	649	6	712.7	1.3
45	680	6	803.0	1.3	**45**	645	6	717.2	1.3
45.5	680	6	806.3	1.3	**46**	648	6	721.2	1.3
					47	643	6	724.0	1.3
					48	645	6	724.1	1.3

A2. Tabulated Values of Section 4.2

Table A2 - 1 – Digitized experimental axial neutron flux profile data at several radial locations (up to 31.5 cm) for HEU core at 57.8 MW

axial distance from bottom of the vessel (cm)	Digitized experimental neutron flux data ($n/cm^2/s$) at r = 23.5 cm	axial distance from bottom of the vessel (cm)	Digitized experimental neutron flux data ($n/cm^2/s$) at r = 27.5 cm	axial distance from bottom of the vessel (cm)	Digitized experimental neutron flux data ($n/cm^2/s$) at r = 31.5 cm
50.48	3.56E+14	62.12	5.31E+14	50.46	4.40E+14
60.84	4.60E+14	70.53	6.56E+14	59.73	6.02E+14
74.44	5.40E+14	79.37	8.06E+14	70.30	7.47E+14
86.09	7.27E+14	91.22	1.01E+15	79.56	9.40E+14
103.13	9.36E+14	100.28	1.17E+15	91.42	1.13E+15
121.49	1.01E+15	111.07	1.29E+15	102.63	1.31E+15
136.00	8.99E+14	121.23	1.28E+15	110.39	1.42E+15
150.52	7.22E+14	130.76	1.21E+15	120.99	1.43E+15
161.32	7.81E+14	141.16	1.05E+15	130.51	1.35E+15
172.80	6.80E+14	149.84	8.99E+14	138.54	1.21E+15
181.47	5.33E+14	158.72	8.13E+14	150.03	1.06E+15
		169.34	6.44E+14		
		178.24	4.84E+14		

Table A2 - 2 – Digitized experimental axial neutron flux profile data at several radial locations (from 35.5 to 83.5 cm) for HEU core at 57.8 MW

axial distance from bottom of the vessel (cm)	Digitized experimental neutron flux data ($n/cm^2/s$) at r = 35.5 cm	axial distance from bottom of the vessel (cm)	Digitized experimental neutron flux data ($n/cm^2/s$) at r = 43.5 cm	axial distance from bottom of the vessel (cm)	Digitized experimental neutron flux data ($n/cm^2/s$) at r = 51.5 cm	axial distance from bottom of the vessel (cm)	Digitized experimental neutron flux data ($n/cm^2/s$) at r = 83.5 cm
81.96	9.68E+14	**70.26**	6.74E+14	**81.22**	7.39E+14	**70.92**	2.47E+14
91.55	1.17E+15	**80.94**	8.59E+14	**101.37**	9.57E+14	**81.46**	2.96E+14
101.81	1.35E+15	**92.46**	1.08E+15	**121.83**	1.01E+15	**93.08**	3.34E+14
116.63	1.46E+15	**102.96**	1.21E+15	**141.31**	8.63E+14	**103.85**	3.57E+14
131.56	1.35E+15	**111.99**	1.26E+15			**112.69**	3.52E+14
142.65	1.18E+15	**120.83**	1.26E+15			**121.54**	3.48E+14
152.23	1.01E+15	**131.22**	1.18E+15			**131.89**	3.36E+14
161.62	8.03E+14	**140.77**	1.06E+15			**141.18**	3.05E+14
172.06	6.24E+14	**152.31**	8.64E+14			**152.63**	2.66E+14
182.07	4.55E+14	**162.33**	6.80E+14			**162.79**	2.20E+14

Table A2 - 3 – Calculated HEU core thermal neutron flux axial profile at several radial locations (up to 31.5 cm) at a power of 57.8 MW

axial distance from bottom of the vessel (cm)	calculated neutron flux (n/cm^2/s) at a radius (cm) of			axial distance from bottom of the vessel (cm)	calculated neutron flux (n/cm^2/s) at a radius (cm) of		
	23.5 cm	27.5 cm	31.5 cm		23.5 cm	27.5 cm	31.5 cm
38.5	2.14E+14	2.42E+14	2.58E+14	**120.5**	9.74E+14	1.31E+15	1.43E+15
40.5	2.31E+14	2.62E+14	2.80E+14	**121.5**	9.72E+14	1.30E+15	1.43E+15
42.5	2.50E+14	2.84E+14	3.03E+14	**123.5**	9.67E+14	1.30E+15	1.42E+15
44.5	2.71E+14	3.08E+14	3.27E+14	**125.5**	9.60E+14	1.29E+15	1.41E+15
46.5	2.94E+14	3.33E+14	3.53E+14	**127.5**	9.51E+14	1.28E+15	1.40E+15
48.5	3.18E+14	3.59E+14	3.81E+14	**129.5**	9.41E+14	1.26E+15	1.38E+15
50.5	3.42E+14	3.86E+14	4.10E+14	**131.5**	9.25E+14	1.24E+15	1.36E+15
52.5	3.68E+14	4.15E+14	4.40E+14	**133.5**	9.11E+14	1.22E+15	1.34E+15
54.5	3.93E+14	4.45E+14	4.71E+14	**135.5**	8.93E+14	1.20E+15	1.31E+15
56.5	4.18E+14	4.76E+14	5.04E+14	**137.5**	8.73E+14	1.17E+15	1.29E+15
58.5	4.41E+14	5.06E+14	5.37E+14	**139.5**	8.53E+14	1.14E+15	1.26E+15
60.5	4.63E+14	5.36E+14	5.72E+14	**141.5**	8.31E+14	1.12E+15	1.22E+15
62.5	4.82E+14	5.66E+14	6.07E+14	**143.5**	8.09E+14	1.08E+15	1.19E+15
64.5	4.99E+14	5.96E+14	6.43E+14	**145.5**	7.85E+14	1.05E+15	1.15E+15
66.5	5.14E+14	6.26E+14	6.80E+14	**147.5**	7.64E+14	1.02E+15	1.12E+15
68.5	5.25E+14	6.54E+14	7.16E+14	**149.5**	7.45E+14	9.89E+14	1.08E+15
70.5	5.33E+14	6.84E+14	7.55E+14	**151.5**	7.31E+14	9.59E+14	1.05E+15
72.5	5.42E+14	7.15E+14	7.93E+14	**153.5**	7.22E+14	9.33E+14	1.01E+15
74.5	5.57E+14	7.47E+14	8.31E+14	**155.5**	7.21E+14	9.08E+14	9.76E+14
76.5	5.76E+14	7.81E+14	8.72E+14	**157.5**	7.29E+14	8.87E+14	9.41E+14
78.5	6.00E+14	8.16E+14	9.12E+14	**159.5**	7.43E+14	8.64E+14	9.05E+14
80.5	6.26E+14	8.53E+14	9.53E+14	**161.5**	7.53E+14	8.40E+14	8.69E+14
82.5	6.55E+14	8.91E+14	9.93E+14	**163.5**	7.53E+14	8.15E+14	8.32E+14
84.5	6.83E+14	9.30E+14	1.03E+15	**165.5**	7.40E+14	7.84E+14	7.94E+14
86.5	7.12E+14	9.68E+14	1.07E+15	**167.5**	7.14E+14	7.50E+14	7.55E+14
88.5	7.41E+14	1.01E+15	1.11E+15	**169.5**	6.79E+14	7.11E+14	7.13E+14
90.5	7.69E+14	1.04E+15	1.15E+15	**171.5**	6.44E+14	6.71E+14	6.71E+14
92.5	7.96E+14	1.08E+15	1.19E+15	**173.5**	6.07E+14	6.31E+14	6.29E+14
94.5	8.21E+14	1.11E+15	1.23E+15	**175.5**	5.69E+14	5.90E+14	5.88E+14
96.5	8.46E+14	1.14E+15	1.26E+15	**177.5**	5.31E+14	5.48E+14	5.46E+14
98.5	8.68E+14	1.17E+15	1.29E+15	**179.5**	4.92E+14	5.07E+14	5.05E+14
100.5	8.89E+14	1.20E+15	1.32E+15	**181.5**	4.53E+14	4.66E+14	4.63E+14
102.5	9.07E+14	1.22E+15	1.34E+15	**183.5**	4.15E+14	4.25E+14	4.23E+14
104.5	9.22E+14	1.24E+15	1.36E+15	**185.5**	3.76E+14	3.84E+14	3.82E+14
106.5	9.37E+14	1.26E+15	1.38E+15	**187.5**	3.38E+14	3.43E+14	3.42E+14
108.5	9.48E+14	1.27E+15	1.39E+15	**189.5**	3.01E+14	3.03E+14	3.02E+14
110.5	9.58E+14	1.29E+15	1.41E+15	**191.5**	2.63E+14	2.62E+14	2.60E+14
112.5	9.65E+14	1.30E+15	1.42E+15	**193.5**	2.27E+14	2.19E+14	2.14E+14
114.5	9.71E+14	1.30E+15	1.42E+15	**195.5**	1.93E+14	1.76E+14	1.73E+14

Table A2 - 4 – Calculated HEU core thermal neutron flux axial profile at several radial locations (from 35.5 to 83.5 cm) at a power of 57.8 MW

axial distance from bottom of the vessel (cm)	calculated neutron flux (n/cm^2/s) at a radius (cm) of				axial distance from bottom of the vessel (cm)	calculated neutron flux (n/cm^2/s) at a radius (cm) of			
	35.5 cm	43.5 cm	51.5 cm	83.5 cm		35.5 cm	43.5 cm	51.5 cm	83.5 cm
38.5	2.67E+14	2.63E+14	1.18E+14	2.44E+14	**120.5**	1.40E+15	1.17E+15	3.70E+14	9.07E+14
40.5	2.88E+14	2.83E+14	1.27E+14	2.61E+14	**122.5**	1.39E+15	1.16E+15	3.69E+14	9.01E+14
44.5	3.35E+14	3.27E+14	1.46E+14	2.99E+14	**126.5**	1.38E+15	1.16E+15	3.66E+14	8.89E+14
50.5	4.17E+14	4.00E+14	1.75E+14	3.61E+14	**132.5**	1.33E+15	1.12E+15	3.61E+14	8.60E+14
52.5	4.47E+14	4.27E+14	1.84E+14	3.83E+14	**134.5**	1.30E+15	1.10E+15	3.59E+14	8.49E+14
54.5	4.78E+14	4.55E+14	1.94E+14	4.06E+14	**136.5**	1.28E+15	1.08E+15	3.56E+14	8.37E+14
56.5	5.10E+14	4.84E+14	2.03E+14	4.29E+14	**138.5**	1.25E+15	1.06E+15	3.53E+14	8.25E+14
58.5	5.45E+14	5.14E+14	2.13E+14	4.54E+14	**140.5**	1.22E+15	1.04E+15	3.50E+14	8.12E+14
60.5	5.79E+14	5.44E+14	2.23E+14	4.79E+14	**142.5**	1.19E+15	1.01E+15	3.46E+14	8.00E+14
62.5	6.15E+14	5.76E+14	2.32E+14	5.03E+14	**144.5**	1.16E+15	9.91E+14	3.42E+14	7.88E+14
64.5	6.52E+14	6.08E+14	2.42E+14	5.28E+14	**146.5**	1.12E+15	9.68E+14	3.38E+14	7.75E+14
66.5	6.90E+14	6.40E+14	2.51E+14	5.53E+14	**148.5**	1.09E+15	9.44E+14	3.33E+14	7.61E+14
68.5	7.28E+14	6.73E+14	2.60E+14	5.78E+14	**150.5**	1.06E+15	9.17E+14	3.28E+14	7.45E+14
70.5	7.67E+14	7.06E+14	2.69E+14	6.02E+14	**152.5**	1.02E+15	8.90E+14	3.21E+14	7.28E+14
72.5	8.06E+14	7.39E+14	2.78E+14	6.26E+14	**154.5**	9.83E+14	8.61E+14	3.14E+14	7.10E+14
74.5	8.45E+14	7.71E+14	2.87E+14	6.48E+14	**156.5**	9.45E+14	8.32E+14	3.05E+14	6.90E+14
76.5	8.84E+14	8.02E+14	2.95E+14	6.69E+14	**158.5**	9.09E+14	8.03E+14	2.97E+14	6.68E+14
78.5	9.24E+14	8.32E+14	3.02E+14	6.90E+14	**160.5**	8.70E+14	7.70E+14	2.89E+14	6.45E+14
80.5	9.62E+14	8.61E+14	3.09E+14	7.10E+14	**162.5**	8.31E+14	7.37E+14	2.81E+14	6.20E+14
82.5	1.00E+15	8.88E+14	3.15E+14	7.31E+14	**164.5**	7.91E+14	7.03E+14	2.73E+14	5.94E+14
84.5	1.04E+15	9.15E+14	3.21E+14	7.52E+14	**166.5**	7.51E+14	6.69E+14	2.64E+14	5.68E+14
86.5	1.07E+15	9.42E+14	3.26E+14	7.74E+14	**168.5**	7.10E+14	6.35E+14	2.55E+14	5.42E+14
88.5	1.11E+15	9.68E+14	3.31E+14	7.93E+14	**170.5**	6.69E+14	6.00E+14	2.47E+14	5.16E+14
90.5	1.15E+15	9.94E+14	3.36E+14	8.10E+14	**172.5**	6.29E+14	5.66E+14	2.39E+14	4.90E+14
92.5	1.18E+15	1.02E+15	3.40E+14	8.26E+14	**174.5**	5.89E+14	5.32E+14	2.30E+14	4.63E+14
94.5	1.22E+15	1.04E+15	3.44E+14	8.41E+14	**176.5**	5.49E+14	4.99E+14	2.21E+14	4.37E+14
96.5	1.25E+15	1.07E+15	3.48E+14	8.57E+14	**178.5**	5.10E+14	4.67E+14	2.13E+14	4.11E+14
98.5	1.28E+15	1.09E+15	3.52E+14	8.73E+14	**180.5**	4.71E+14	4.34E+14	2.04E+14	3.86E+14
100.5	1.30E+15	1.12E+15	3.56E+14	8.88E+14	**182.5**	4.32E+14	4.02E+14	1.96E+14	3.62E+14
102.5	1.33E+15	1.13E+15	3.60E+14	9.01E+14	**184.5**	3.95E+14	3.72E+14	1.88E+14	3.38E+14
104.5	1.35E+15	1.14E+15	3.63E+14	9.10E+14	**186.5**	3.57E+14	3.42E+14	1.80E+14	3.15E+14
106.5	1.36E+15	1.15E+15	3.66E+14	9.17E+14	**188.5**	3.19E+14	3.12E+14	1.72E+14	2.93E+14
108.5	1.37E+15	1.16E+15	3.70E+14	9.21E+14	**190.5**	2.81E+14	2.83E+14	1.64E+14	2.72E+14
110.5	1.38E+15	1.16E+15	3.73E+14	9.23E+14					
112.5	1.39E+15	1.17E+15	3.74E+14	9.24E+14					
114.5	1.39E+15	1.17E+15	3.74E+14	9.21E+14					
116.5	1.40E+15	1.17E+15	3.73E+14	9.18E+14					

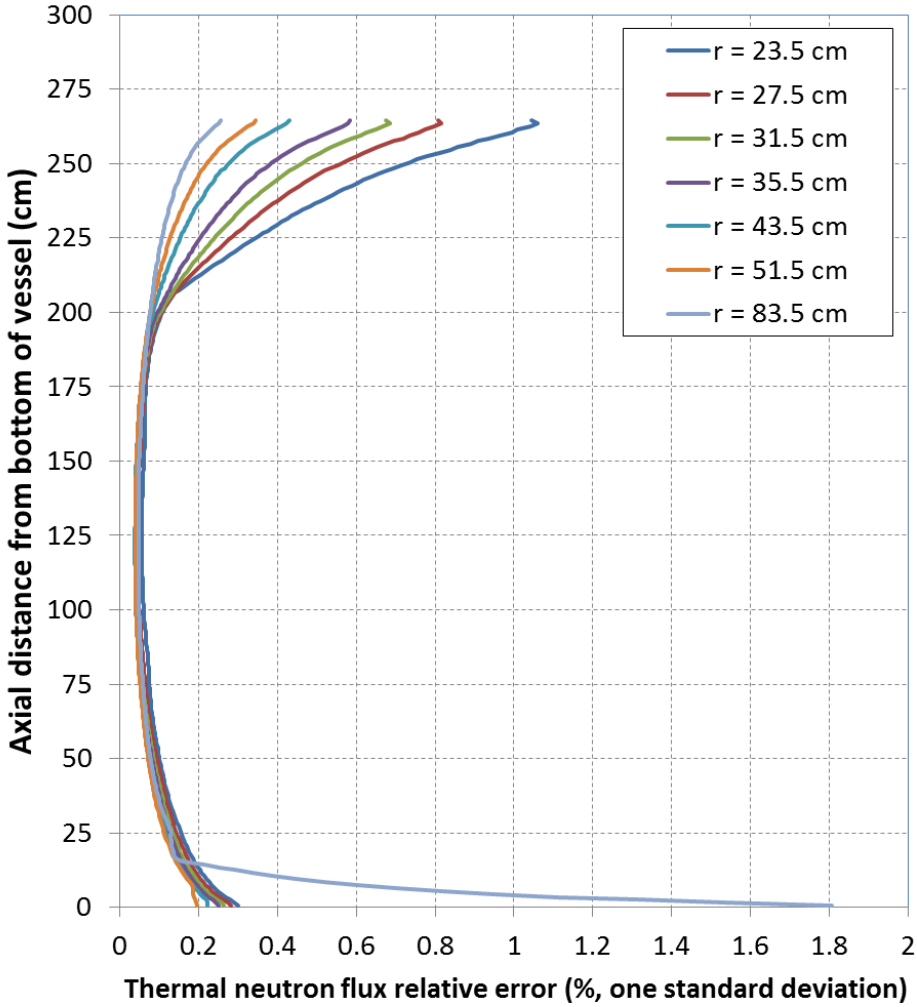

Figure A2 - 1 – relative error associated to the calculated HEU core thermal neutron flux presented in table A2 -3 and A2 - 4 at one standard deviation

Table A2 - 5 – Digitized experimental and calculated (at 57.8MW) neutron flux in midplane for HEU

Digitized experimental neutron flux data (n/cm^2/s)	calculated HEU neutron flux (n/cm^2/s)

radius (cm)	thermal flux (θ<0.625eV)	epithermal flux (0.625eV<θ<5.5 keV)	epithermal flux (5.5 keV<θ<0.821 MeV)	fast flux (θ>0.821 MeV)	radius (cm)	thermal flux (θ<0.625eV)	epithermal flux (0.625eV<θ<5.5 keV)	epithermal flux (5.5keV<θ<0.821MeV)	fast flux (θ>0.821MeV)
0.01	1.37E+15	1.01E+15	4.88E+14	7.82E+13	**0.25**	1.31E+15	1.18E+15	4.22E+14	8.16E+13
2.71	1.31E+15	1.00E+15	5.15E+14	8.60E+13	**3.25**	1.24E+15	1.18E+15	4.54E+14	8.72E+13
3.05	1.30E+15	1.00E+15	5.19E+14	8.81E+13	**6.25**	1.07E+15	1.18E+15	5.44E+14	1.10E+14
5.18	1.21E+15	9.93E+14	5.67E+14	1.02E+14	**9.25**	8.00E+14	1.16E+15	7.01E+14	1.60E+14
6.97	1.10E+15	9.88E+14	6.18E+14	1.24E+14	**12.25**	3.47E+14	1.02E+15	9.36E+14	2.84E+14
8.06	9.55E+14	9.88E+14	6.52E+14	1.44E+14	**15.25**	1.90E+14	9.19E+14	1.14E+15	5.07E+14
11.04	6.09E+14	9.65E+14	7.58E+14	2.44E+14	**18.25**	2.81E+14	8.64E+14	1.11E+15	5.61E+14
13.96	2.43E+14	9.24E+14	9.78E+14	4.30E+14	**21.25**	6.94E+14	8.51E+14	7.81E+14	2.49E+14
15.78	1.66E+14	8.93E+14	9.92E+14	4.79E+14	**24.25**	1.08E+15	7.41E+14	4.66E+14	1.12E+14
17.01	2.05E+14	8.61E+14	9.82E+14	4.69E+14	**27.25**	1.30E+15	5.90E+14	2.73E+14	5.80E+13
19.03	4.54E+14	8.17E+14	8.70E+14	4.13E+14	**30.25**	1.41E+15	4.43E+14	1.58E+14	3.21E+13
24.85	1.07E+15	6.52E+14	4.00E+14	1.09E+14	**36.75**	1.37E+15	2.05E+14	4.70E+13	9.97E+12
26.25	1.16E+15	5.74E+14	3.26E+14	8.03E+13	**40.25**	1.26E+15	1.30E+14	2.48E+13	5.70E+12
28.34	1.25E+15	4.71E+14	2.43E+14	4.80E+13	**43.25**	1.17E+15	8.95E+13	1.54E+13	3.72E+12
30.16	1.30E+15	3.92E+14	1.83E+14	3.13E+13	**46.25**	1.07E+15	6.23E+13	9.70E+12	2.49E+12
32.47	1.32E+15	3.12E+14	1.28E+14	1.87E+13	**49.25**	9.79E+14	4.36E+13	6.26E+12	1.72E+12
34.11	1.30E+15	2.63E+14	1.02E+14	1.29E+13	**55.25**	8.22E+14	2.25E+13	3.01E+12	8.73E+11
36.08	1.29E+15	2.15E+14	7.46E+13	8.21E+12	**58.25**	7.58E+14	1.66E+13	2.21E+12	6.43E+11
38.26	1.26E+15	1.72E+14	5.15E+13	5.17E+12	**64.25**	6.45E+14	9.01E+12	1.21E+12	3.63E+11
41.33	1.20E+15	1.22E+14	3.10E+13	2.76E+12	**67.25**	5.94E+14	6.48E+12	8.78E+11	2.61E+11
43.14	1.15E+15	1.00E+14	2.29E+13	1.89E+12	**70.75**	5.38E+14	4.31E+12	5.80E+11	1.72E+11
45.08	1.09E+15	7.98E+13	1.64E+13	1.28E+12	**73.75**	4.93E+14	3.10E+12	4.14E+11	1.24E+11
48.67	9.88E+14	5.29E+13	9.62E+12	6.03E+11	**76.75**	4.52E+14	2.24E+12	2.92E+11	8.56E+10
50.85	9.44E+14	4.20E+13	6.80E+12	3.87E+11	**79.75**	4.14E+14	1.66E+12	2.11E+11	6.50E+10
52.10	9.26E+14	3.66E+13	5.59E+12	3.00E+11	**82.75**	3.79E+14	1.22E+12	1.61E+11	4.87E+10
54.77	8.60E+14	2.74E+13	3.76E+12	1.74E+11	**85.75**	3.47E+14	9.09E+11	1.17E+11	3.82E+10
56.59	8.12E+14	2.24E+13	2.86E+12	1.20E+11	**88.75**	3.16E+14	6.91E+11	8.66E+10	2.73E+10
61.50	7.12E+14	1.28E+13	1.37E+12	4.39E+10	**94.75**	2.59E+14	3.72E+11	5.17E+10	1.53E+10
64.44	6.59E+14	9.63E+12	8.95E+11	2.41E+10	**97.75**	2.33E+14	2.76E+11	3.65E+10	1.02E+10
66.32	6.22E+14	7.89E+12	6.79E+11	1.64E+10	**100.75**	2.10E+14	2.09E+11	2.76E+10	7.77E+09
68.50	5.67E+14	6.01E+12	4.98E+11	1.05E+10	**103.75**	1.88E+14	1.63E+11	2.24E+10	5.80E+09
69.21	5.56E+14	5.48E+12	4.54E+11	9.09E+09	**106.75**	1.68E+14	1.31E+11	1.77E+10	3.70E+09
71.71	5.13E+14	4.19E+12	3.04E+11	5.45E+09	**109.75**	1.48E+14	1.05E+11	1.30E+10	2.98E+09
75.41	4.45E+14	2.74E+12	1.53E+11	2.56E+09	**112.75**	1.30E+14	8.40E+10	1.11E+10	3.14E+09
79.46	3.80E+14	1.76E+12	7.21E+10	1.12E+09	**115.75**	1.12E+14	7.10E+10	9.52E+09	2.09E+09
83.26	3.18E+14	1.17E+12	3.57E+10	5.15E+08	**118.75**	9.41E+13	5.84E+10	6.25E+09	1.40E+09
89.93	2.25E+14	5.74E+11	1.03E+10	1.32E+08	**124.75**	5.89E+13	3.65E+10	4.91E+09	1.19E+09
93.50	1.84E+14	3.92E+11	5.34E+09	6.35E+07	**129.75**	3.12E+13	2.06E+10	3.00E+09	9.93E+08

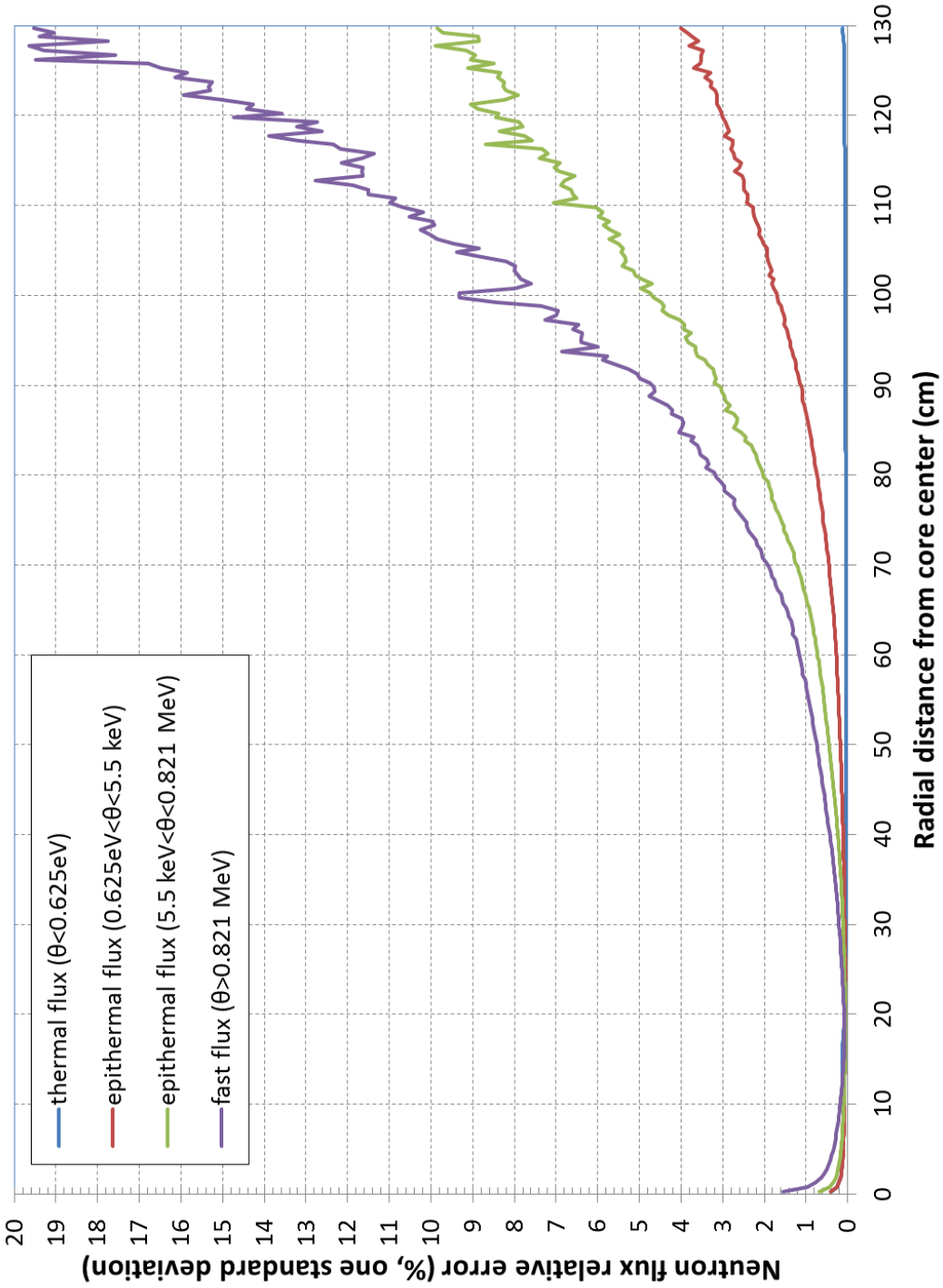

Figure A2 - 2 – relative error associated to the calculated HEU core neutron flux presented in table A2 - 1 at one standard deviation

Table A2 - 6 – HEU (52.8 MW) and LEU (57.8 MW) thermal neutron flux profile at a distance of 30 cm from the core center

axial position relative to core midplane (cm)	neutron flux (n/cm^2/s)				axial position relative to core midplane (cm)	neutron flux (n/cm^2/s)			
	HEU BOC	HEU EOC	LEU BOC	LEU EOC		HEU BOC	HEU EOC	LEU BOC	LEU EOC
-65.5	3.45E+14	4.73E+14	4.01E+14	4.68E+14	**2.5**	1.29E+15	1.26E+15	1.20E+15	1.18E+15
-63.5	3.72E+14	5.10E+14	4.30E+14	5.01E+14	**4.5**	1.29E+15	1.26E+15	1.21E+15	1.17E+15
-61.5	3.99E+14	5.48E+14	4.59E+14	5.36E+14	**6.5**	1.29E+15	1.25E+15	1.21E+15	1.17E+15
-59.5	4.27E+14	5.86E+14	4.90E+14	5.71E+14	**8.5**	1.29E+15	1.23E+15	1.20E+15	1.16E+15
-57.5	4.56E+14	6.26E+14	5.21E+14	6.06E+14	**10.5**	1.28E+15	1.22E+15	1.20E+15	1.15E+15
-55.5	4.87E+14	6.66E+14	5.52E+14	6.41E+14	**12.5**	1.27E+15	1.21E+15	1.19E+15	1.14E+15
-53.5	5.19E+14	7.07E+14	5.83E+14	6.77E+14	**14.5**	1.25E+15	1.19E+15	1.18E+15	1.13E+15
-51.5	5.50E+14	7.47E+14	6.15E+14	7.11E+14	**16.5**	1.24E+15	1.17E+15	1.17E+15	1.12E+15
-49.5	5.84E+14	7.87E+14	6.45E+14	7.43E+14	**18.5**	1.22E+15	1.15E+15	1.16E+15	1.10E+15
-47.5	6.17E+14	8.24E+14	6.75E+14	7.74E+14	**20.5**	1.20E+15	1.12E+15	1.14E+15	1.08E+15
-45.5	6.51E+14	8.61E+14	7.06E+14	8.04E+14	**22.5**	1.18E+15	1.10E+15	1.13E+15	1.06E+15
-43.5	6.85E+14	8.97E+14	7.35E+14	8.33E+14	**24.5**	1.15E+15	1.08E+15	1.11E+15	1.04E+15
-41.5	7.21E+14	9.30E+14	7.65E+14	8.61E+14	**26.5**	1.12E+15	1.05E+15	1.08E+15	1.02E+15
-39.5	7.56E+14	9.62E+14	7.94E+14	8.89E+14	**28.5**	1.09E+15	1.02E+15	1.06E+15	1.00E+15
-37.5	7.93E+14	9.93E+14	8.25E+14	9.16E+14	**30.5**	1.06E+15	9.97E+14	1.04E+15	9.77E+14
-35.5	8.29E+14	1.02E+15	8.54E+14	9.43E+14	**32.5**	1.03E+15	9.71E+14	1.01E+15	9.55E+14
-33.5	8.65E+14	1.05E+15	8.83E+14	9.68E+14	**34.5**	9.97E+14	9.44E+14	9.81E+14	9.31E+14
-31.5	9.01E+14	1.08E+15	9.12E+14	9.92E+14	**36.5**	9.64E+14	9.17E+14	9.52E+14	9.08E+14
-29.5	9.38E+14	1.11E+15	9.39E+14	1.02E+15	**38.5**	9.31E+14	8.92E+14	9.21E+14	8.84E+14
-27.5	9.74E+14	1.13E+15	9.67E+14	1.04E+15	**40.5**	8.98E+14	8.65E+14	8.90E+14	8.61E+14
-25.5	1.01E+15	1.16E+15	9.93E+14	1.06E+15	**42.5**	8.65E+14	8.39E+14	8.59E+14	8.37E+14
-23.5	1.04E+15	1.18E+15	1.02E+15	1.08E+15	**44.5**	8.32E+14	8.10E+14	8.27E+14	8.13E+14
-21.5	1.08E+15	1.20E+15	1.05E+15	1.10E+15	**46.5**	7.98E+14	7.80E+14	7.96E+14	7.88E+14
-19.5	1.11E+15	1.22E+15	1.07E+15	1.12E+15	**48.5**	7.65E+14	7.49E+14	7.64E+14	7.61E+14
-17.5	1.14E+15	1.24E+15	1.09E+15	1.13E+15	**50.5**	7.30E+14	7.16E+14	7.33E+14	7.32E+14
-15.5	1.17E+15	1.25E+15	1.11E+15	1.15E+15	**52.5**	6.94E+14	6.80E+14	7.01E+14	7.03E+14
-13.5	1.19E+15	1.26E+15	1.13E+15	1.16E+15	**54.5**	6.57E+14	6.45E+14	6.69E+14	6.70E+14
-11.5	1.21E+15	1.27E+15	1.15E+15	1.17E+15	**56.5**	6.20E+14	6.08E+14	6.36E+14	6.36E+14
-9.5	1.23E+15	1.28E+15	1.16E+15	1.18E+15	**58.5**	5.82E+14	5.71E+14	6.02E+14	6.01E+14
-7.5	1.25E+15	1.28E+15	1.17E+15	1.18E+15	**60.5**	5.45E+14	5.33E+14	5.67E+14	5.66E+14
-5.5	1.26E+15	1.28E+15	1.18E+15	1.18E+15	**62.5**	5.08E+14	4.97E+14	5.31E+14	5.29E+14
-3.5	1.27E+15	1.28E+15	1.19E+15	1.18E+15	**64.5**	4.70E+14	4.60E+14	4.95E+14	4.92E+14
-1.5	1.28E+15	1.28E+15	1.20E+15	1.18E+15	**65.5**	4.52E+14	4.42E+14	4.77E+14	4.73E+14
0.5	1.29E+15	1.27E+15	1.20E+15	1.18E+15					

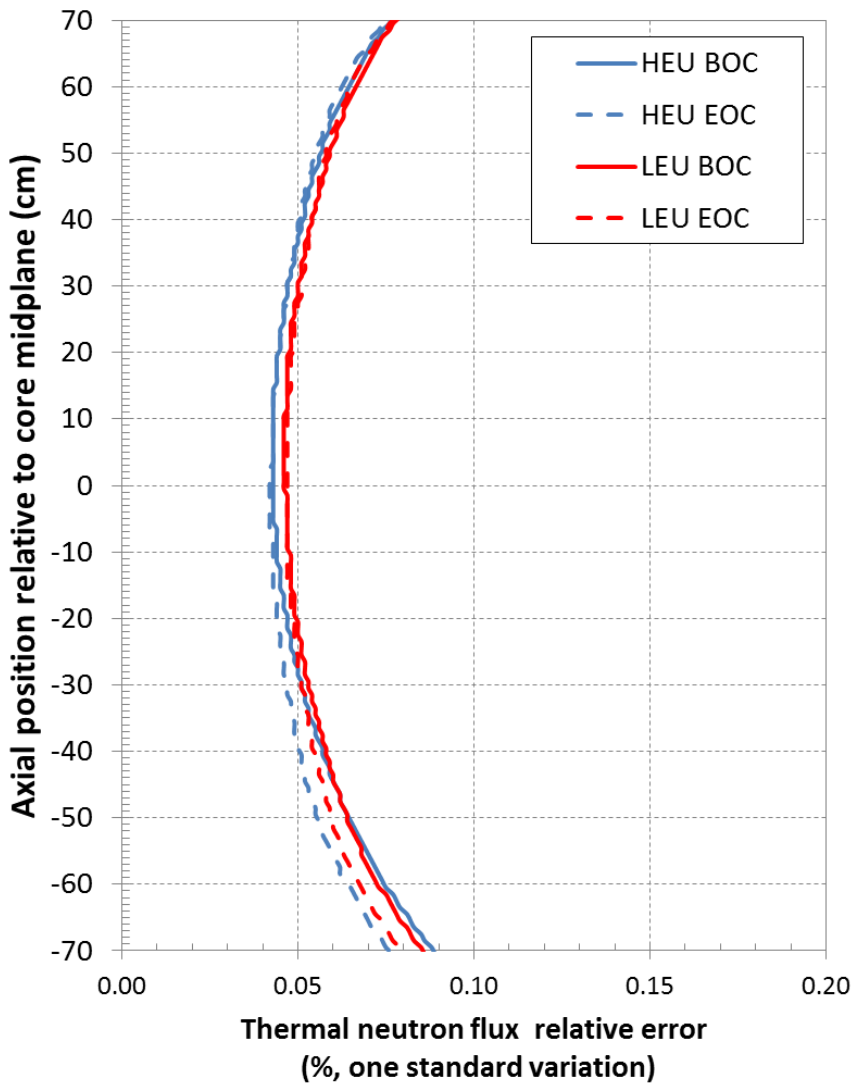

Figure A2 - 3 – relative error associated to the calculated HEU and LEU cores neutron flux presented in table A2 - 6 at one standard deviation

A3. Tabulated Values of Section 4.3

Table A3 - 1 – digitized experimental data representing the ratio between stripe averaged power and average core power at several radial locations of the HEU core

radial distance from core center (cm)	digitized experimental data
14.37	1.005
14.65	0.898
14.96	0.820
15.25	0.769
15.90	0.727
17.68	0.893
18.59	1.228
18.98	1.493
19.39	1.933

Table A3 - 2 – digitized experimental data representing the ratio between local power and average core power at several radial locations of the HEU core

axial distance from fuel bottom (cm)	digitized experimental data at r = 17.6 cm	axial distance from fuel bottom (cm)	digitized experimental data at r = 18.55 cm	axial distance from fuel bottom (cm)	digitized experimental data at r = 18.85 cm	axial distance from fuel bottom (cm)	digitized experimental data at r = 19.39 cm
18.42	0.739	**1.20**	0.812	**1.05**	0.927	**1.28**	1.196
40.16	1.022	**5.59**	0.788	**4.90**	0.933	**3.15**	1.223
61.80	0.989	**18.16**	1.070	**16.92**	1.238	**5.20**	1.257
74.96	0.806	**39.55**	1.416	**39.24**	1.617	**7.27**	1.341
79.04	0.968	**61.18**	1.357	**61.43**	1.561	**10.36**	1.429
		74.70	1.174	**74.37**	1.278	**17.60**	1.719
		78.22	1.277	**78.44**	1.403	**24.81**	1.938
						32.68	2.123
						40.01	2.251
						47.15	2.317
						54.73	2.262
						62.28	2.135
						69.78	1.907
						72.45	1.818
						74.79	1.777
						76.81	1.746
						79.37	1.793
						79.39	1.841

Table A3 - 3 – HEU fuel power density at BOC (core power at 57.8 MW)

radial node width (cm)		0.3	0.3	0.3	0.3	1	1.734	1	0.3	0.3	0.3	0.3	0.3	0.3
distance (cm) from - inner edge of the fuel	0	0.3	0.6	0.9	1.2	2.2	3.934	4.934	5.234	5.534	5.834	6.134	6.434	6.734
- core center	14	14.29	14.57	14.85	15.13	16.01	17.43	18.19	18.42	18.64	18.86	19.07	19.29	19.5
axial node height (cm)	position to core midplane (cm)	volumetric heat generation rate (W/mm^3)												
	40													
0.3	39.7	9.26	8.33	7.65	7.18	6.55	6.32	7.23	8.09	8.58	9.20	9.93	10.80	11.93
0.3	39.4	8.89	7.85	7.21	6.73	6.08	5.89	6.74	7.55	8.05	8.66	9.39	10.32	11.57
0.3	39.1	8.74	7.66	6.98	6.49	5.86	5.65	6.47	7.31	7.83	8.41	9.19	10.07	11.47
0.3	38.8	8.61	7.54	6.84	6.33	5.71	5.49	6.32	7.14	7.64	8.27	9.05	10.03	11.29
0.3	38.5	8.49	7.45	6.73	6.22	5.58	5.36	6.21	7.04	7.55	8.21	8.96	9.92	11.24
0.3	38.2	8.42	7.34	6.63	6.14	5.51	5.29	6.10	6.95	7.48	8.16	8.91	9.86	11.20
0.3	37.9	8.35	7.27	6.58	6.10	5.45	5.22	6.06	6.94	7.42	8.07	8.87	9.87	11.19
0.3	37.6	8.32	7.24	6.50	5.99	5.40	5.17	6.02	6.83	7.38	8.05	8.83	9.87	11.16
0.3	37.3	8.25	7.22	6.48	5.97	5.37	5.16	5.99	6.87	7.36	8.05	8.82	9.83	11.15
0.3	37	8.19	7.18	6.44	5.98	5.34	5.14	5.98	6.84	7.37	8.07	8.83	9.79	11.15
0.3	36.7	8.18	7.15	6.45	5.94	5.33	5.12	5.96	6.85	7.35	8.02	8.81	9.83	11.12
0.3	36.4	8.15	7.11	6.43	5.95	5.33	5.11	5.96	6.82	7.36	8.00	8.82	9.80	11.09
0.3	36.1	8.17	7.15	6.45	5.94	5.31	5.11	5.96	6.83	7.37	8.01	8.80	9.81	11.16
0.3	35.8	8.16	7.15	6.42	5.94	5.31	5.11	5.97	6.82	7.35	8.04	8.83	9.85	11.17
0.3	35.5	8.20	7.14	6.44	5.94	5.30	5.13	6.00	6.84	7.39	8.06	8.88	9.88	11.21
3.6	31.9	8.20	7.18	6.51	6.02	5.39	5.22	6.11	7.00	7.56	8.22	9.04	10.06	11.41
3.6	28.3	8.29	7.30	6.65	6.18	5.57	5.44	6.40	7.33	7.93	8.63	9.48	10.52	11.94
3.6	24.7	7.76	6.93	6.37	5.98	5.52	5.57	6.66	7.66	8.27	9.02	9.90	11.02	12.49
3.6	21.1	6.68	6.13	5.77	5.54	5.29	5.59	6.85	7.91	8.58	9.35	10.30	11.46	13.00
3.6	17.5	6.55	6.05	5.73	5.51	5.32	5.71	7.05	8.17	8.86	9.67	10.64	11.84	13.43
3.6	13.9	6.69	6.17	5.86	5.64	5.45	5.87	7.25	8.40	9.11	9.95	10.94	12.19	13.82
3.6	10.3	6.81	6.29	5.97	5.75	5.56	5.99	7.40	8.59	9.31	10.16	11.17	12.44	14.12
3.6	6.7	6.90	6.37	6.04	5.83	5.64	6.07	7.50	8.70	9.42	10.28	11.31	12.59	14.30
3.6	3.1	6.92	6.40	6.07	5.85	5.66	6.10	7.53	8.74	9.46	10.34	11.38	12.66	14.36
3.6	-0.5	6.91	6.38	6.05	5.83	5.64	6.07	7.51	8.71	9.44	10.30	11.35	12.63	14.32
3.6	-4.1	6.83	6.30	5.98	5.76	5.58	6.01	7.43	8.62	9.35	10.19	11.23	12.48	14.17
3.6	-7.7	6.69	6.17	5.86	5.65	5.47	5.89	7.29	8.45	9.17	10.00	11.03	12.27	13.94
3.6	-11.3	6.48	5.99	5.69	5.49	5.31	5.73	7.10	8.24	8.95	9.76	10.75	11.97	13.58
3.6	-14.9	6.22	5.75	5.46	5.27	5.10	5.51	6.84	7.94	8.61	9.41	10.36	11.54	13.09
3.6	-18.5	5.91	5.46	5.19	5.00	4.85	5.26	6.54	7.59	8.23	9.00	9.92	11.04	12.55
3.6	-22.1	5.54	5.13	4.87	4.70	4.56	4.95	6.17	7.18	7.80	8.52	9.40	10.48	11.90
3.6	-25.7	5.12	4.74	4.50	4.35	4.23	4.61	5.77	6.72	7.30	8.00	8.83	9.83	11.17
3.6	-29.3	4.64	4.29	4.10	3.96	3.86	4.24	5.34	6.24	6.78	7.43	8.19	9.14	10.41
3.6	-32.9	4.10	3.81	3.64	3.53	3.46	3.84	4.88	5.72	6.22	6.84	7.56	8.44	9.63
3.6	-36.5	3.48	3.26	3.13	3.06	3.04	3.45	4.45	5.24	5.73	6.29	6.96	7.80	8.91
0.5	-37	3.15	2.96	2.86	2.82	2.84	3.27	4.24	5.02	5.50	6.04	6.69	7.48	8.55
0.3	-37.3	3.11	2.94	2.84	2.80	2.82	3.25	4.21	5.00	5.46	6.01	6.68	7.47	8.50
0.3	-37.6	3.08	2.92	2.81	2.78	2.81	3.24	4.21	4.98	5.44	5.98	6.64	7.44	8.49
0.3	-37.9	3.07	2.89	2.80	2.76	2.80	3.24	4.21	4.98	5.44	5.95	6.62	7.36	8.46
0.3	-38.2	3.06	2.89	2.80	2.76	2.80	3.24	4.21	4.97	5.41	5.93	6.57	7.38	8.41
0.3	-38.5	3.03	2.89	2.80	2.76	2.80	3.26	4.23	4.98	5.43	5.94	6.58	7.34	8.42
0.3	-38.8	3.05	2.92	2.82	2.77	2.82	3.28	4.26	5.01	5.43	5.97	6.59	7.39	8.41
0.3	-39.1	3.05	2.91	2.84	2.80	2.85	3.32	4.30	5.02	5.47	6.03	6.60	7.39	8.40
0.3	-39.4	3.09	2.94	2.88	2.84	2.91	3.40	4.38	5.11	5.55	6.05	6.66	7.41	8.46
0.3	-39.7	3.13	3.01	2.95	2.91	2.99	3.51	4.51	5.27	5.70	6.19	6.77	7.52	8.50
0.3	-40	3.26	3.11	3.10	3.08	3.16	3.72	4.79	5.58	6.05	6.53	7.09	7.78	8.68

Table A3 - 4 – HEU fuel power density at day 1 (core power at 57.8 MW)

radial node width (cm)		0.3	0.3	0.3	0.3	1	1.734	1	0.3	0.3	0.3	0.3	0.3	0.3
distance (cm) from - inner edge of the fuel	0	0.3	0.6	0.9	1.2	2.2	3.934	4.934	5.234	5.534	5.834	6.134	6.434	6.734
- core center	14	14.29	14.57	14.85	15.13	16.01	17.43	18.19	18.42	18.64	18.86	19.07	19.29	19.5
axial node height (cm)	position to core midplane (cm)	volumetric heat generation rate (W/mm^3)												
	40													
0.3	39.7	9.72	8.72	8.04	7.53	6.84	6.60	7.50	8.38	8.95	9.56	10.26	11.14	12.29
0.3	39.4	9.33	8.25	7.53	7.00	6.34	6.09	6.95	7.80	8.29	8.95	9.70	10.65	11.91
0.3	39.1	9.18	7.99	7.29	6.75	6.11	5.83	6.65	7.51	8.04	8.66	9.43	10.42	11.77
0.3	38.8	9.03	7.85	7.11	6.55	5.90	5.63	6.46	7.31	7.87	8.52	9.28	10.30	11.70
0.3	38.5	8.89	7.71	6.99	6.45	5.75	5.50	6.33	7.18	7.73	8.43	9.21	10.24	11.57
0.3	38.2	8.81	7.65	6.92	6.35	5.66	5.40	6.23	7.09	7.64	8.31	9.14	10.13	11.54
0.3	37.9	8.74	7.59	6.83	6.27	5.59	5.33	6.17	7.06	7.62	8.26	9.11	10.14	11.49
0.3	37.6	8.69	7.55	6.78	6.21	5.54	5.27	6.13	7.00	7.56	8.23	9.05	10.08	11.47
0.3	37.3	8.65	7.50	6.72	6.20	5.50	5.24	6.08	6.97	7.53	8.24	9.04	10.04	11.47
0.3	37	8.61	7.46	6.73	6.16	5.47	5.22	6.09	6.94	7.51	8.18	9.00	10.03	11.42
0.3	36.7	8.60	7.45	6.70	6.15	5.45	5.20	6.04	6.93	7.50	8.20	9.03	10.07	11.45
0.3	36.4	8.61	7.44	6.69	6.16	5.45	5.19	6.05	6.93	7.51	8.18	9.04	10.08	11.46
0.3	36.1	8.54	7.43	6.70	6.15	5.45	5.19	6.06	6.94	7.53	8.18	9.05	10.08	11.48
0.3	35.8	8.57	7.42	6.71	6.15	5.45	5.20	6.06	6.97	7.54	8.17	9.04	10.09	11.51
0.3	35.5	8.55	7.43	6.69	6.14	5.47	5.21	6.08	6.96	7.57	8.22	9.08	10.15	11.53
3.6	31.9	8.67	7.55	6.81	6.25	5.56	5.32	6.21	7.12	7.71	8.41	9.26	10.32	11.74
3.6	28.3	9.08	7.93	7.16	6.60	5.89	5.64	6.58	7.53	8.13	8.86	9.74	10.84	12.30
3.6	24.7	9.59	8.37	7.58	6.99	6.25	5.99	6.97	7.96	8.58	9.33	10.25	11.39	12.92
3.6	21.1	10.04	8.79	7.95	7.34	6.56	6.29	7.29	8.33	8.97	9.76	10.72	11.91	13.49
3.6	17.5	10.35	9.07	8.21	7.59	6.79	6.52	7.56	8.61	9.31	10.10	11.09	12.31	13.94
3.6	13.9	10.50	9.21	8.34	7.71	6.91	6.65	7.73	8.81	9.49	10.33	11.33	12.57	14.23
3.6	10.3	10.27	9.01	8.19	7.58	6.83	6.63	7.76	8.87	9.56	10.41	11.43	12.70	14.38
3.6	6.7	8.94	7.97	7.34	6.89	6.34	6.38	7.62	8.78	9.49	10.34	11.37	12.64	14.33
3.6	3.1	7.31	6.68	6.29	6.01	5.73	6.05	7.41	8.59	9.30	10.17	11.20	12.47	14.17
3.6	-0.5	6.82	6.26	5.91	5.67	5.45	5.83	7.21	8.38	9.10	9.97	10.98	12.25	13.92
3.6	-4.1	6.55	6.02	5.69	5.46	5.26	5.66	7.04	8.18	8.89	9.72	10.74	11.96	13.60
3.6	-7.7	6.29	5.78	5.47	5.26	5.07	5.47	6.81	7.93	8.62	9.43	10.42	11.62	13.21
3.6	-11.3	6.01	5.54	5.23	5.04	4.86	5.25	6.55	7.64	8.32	9.10	10.04	11.21	12.76
3.6	-14.9	5.71	5.26	4.98	4.79	4.63	5.01	6.26	7.31	7.95	8.71	9.61	10.73	12.22
3.6	-18.5	5.37	4.96	4.69	4.51	4.37	4.73	5.92	6.93	7.54	8.27	9.13	10.20	11.63
3.6	-22.1	5.02	4.62	4.38	4.21	4.08	4.43	5.57	6.52	7.10	7.78	8.60	9.62	10.96
3.6	-25.7	4.63	4.26	4.03	3.89	3.77	4.11	5.18	6.07	6.61	7.26	8.03	8.99	10.25
3.6	-29.3	4.22	3.89	3.69	3.55	3.44	3.77	4.78	5.62	6.13	6.73	7.46	8.35	9.53
3.6	-32.9	3.82	3.52	3.34	3.22	3.12	3.44	4.38	5.16	5.64	6.20	6.88	7.71	8.82
3.6	-36.5	3.47	3.19	3.02	2.91	2.83	3.13	4.02	4.76	5.20	5.72	6.35	7.13	8.17
0.5	-37	3.34	3.05	2.89	2.78	2.73	3.02	3.88	4.58	4.99	5.50	6.12	6.86	7.87
0.3	-37.3	3.33	3.06	2.90	2.79	2.71	3.00	3.85	4.57	4.96	5.47	6.08	6.84	7.82
0.3	-37.6	3.34	3.07	2.89	2.78	2.72	3.01	3.85	4.53	4.97	5.49	6.11	6.82	7.85
0.3	-37.9	3.30	3.05	2.89	2.80	2.72	3.02	3.86	4.55	4.98	5.48	6.06	6.80	7.82
0.3	-38.2	3.31	3.05	2.89	2.79	2.74	3.03	3.87	4.57	4.97	5.46	6.05	6.80	7.77
0.3	-38.5	3.32	3.07	2.91	2.82	2.74	3.05	3.89	4.57	4.99	5.48	6.06	6.80	7.77
0.3	-38.8	3.34	3.08	2.92	2.82	2.78	3.08	3.91	4.62	5.01	5.50	6.09	6.81	7.79
0.3	-39.1	3.36	3.11	2.96	2.89	2.82	3.14	3.98	4.65	5.06	5.56	6.14	6.82	7.76
0.3	-39.4	3.41	3.17	3.02	2.95	2.90	3.22	4.07	4.75	5.15	5.61	6.22	6.91	7.82
0.3	-39.7	3.45	3.24	3.11	3.03	3.01	3.35	4.23	4.91	5.28	5.78	6.30	6.97	7.90
0.3	-40	3.58	3.40	3.29	3.21	3.20	3.59	4.53	5.24	5.64	6.08	6.65	7.25	8.09

Table A3 - 5 – HEU fuel power density at day 5 (core power at 57.8 MW)

radial node width (cm)		**0.3**	**0.3**	**0.3**	**0.3**	**1**	**1.734**	**1**	**0.3**	**0.3**	**0.3**	**0.3**	**0.3**	**0.3**
distance (cm) from - inner edge of the fuel	**0**	**0.3**	**0.6**	**0.9**	**1.2**	**2.2**	**3.934**	**4.934**	**5.234**	**5.534**	**5.834**	**6.134**	**6.434**	**6.734**
- core center	**14**	**14.29**	**14.57**	**14.85**	**15.13**	**16.01**	**17.43**	**18.19**	**18.42**	**18.64**	**18.86**	**19.07**	**19.29**	**19.5**
axial node height (cm)	**position to core midplane (cm)**	**volumetric heat generation rate (W/mm^3)**												
	40													
0.3	**39.7**	10.01	9.10	8.42	7.96	7.29	7.09	7.95	8.82	9.26	9.84	10.46	11.20	12.29
0.3	**39.4**	9.58	8.57	7.87	7.39	6.76	6.51	7.30	8.14	8.61	9.20	9.90	10.76	11.91
0.3	**39.1**	9.36	8.29	7.59	7.05	6.41	6.18	6.97	7.77	8.34	8.87	9.61	10.50	11.72
0.3	**38.8**	9.15	8.04	7.33	6.82	6.16	5.94	6.72	7.53	8.04	8.66	9.42	10.35	11.58
0.3	**38.5**	9.06	7.91	7.17	6.68	6.01	5.76	6.55	7.37	7.92	8.52	9.27	10.22	11.46
0.3	**38.2**	8.91	7.82	7.08	6.56	5.88	5.63	6.44	7.27	7.77	8.42	9.18	10.13	11.37
0.3	**37.9**	8.85	7.72	7.03	6.47	5.79	5.53	6.35	7.18	7.68	8.35	9.13	10.05	11.29
0.3	**37.6**	8.72	7.64	6.94	6.37	5.71	5.45	6.27	7.09	7.65	8.26	9.06	9.99	11.28
0.3	**37.3**	8.69	7.57	6.88	6.32	5.64	5.38	6.21	7.05	7.59	8.25	9.04	9.98	11.28
0.3	**37**	8.64	7.54	6.82	6.28	5.60	5.35	6.16	7.02	7.56	8.19	8.99	9.93	11.23
0.3	**36.7**	8.62	7.53	6.77	6.26	5.56	5.31	6.15	7.00	7.53	8.15	8.95	9.92	11.20
0.3	**36.4**	8.52	7.49	6.76	6.22	5.54	5.29	6.13	6.99	7.54	8.20	8.98	9.96	11.21
0.3	**36.1**	8.55	7.49	6.74	6.21	5.53	5.27	6.12	7.00	7.52	8.21	8.96	9.91	11.19
0.3	**35.8**	8.54	7.45	6.75	6.21	5.52	5.27	6.11	7.02	7.53	8.20	8.99	9.89	11.21
0.3	**35.5**	8.52	7.44	6.73	6.21	5.52	5.28	6.12	6.97	7.53	8.19	8.95	9.95	11.23
3.6	**31.9**	8.60	7.52	6.80	6.27	5.60	5.36	6.23	7.12	7.68	8.33	9.12	10.09	11.37
3.6	**28.3**	8.93	7.83	7.12	6.58	5.89	5.65	6.57	7.48	8.06	8.74	9.55	10.54	11.86
3.6	**24.7**	9.38	8.25	7.52	6.95	6.23	5.98	6.93	7.88	8.46	9.17	10.01	11.06	12.40
3.6	**21.1**	9.83	8.66	7.88	7.30	6.56	6.29	7.27	8.25	8.86	9.58	10.46	11.52	12.91
3.6	**17.5**	10.19	9.00	8.19	7.58	6.82	6.54	7.54	8.55	9.18	9.92	10.82	11.92	13.33
3.6	**13.9**	10.42	9.20	8.38	7.77	6.98	6.70	7.72	8.75	9.41	10.17	11.08	12.19	13.63
3.6	**10.3**	10.50	9.26	8.44	7.83	7.05	6.77	7.82	8.86	9.51	10.30	11.22	12.34	13.79
3.6	**6.7**	10.36	9.16	8.35	7.75	6.99	6.75	7.81	8.87	9.52	10.30	11.23	12.35	13.81
3.6	**3.1**	9.72	8.62	7.88	7.34	6.66	6.54	7.65	8.71	9.38	10.16	11.07	12.21	13.68
3.6	**-0.5**	7.85	7.13	6.66	6.31	5.93	6.11	7.37	8.46	9.12	9.89	10.82	11.94	13.40
3.6	**-4.1**	6.72	6.18	5.84	5.60	5.38	5.74	7.05	8.14	8.80	9.58	10.48	11.60	13.05
3.6	**-7.7**	6.28	5.78	5.48	5.27	5.08	5.46	6.77	7.85	8.49	9.24	10.13	11.23	12.63
3.6	**-11.3**	5.94	5.48	5.19	5.00	4.83	5.22	6.48	7.52	8.15	8.88	9.75	10.78	12.16
3.6	**-14.9**	5.60	5.18	4.92	4.74	4.57	4.96	6.18	7.18	7.77	8.48	9.33	10.32	11.63
3.6	**-18.5**	5.26	4.86	4.61	4.44	4.30	4.67	5.84	6.80	7.37	8.05	8.84	9.81	11.08
3.6	**-22.1**	4.90	4.52	4.29	4.14	4.01	4.37	5.47	6.37	6.93	7.57	8.32	9.25	10.45
3.6	**-25.7**	4.51	4.16	3.95	3.81	3.70	4.04	5.08	5.93	6.45	7.07	7.77	8.64	9.79
3.6	**-29.3**	4.12	3.80	3.61	3.48	3.38	3.70	4.68	5.48	5.97	6.54	7.20	8.03	9.10
3.6	**-32.9**	3.73	3.44	3.27	3.15	3.06	3.38	4.29	5.04	5.49	6.03	6.65	7.44	8.45
3.6	**-36.5**	3.41	3.14	2.97	2.87	2.80	3.10	3.96	4.66	5.09	5.60	6.18	6.90	7.87
0.5	**-37**	3.29	3.04	2.86	2.77	2.69	2.99	3.83	4.51	4.91	5.41	5.98	6.65	7.63
0.3	**-37.3**	3.28	3.02	2.87	2.78	2.69	2.99	3.82	4.49	4.90	5.39	5.97	6.66	7.59
0.3	**-37.6**	3.30	3.03	2.87	2.77	2.71	2.99	3.80	4.47	4.89	5.36	5.92	6.63	7.57
0.3	**-37.9**	3.30	3.02	2.88	2.79	2.71	3.01	3.83	4.51	4.89	5.37	5.93	6.60	7.50
0.3	**-38.2**	3.28	3.04	2.88	2.78	2.72	3.02	3.84	4.51	4.90	5.39	5.94	6.63	7.54
0.3	**-38.5**	3.32	3.05	2.91	2.82	2.75	3.06	3.88	4.56	4.94	5.38	5.98	6.63	7.57
0.3	**-38.8**	3.34	3.09	2.94	2.85	2.80	3.10	3.92	4.58	4.96	5.44	5.98	6.64	7.57
0.3	**-39.1**	3.37	3.11	2.97	2.88	2.85	3.17	3.98	4.63	5.00	5.46	6.05	6.69	7.60
0.3	**-39.4**	3.42	3.16	3.03	2.96	2.93	3.27	4.10	4.73	5.14	5.56	6.12	6.75	7.62
0.3	**-39.7**	3.50	3.27	3.15	3.06	3.04	3.40	4.26	4.91	5.28	5.71	6.23	6.87	7.71
0.3	**-40**	3.64	3.46	3.34	3.26	3.26	3.67	4.59	5.25	5.63	6.03	6.56	7.16	7.89

Table A3 - 6 – HEU fuel power density at day 12 (core power at 57.8 MW)

radial node width (cm)		0.3	0.3	0.3	0.3	1	1.734	1	0.3	0.3	0.3	0.3	0.3	0.3
distance (cm) from - inner edge of the fuel	0	0.3	0.6	0.9	1.2	2.2	3.934	4.934	5.234	5.534	5.834	6.134	6.434	6.734
- core center	14	14.29	14.57	14.85	15.13	16.01	17.43	18.19	18.42	18.64	18.86	19.07	19.29	19.5
axial node height (cm)	position to core midplane (cm)	volumetric heat generation rate (W/mm^3)												
	40													
0.3	39.7	10.75	9.96	9.43	9.02	8.50	8.31	9.07	9.70	10.14	10.64	11.13	11.71	12.55
0.3	39.4	10.26	9.34	8.77	8.33	7.75	7.55	8.31	9.03	9.42	9.90	10.49	11.18	12.10
0.3	39.1	9.92	8.99	8.36	7.87	7.29	7.08	7.83	8.54	8.97	9.48	10.07	10.80	11.81
0.3	38.8	9.67	8.71	8.05	7.56	6.94	6.73	7.49	8.24	8.69	9.21	9.84	10.58	11.60
0.3	38.5	9.49	8.47	7.81	7.33	6.69	6.47	7.22	7.99	8.46	8.98	9.64	10.43	11.42
0.3	38.2	9.33	8.34	7.65	7.11	6.49	6.26	7.02	7.80	8.28	8.85	9.49	10.31	11.29
0.3	37.9	9.21	8.18	7.49	6.99	6.33	6.08	6.86	7.68	8.14	8.72	9.36	10.18	11.21
0.3	37.6	9.08	8.06	7.38	6.88	6.21	5.95	6.74	7.53	8.03	8.59	9.26	10.10	11.11
0.3	37.3	8.98	7.99	7.26	6.78	6.10	5.86	6.65	7.45	7.92	8.54	9.21	10.02	11.05
0.3	37	8.89	7.91	7.20	6.70	6.04	5.77	6.56	7.39	7.87	8.45	9.17	9.95	11.01
0.3	36.7	8.83	7.87	7.15	6.64	5.98	5.71	6.51	7.32	7.84	8.44	9.11	9.93	10.97
0.3	36.4	8.77	7.79	7.09	6.57	5.94	5.67	6.47	7.28	7.80	8.39	9.06	9.91	10.92
0.3	36.1	8.68	7.71	7.06	6.53	5.88	5.62	6.42	7.19	7.74	8.35	9.02	9.87	10.92
0.3	35.8	8.70	7.71	7.00	6.49	5.85	5.58	6.42	7.24	7.74	8.32	9.03	9.84	10.89
0.3	35.5	8.61	7.67	7.00	6.47	5.83	5.57	6.38	7.23	7.71	8.35	9.02	9.83	10.89
3.6	31.9	8.58	7.63	6.97	6.47	5.82	5.58	6.43	7.26	7.77	8.36	9.06	9.87	10.91
3.6	28.3	8.76	7.81	7.14	6.66	6.02	5.79	6.66	7.50	8.02	8.63	9.33	10.16	11.21
3.6	24.7	9.09	8.13	7.48	6.97	6.30	6.09	6.98	7.85	8.37	8.98	9.70	10.54	11.60
3.6	21.1	9.46	8.48	7.80	7.28	6.60	6.37	7.29	8.17	8.71	9.33	10.06	10.91	11.98
3.6	17.5	9.76	8.77	8.07	7.55	6.85	6.60	7.54	8.43	8.99	9.63	10.37	11.22	12.31
3.6	13.9	9.98	8.96	8.26	7.72	7.02	6.76	7.71	8.62	9.19	9.83	10.58	11.45	12.53
3.6	10.3	10.09	9.07	8.35	7.81	7.10	6.85	7.81	8.74	9.29	9.94	10.70	11.57	12.66
3.6	6.7	10.06	9.04	8.33	7.78	7.08	6.84	7.82	8.75	9.31	9.96	10.71	11.59	12.68
3.6	3.1	9.92	8.90	8.19	7.65	6.96	6.75	7.73	8.66	9.23	9.88	10.63	11.50	12.58
3.6	-0.5	9.42	8.42	7.77	7.26	6.63	6.50	7.51	8.46	9.02	9.67	10.42	11.29	12.37
3.6	-4.1	7.75	7.07	6.61	6.28	5.90	6.05	7.18	8.15	8.71	9.36	10.11	10.98	12.06
3.6	-7.7	6.42	5.94	5.65	5.44	5.25	5.60	6.81	7.77	8.34	8.99	9.73	10.59	11.68
3.6	-11.3	5.90	5.48	5.22	5.03	4.89	5.27	6.48	7.43	7.98	8.60	9.34	10.18	11.23
3.6	-14.9	5.52	5.13	4.89	4.73	4.59	4.98	6.14	7.06	7.59	8.20	8.92	9.74	10.76
3.6	-18.5	5.17	4.80	4.57	4.42	4.30	4.68	5.79	6.68	7.20	7.79	8.47	9.26	10.27
3.6	-22.1	4.80	4.46	4.25	4.11	4.00	4.37	5.42	6.27	6.77	7.34	8.00	8.75	9.73
3.6	-25.7	4.42	4.10	3.91	3.79	3.69	4.04	5.05	5.85	6.31	6.85	7.49	8.22	9.15
3.6	-29.3	4.05	3.75	3.58	3.46	3.37	3.71	4.66	5.42	5.86	6.37	6.97	7.68	8.57
3.6	-32.9	3.69	3.41	3.25	3.14	3.06	3.39	4.28	4.99	5.42	5.91	6.47	7.14	8.00
3.6	-36.5	3.40	3.14	2.98	2.88	2.81	3.12	3.97	4.64	5.03	5.50	6.04	6.69	7.52
0.5	-37	3.30	3.06	2.92	2.81	2.74	3.05	3.86	4.52	4.91	5.36	5.88	6.50	7.31
0.3	-37.3	3.31	3.05	2.90	2.80	2.75	3.05	3.87	4.51	4.89	5.33	5.86	6.49	7.28
0.3	-37.6	3.34	3.06	2.91	2.81	2.77	3.06	3.88	4.51	4.91	5.34	5.84	6.49	7.31
0.3	-37.9	3.32	3.07	2.92	2.84	2.78	3.08	3.89	4.54	4.91	5.32	5.87	6.50	7.29
0.3	-38.2	3.34	3.09	2.95	2.85	2.80	3.11	3.92	4.55	4.92	5.38	5.88	6.48	7.27
0.3	-38.5	3.36	3.13	2.98	2.89	2.84	3.15	3.95	4.58	4.96	5.42	5.89	6.47	7.30
0.3	-38.8	3.39	3.15	3.02	2.94	2.90	3.22	4.02	4.65	5.03	5.44	5.94	6.56	7.33
0.3	-39.1	3.48	3.23	3.08	3.00	2.96	3.30	4.10	4.72	5.10	5.49	5.98	6.60	7.37
0.3	-39.4	3.52	3.28	3.15	3.08	3.07	3.41	4.24	4.85	5.21	5.61	6.10	6.68	7.42
0.3	-39.7	3.62	3.40	3.28	3.21	3.22	3.58	4.43	5.01	5.37	5.78	6.27	6.78	7.51
0.3	-40	3.80	3.58	3.51	3.47	3.47	3.89	4.77	5.37	5.75	6.12	6.55	7.04	7.74

Table A3 - 7 – HEU fuel power density at day 18 (core power at 57.8 MW)

radial node width (cm)		0.3	0.3	0.3	0.3	1	1.734	1	0.3	0.3	0.3	0.3	0.3	0.3
distance (cm) from - inner edge of the fuel	0	0.3	0.6	0.9	1.2	2.2	3.934	4.934	5.234	5.534	5.834	6.134	6.434	6.734
- core center	14	14.29	14.57	14.85	15.13	16.01	17.43	18.19	18.42	18.64	18.86	19.07	19.29	19.5
axial node height (cm)	**position to core midplane (cm)**	**volumetric heat generation rate (W/mm^3)**												
	40													
0.3	**39.7**	11.45	10.83	10.38	10.07	9.62	9.48	10.05	10.61	10.89	11.25	11.67	12.08	12.65
0.3	**39.4**	10.87	10.10	9.62	9.26	8.76	8.58	9.18	9.80	10.08	10.51	10.96	11.52	12.17
0.3	**39.1**	10.49	9.68	9.10	8.73	8.19	7.98	8.62	9.21	9.60	10.05	10.51	11.11	11.89
0.3	**38.8**	10.18	9.35	8.77	8.33	7.76	7.53	8.17	8.81	9.21	9.69	10.22	10.85	11.60
0.3	**38.5**	9.93	9.08	8.44	8.00	7.41	7.16	7.86	8.52	8.95	9.41	9.93	10.63	11.40
0.3	**38.2**	9.73	8.84	8.22	7.75	7.13	6.87	7.59	8.25	8.70	9.22	9.76	10.44	11.25
0.3	**37.9**	9.54	8.65	8.02	7.53	6.91	6.65	7.38	8.08	8.53	9.04	9.62	10.31	11.08
0.3	**37.6**	9.40	8.49	7.87	7.37	6.74	6.48	7.21	7.93	8.42	8.90	9.51	10.15	11.00
0.3	**37.3**	9.30	8.39	7.72	7.22	6.58	6.32	7.08	7.83	8.29	8.78	9.39	10.06	10.90
0.3	**37**	9.14	8.25	7.60	7.11	6.47	6.21	6.95	7.73	8.15	8.68	9.26	10.00	10.84
0.3	**36.7**	9.03	8.14	7.52	7.00	6.36	6.11	6.88	7.62	8.07	8.58	9.19	9.92	10.77
0.3	**36.4**	8.96	8.07	7.41	6.93	6.30	6.02	6.80	7.58	8.03	8.57	9.17	9.86	10.72
0.3	**36.1**	8.88	8.00	7.36	6.85	6.23	5.97	6.75	7.52	7.94	8.53	9.10	9.80	10.66
0.3	**35.8**	8.80	7.93	7.27	6.80	6.18	5.91	6.70	7.47	7.95	8.47	9.06	9.77	10.60
0.3	**35.5**	8.75	7.85	7.22	6.76	6.11	5.87	6.69	7.45	7.91	8.44	9.05	9.75	10.59
3.6	**31.9**	8.58	7.72	7.11	6.64	6.02	5.80	6.60	7.38	7.84	8.36	8.96	9.66	10.50
3.6	**28.3**	8.58	7.76	7.17	6.73	6.12	5.92	6.75	7.52	7.99	8.52	9.12	9.80	10.62
3.6	**24.7**	8.82	8.01	7.42	6.97	6.37	6.17	7.01	7.80	8.27	8.80	9.40	10.08	10.88
3.6	**21.1**	9.12	8.29	7.69	7.24	6.62	6.43	7.29	8.08	8.56	9.09	9.68	10.37	11.17
3.6	**17.5**	9.36	8.54	7.93	7.46	6.84	6.63	7.51	8.32	8.79	9.33	9.93	10.61	11.40
3.6	**13.9**	9.55	8.71	8.11	7.64	7.00	6.79	7.67	8.49	8.97	9.51	10.11	10.80	11.58
3.6	**10.3**	9.65	8.81	8.20	7.73	7.09	6.88	7.77	8.59	9.07	9.60	10.21	10.89	11.69
3.6	**6.7**	9.68	8.83	8.22	7.75	7.10	6.89	7.79	8.61	9.09	9.64	10.24	10.92	11.72
3.6	**3.1**	9.62	8.75	8.13	7.66	7.02	6.82	7.72	8.55	9.03	9.57	10.17	10.85	11.64
3.6	**-0.5**	9.48	8.60	7.96	7.48	6.85	6.66	7.56	8.38	8.87	9.40	10.01	10.70	11.50
3.6	**-4.1**	8.97	8.11	7.49	7.05	6.47	6.36	7.30	8.12	8.61	9.15	9.77	10.44	11.24
3.6	**-7.7**	7.30	6.71	6.32	6.03	5.69	5.86	6.91	7.77	8.25	8.79	9.39	10.09	10.91
3.6	**-11.3**	6.02	5.62	5.36	5.18	5.03	5.39	6.50	7.35	7.85	8.41	9.02	9.71	10.52
3.6	**-14.9**	5.51	5.15	4.92	4.76	4.65	5.03	6.13	6.98	7.46	8.00	8.61	9.29	10.09
3.6	**-18.5**	5.12	4.78	4.57	4.44	4.33	4.71	5.78	6.58	7.05	7.59	8.17	8.85	9.64
3.6	**-22.1**	4.75	4.43	4.24	4.11	4.02	4.38	5.41	6.19	6.65	7.16	7.72	8.38	9.16
3.6	**-25.7**	4.37	4.09	3.91	3.78	3.70	4.05	5.03	5.79	6.21	6.70	7.25	7.89	8.66
3.6	**-29.3**	4.01	3.73	3.57	3.45	3.38	3.72	4.65	5.36	5.78	6.24	6.78	7.40	8.15
3.6	**-32.9**	3.66	3.41	3.25	3.15	3.08	3.41	4.28	4.96	5.36	5.80	6.32	6.91	7.65
3.6	**-36.5**	3.40	3.15	3.01	2.91	2.85	3.16	4.00	4.64	5.02	5.45	5.93	6.52	7.24
0.5	**-37**	3.33	3.08	2.96	2.85	2.81	3.11	3.93	4.57	4.91	5.34	5.80	6.38	7.09
0.3	**-37.3**	3.36	3.11	2.96	2.88	2.82	3.13	3.94	4.54	4.90	5.34	5.82	6.39	7.10
0.3	**-37.6**	3.37	3.11	2.98	2.89	2.84	3.15	3.96	4.59	4.93	5.35	5.83	6.39	7.10
0.3	**-37.9**	3.40	3.14	3.02	2.92	2.86	3.18	3.99	4.61	4.96	5.36	5.82	6.36	7.08
0.3	**-38.2**	3.42	3.17	3.03	2.94	2.91	3.22	4.00	4.63	4.97	5.39	5.85	6.35	7.11
0.3	**-38.5**	3.46	3.19	3.09	2.99	2.95	3.28	4.06	4.65	5.03	5.42	5.87	6.42	7.15
0.3	**-38.8**	3.48	3.24	3.12	3.05	3.03	3.35	4.14	4.73	5.08	5.47	5.93	6.49	7.17
0.3	**-39.1**	3.55	3.30	3.21	3.14	3.11	3.45	4.24	4.84	5.20	5.57	5.98	6.53	7.22
0.3	**-39.4**	3.62	3.41	3.28	3.23	3.23	3.58	4.39	4.97	5.32	5.73	6.10	6.61	7.29
0.3	**-39.7**	3.74	3.54	3.43	3.40	3.40	3.78	4.60	5.18	5.51	5.86	6.28	6.80	7.37
0.3	**-40**	3.93	3.77	3.69	3.63	3.67	4.11	4.96	5.57	5.88	6.21	6.58	7.07	7.62

Table A3 - 8 – HEU fuel power density at day 24 (core power at 57.8 MW)

radial node width (cm)		0.3	0.3	0.3	0.3	1	1.734	1	0.3	0.3	0.3	0.3	0.3	0.3
distance (cm) from - inner edge of the fuel	0	0.3	0.6	0.9	1.2	2.2	3.934	4.934	5.234	5.534	5.834	6.134	6.434	6.734
- core center	14	14.29	14.57	14.85	15.13	16.01	17.43	18.19	18.42	18.64	18.86	19.07	19.29	19.5
axial node height (cm)	position to core midplane (cm)	volumetric heat generation rate (W/mm^3)												
	40													
0.3	39.7	11.72	11.34	11.03	10.77	10.47	10.33	10.75	11.11	11.35	11.52	11.78	12.04	12.35
0.3	39.4	11.17	10.67	10.24	9.95	9.57	9.39	9.87	10.29	10.55	10.81	11.14	11.50	11.91
0.3	39.1	10.79	10.14	9.70	9.34	8.92	8.74	9.25	9.72	10.02	10.34	10.70	11.13	11.64
0.3	38.8	10.43	9.75	9.27	8.88	8.41	8.20	8.76	9.30	9.61	9.99	10.39	10.83	11.39
0.3	38.5	10.16	9.42	8.96	8.52	8.00	7.79	8.36	8.95	9.29	9.68	10.12	10.61	11.16
0.3	38.2	9.90	9.16	8.64	8.23	7.68	7.43	8.06	8.69	9.05	9.43	9.87	10.36	10.97
0.3	37.9	9.71	8.96	8.43	7.96	7.42	7.16	7.80	8.42	8.84	9.23	9.69	10.23	10.82
0.3	37.6	9.52	8.75	8.17	7.77	7.17	6.93	7.59	8.27	8.63	9.04	9.53	10.05	10.69
0.3	37.3	9.36	8.60	8.03	7.59	6.99	6.74	7.43	8.08	8.49	8.91	9.41	9.95	10.59
0.3	37	9.24	8.47	7.90	7.45	6.85	6.59	7.29	7.98	8.37	8.81	9.29	9.89	10.52
0.3	36.7	9.10	8.34	7.79	7.32	6.72	6.46	7.18	7.86	8.24	8.71	9.21	9.79	10.40
0.3	36.4	9.01	8.25	7.69	7.25	6.63	6.35	7.08	7.80	8.18	8.67	9.15	9.67	10.29
0.3	36.1	8.89	8.14	7.54	7.14	6.54	6.27	7.01	7.71	8.07	8.56	9.05	9.63	10.23
0.3	35.8	8.84	8.05	7.49	7.01	6.45	6.20	6.94	7.65	8.04	8.51	9.00	9.57	10.19
0.3	35.5	8.73	7.99	7.46	6.98	6.39	6.15	6.89	7.56	7.97	8.43	8.95	9.52	10.15
3.6	31.9	8.49	7.76	7.20	6.78	6.20	5.99	6.74	7.45	7.85	8.31	8.81	9.37	10.01
3.6	28.3	8.37	7.68	7.16	6.75	6.21	6.02	6.80	7.50	7.91	8.35	8.84	9.38	9.99
3.6	24.7	8.52	7.85	7.33	6.94	6.40	6.23	7.00	7.70	8.11	8.55	9.04	9.56	10.15
3.6	21.1	8.73	8.06	7.56	7.17	6.62	6.45	7.23	7.93	8.33	8.78	9.25	9.76	10.34
3.6	17.5	8.94	8.28	7.76	7.36	6.82	6.66	7.44	8.15	8.55	8.99	9.45	9.96	10.52
3.6	13.9	9.09	8.43	7.92	7.53	6.98	6.80	7.59	8.31	8.70	9.14	9.60	10.11	10.65
3.6	10.3	9.19	8.53	8.01	7.61	7.06	6.88	7.68	8.39	8.79	9.22	9.68	10.18	10.72
3.6	6.7	9.23	8.55	8.04	7.64	7.08	6.91	7.71	8.41	8.82	9.25	9.72	10.21	10.75
3.6	3.1	9.25	8.54	8.02	7.60	7.03	6.86	7.67	8.38	8.78	9.22	9.68	10.18	10.72
3.6	-0.5	9.24	8.48	7.94	7.50	6.92	6.75	7.55	8.26	8.66	9.11	9.58	10.09	10.63
3.6	-4.1	9.09	8.30	7.74	7.29	6.71	6.55	7.36	8.07	8.47	8.91	9.38	9.90	10.46
3.6	-7.7	8.64	7.85	7.29	6.86	6.32	6.22	7.07	7.77	8.18	8.63	9.11	9.63	10.20
3.6	-11.3	7.11	6.56	6.18	5.89	5.57	5.70	6.65	7.39	7.80	8.27	8.76	9.28	9.89
3.6	-14.9	5.73	5.37	5.14	4.98	4.84	5.18	6.21	6.96	7.38	7.83	8.34	8.88	9.49
3.6	-18.5	5.17	4.85	4.64	4.52	4.42	4.79	5.81	6.56	6.98	7.43	7.93	8.48	9.10
3.6	-22.1	4.76	4.47	4.28	4.16	4.08	4.45	5.43	6.16	6.57	7.02	7.50	8.06	8.68
3.6	-25.7	4.38	4.10	3.94	3.82	3.75	4.11	5.06	5.76	6.15	6.58	7.08	7.62	8.24
3.6	-29.3	4.02	3.76	3.60	3.50	3.43	3.78	4.68	5.35	5.73	6.15	6.63	7.16	7.80
3.6	-32.9	3.68	3.43	3.29	3.20	3.13	3.46	4.32	4.97	5.34	5.75	6.22	6.74	7.37
3.6	-36.5	3.44	3.20	3.06	2.97	2.92	3.24	4.06	4.68	5.04	5.43	5.88	6.40	7.04
0.5	-37	3.41	3.17	3.03	2.94	2.89	3.21	4.01	4.60	4.94	5.35	5.81	6.31	6.93
0.3	-37.3	3.42	3.18	3.04	2.97	2.92	3.22	4.01	4.62	4.99	5.37	5.81	6.34	6.91
0.3	-37.6	3.45	3.20	3.06	2.98	2.94	3.25	4.04	4.63	5.00	5.39	5.83	6.36	6.93
0.3	-37.9	3.48	3.22	3.11	3.01	2.98	3.29	4.08	4.67	5.01	5.38	5.81	6.31	6.93
0.3	-38.2	3.52	3.26	3.15	3.06	3.03	3.34	4.12	4.71	5.06	5.45	5.84	6.34	7.01
0.3	-38.5	3.55	3.32	3.20	3.11	3.09	3.42	4.20	4.77	5.13	5.48	5.90	6.38	6.97
0.3	-38.8	3.62	3.39	3.28	3.18	3.17	3.52	4.28	4.85	5.15	5.54	5.98	6.46	7.06
0.3	-39.1	3.69	3.46	3.35	3.30	3.29	3.63	4.42	4.97	5.27	5.65	6.04	6.52	7.12
0.3	-39.4	3.78	3.58	3.47	3.43	3.43	3.80	4.59	5.12	5.43	5.78	6.15	6.64	7.23
0.3	-39.7	3.93	3.71	3.65	3.60	3.62	4.02	4.82	5.34	5.64	5.97	6.34	6.77	7.30
0.3	-40	4.12	3.98	3.91	3.89	3.93	4.39	5.21	5.76	6.01	6.29	6.65	7.04	7.53

Table A3 - 9 – HEU fuel power density at day 30 (core power at 57.8 MW)

radial node width (cm)		0.3	0.3	0.3	0.3	1	1.734	1	0.3	0.3	0.3	0.3	0.3	0.3
distance (cm) from - inner edge of the fuel	0	0.3	0.6	0.9	1.2	2.2	3.934	4.934	5.234	5.534	5.834	6.134	6.434	6.734
- core center	14	14.29	14.57	14.85	15.13	16.01	17.43	18.19	18.42	18.64	18.86	19.07	19.29	19.5
axial node height (cm)	position to core midplane (cm)	volumetric heat generation rate (W/mm^3)												
	40													
0.3	39.7	11.25	10.95	10.83	10.67	10.51	10.41	10.65	10.84	10.95	11.07	11.17	11.24	11.38
0.3	39.4	10.76	10.44	10.16	9.96	9.69	9.57	9.89	10.18	10.36	10.56	10.68	10.87	11.09
0.3	39.1	10.40	9.98	9.65	9.43	9.06	8.93	9.31	9.70	9.86	10.07	10.31	10.55	10.84
0.3	38.8	10.13	9.64	9.27	9.00	8.59	8.41	8.86	9.26	9.50	9.72	10.02	10.30	10.62
0.3	38.5	9.85	9.34	8.94	8.64	8.19	8.00	8.47	8.95	9.19	9.46	9.76	10.10	10.45
0.3	38.2	9.63	9.09	8.65	8.33	7.86	7.66	8.17	8.64	8.95	9.23	9.56	9.90	10.27
0.3	37.9	9.44	8.86	8.43	8.08	7.58	7.36	7.92	8.44	8.70	9.03	9.38	9.71	10.12
0.3	37.6	9.25	8.71	8.23	7.85	7.35	7.12	7.68	8.21	8.52	8.84	9.19	9.55	9.99
0.3	37.3	9.12	8.51	8.09	7.66	7.15	6.91	7.52	8.08	8.37	8.72	9.08	9.48	9.89
0.3	37	9.01	8.38	7.87	7.49	6.98	6.74	7.36	7.96	8.26	8.60	8.97	9.39	9.80
0.3	36.7	8.86	8.25	7.75	7.37	6.83	6.60	7.23	7.81	8.17	8.50	8.90	9.33	9.71
0.3	36.4	8.72	8.10	7.65	7.26	6.72	6.50	7.13	7.72	8.08	8.44	8.83	9.20	9.66
0.3	36.1	8.64	8.03	7.55	7.14	6.63	6.40	7.05	7.65	7.97	8.35	8.75	9.16	9.56
0.3	35.8	8.53	7.95	7.44	7.09	6.54	6.31	6.99	7.57	7.92	8.27	8.67	9.11	9.54
0.3	35.5	8.48	7.85	7.42	7.01	6.46	6.24	6.89	7.49	7.85	8.24	8.60	9.02	9.50
3.6	31.9	8.17	7.57	7.11	6.74	6.22	6.04	6.72	7.33	7.67	8.04	8.44	8.87	9.31
3.6	28.3	7.98	7.43	7.00	6.65	6.17	6.02	6.72	7.33	7.66	8.02	8.41	8.80	9.22
3.6	24.7	8.07	7.55	7.13	6.79	6.33	6.19	6.89	7.50	7.83	8.18	8.54	8.93	9.30
3.6	21.1	8.25	7.74	7.33	7.00	6.53	6.40	7.11	7.70	8.03	8.37	8.73	9.08	9.45
3.6	17.5	8.42	7.92	7.51	7.19	6.73	6.60	7.29	7.89	8.21	8.55	8.89	9.24	9.57
3.6	13.9	8.56	8.07	7.66	7.34	6.88	6.75	7.45	8.04	8.35	8.68	9.02	9.36	9.68
3.6	10.3	8.68	8.18	7.78	7.44	6.98	6.85	7.55	8.14	8.45	8.78	9.12	9.45	9.76
3.6	6.7	8.76	8.25	7.84	7.50	7.03	6.90	7.60	8.19	8.49	8.82	9.16	9.51	9.82
3.6	3.1	8.83	8.28	7.86	7.51	7.02	6.88	7.58	8.17	8.49	8.83	9.15	9.50	9.82
3.6	-0.5	8.90	8.31	7.84	7.47	6.96	6.80	7.51	8.11	8.42	8.76	9.11	9.45	9.78
3.6	-4.1	8.93	8.27	7.77	7.37	6.84	6.67	7.38	7.98	8.30	8.64	9.00	9.35	9.70
3.6	-7.7	8.85	8.12	7.59	7.18	6.64	6.46	7.17	7.78	8.12	8.46	8.83	9.19	9.57
3.6	-11.3	8.53	7.78	7.25	6.84	6.31	6.16	6.89	7.51	7.85	8.21	8.58	8.97	9.37
3.6	-14.9	7.62	6.95	6.49	6.15	5.73	5.71	6.50	7.14	7.49	7.86	8.25	8.66	9.08
3.6	-18.5	5.88	5.49	5.23	5.07	4.89	5.14	6.04	6.70	7.06	7.45	7.86	8.29	8.76
3.6	-22.1	4.99	4.70	4.52	4.40	4.30	4.65	5.59	6.27	6.62	7.02	7.43	7.89	8.37
3.6	-25.7	4.52	4.25	4.08	3.98	3.91	4.26	5.18	5.85	6.21	6.59	7.01	7.46	7.97
3.6	-29.3	4.12	3.88	3.72	3.62	3.56	3.91	4.80	5.44	5.80	6.19	6.60	7.07	7.58
3.6	-32.9	3.78	3.55	3.41	3.31	3.26	3.59	4.45	5.07	5.42	5.80	6.22	6.69	7.21
3.6	-36.5	3.57	3.33	3.19	3.10	3.05	3.38	4.20	4.80	5.14	5.52	5.93	6.39	6.93
0.5	-37	3.55	3.33	3.18	3.11	3.05	3.39	4.17	4.76	5.11	5.46	5.87	6.33	6.88
0.3	-37.3	3.61	3.36	3.22	3.13	3.10	3.42	4.20	4.77	5.13	5.47	5.88	6.35	6.90
0.3	-37.6	3.62	3.37	3.25	3.15	3.13	3.46	4.24	4.83	5.15	5.50	5.92	6.32	6.93
0.3	-37.9	3.65	3.40	3.30	3.21	3.18	3.51	4.29	4.84	5.18	5.54	5.94	6.37	6.93
0.3	-38.2	3.70	3.48	3.34	3.27	3.23	3.57	4.34	4.90	5.22	5.57	5.98	6.42	6.98
0.3	-38.5	3.77	3.53	3.41	3.33	3.32	3.65	4.40	4.97	5.29	5.64	6.01	6.47	7.00
0.3	-38.8	3.84	3.62	3.48	3.41	3.41	3.76	4.53	5.07	5.36	5.71	6.08	6.54	7.07
0.3	-39.1	3.92	3.70	3.61	3.54	3.54	3.91	4.66	5.19	5.51	5.83	6.17	6.61	7.14
0.3	-39.4	4.04	3.85	3.72	3.68	3.70	4.11	4.85	5.38	5.66	5.99	6.33	6.73	7.21
0.3	-39.7	4.20	4.03	3.94	3.89	3.94	4.36	5.12	5.64	5.90	6.21	6.51	6.88	7.36
0.3	-40	4.42	4.31	4.25	4.24	4.30	4.77	5.56	6.01	6.28	6.54	6.84	7.16	7.54

Table A3 - 10 – HEU fuel power density at day 36 (core power at 57.8 MW)

radial node width (cm)		0.3	0.3	0.3	0.3	1	1.734	1	0.3	0.3	0.3	0.3	0.3	0.3
distance (cm) from - inner edge of the fuel	0	0.3	0.6	0.9	1.2	2.2	3.934	4.934	5.234	5.534	5.834	6.134	6.434	6.734
- core center	14	14.29	14.57	14.85	15.13	16.01	17.43	18.19	18.42	18.64	18.86	19.07	19.29	19.5
axial node height (cm)	position to core midplane (cm)	volumetric heat generation rate (W/mm^3)												
	40													
0.3	39.7	9.97	9.89	9.84	9.78	9.69	9.65	9.75	9.83	9.86	9.89	9.90	9.93	9.86
0.3	39.4	9.71	9.54	9.39	9.26	9.13	9.03	9.22	9.40	9.47	9.56	9.61	9.68	9.69
0.3	39.1	9.45	9.19	9.01	8.86	8.63	8.52	8.79	9.02	9.15	9.26	9.36	9.48	9.53
0.3	38.8	9.23	8.91	8.69	8.52	8.22	8.08	8.43	8.70	8.86	9.00	9.12	9.28	9.42
0.3	38.5	9.02	8.70	8.42	8.20	7.88	7.73	8.11	8.42	8.60	8.76	8.94	9.13	9.28
0.3	38.2	8.83	8.47	8.21	7.97	7.59	7.42	7.83	8.18	8.40	8.59	8.80	8.98	9.14
0.3	37.9	8.65	8.30	7.95	7.70	7.33	7.16	7.61	8.02	8.21	8.44	8.63	8.86	9.04
0.3	37.6	8.56	8.13	7.82	7.54	7.12	6.95	7.41	7.83	8.05	8.30	8.52	8.75	8.96
0.3	37.3	8.41	7.99	7.64	7.35	6.94	6.76	7.25	7.68	7.92	8.17	8.42	8.65	8.85
0.3	37	8.26	7.87	7.51	7.21	6.78	6.60	7.11	7.58	7.80	8.03	8.30	8.54	8.78
0.3	36.7	8.16	7.76	7.41	7.11	6.65	6.47	6.99	7.47	7.70	7.98	8.26	8.45	8.72
0.3	36.4	8.07	7.65	7.27	7.00	6.54	6.35	6.91	7.37	7.63	7.89	8.16	8.40	8.64
0.3	36.1	7.99	7.56	7.16	6.88	6.43	6.25	6.81	7.27	7.53	7.84	8.08	8.36	8.61
0.3	35.8	7.90	7.46	7.12	6.78	6.34	6.17	6.73	7.23	7.46	7.75	8.04	8.29	8.59
0.3	35.5	7.86	7.39	7.03	6.72	6.28	6.10	6.66	7.15	7.43	7.71	7.95	8.26	8.51
3.6	31.9	7.55	7.12	6.77	6.47	6.03	5.88	6.47	6.98	7.25	7.53	7.82	8.09	8.36
3.6	28.3	7.38	6.97	6.63	6.36	5.96	5.84	6.45	6.94	7.21	7.49	7.76	8.02	8.25
3.6	24.7	7.46	7.07	6.75	6.48	6.10	6.00	6.61	7.10	7.36	7.62	7.88	8.12	8.33
3.6	21.1	7.61	7.25	6.94	6.67	6.30	6.20	6.81	7.28	7.53	7.78	8.02	8.24	8.42
3.6	17.5	7.79	7.43	7.13	6.87	6.50	6.41	7.01	7.47	7.71	7.96	8.18	8.38	8.55
3.6	13.9	7.92	7.58	7.28	7.03	6.67	6.58	7.17	7.63	7.86	8.09	8.31	8.51	8.64
3.6	10.3	8.06	7.72	7.43	7.17	6.80	6.70	7.30	7.76	7.98	8.21	8.43	8.61	8.73
3.6	6.7	8.17	7.82	7.53	7.26	6.88	6.79	7.39	7.84	8.07	8.30	8.51	8.70	8.81
3.6	3.1	8.31	7.93	7.61	7.32	6.93	6.82	7.41	7.88	8.12	8.35	8.57	8.76	8.90
3.6	-0.5	8.46	8.03	7.67	7.36	6.93	6.80	7.40	7.87	8.12	8.36	8.59	8.78	8.92
3.6	-4.1	8.63	8.10	7.69	7.35	6.90	6.73	7.34	7.83	8.08	8.33	8.58	8.78	8.95
3.6	-7.7	8.70	8.10	7.65	7.28	6.79	6.61	7.22	7.72	7.97	8.25	8.50	8.72	8.91
3.6	-11.3	8.66	8.00	7.51	7.12	6.60	6.42	7.05	7.56	7.84	8.11	8.39	8.63	8.87
3.6	-14.9	8.48	7.78	7.27	6.88	6.35	6.18	6.81	7.33	7.62	7.91	8.20	8.49	8.74
3.6	-18.5	8.11	7.39	6.89	6.51	6.01	5.86	6.50	7.05	7.33	7.64	7.95	8.27	8.56
3.6	-22.1	7.46	6.79	6.32	5.96	5.52	5.44	6.12	6.67	6.97	7.30	7.63	7.98	8.31
3.6	-25.7	6.03	5.57	5.25	5.00	4.74	4.87	5.64	6.24	6.55	6.89	7.23	7.60	7.98
3.6	-29.3	4.69	4.41	4.23	4.11	4.01	4.31	5.17	5.76	6.09	6.45	6.82	7.20	7.62
3.6	-32.9	4.15	3.90	3.74	3.63	3.57	3.91	4.77	5.38	5.70	6.05	6.44	6.85	7.29
3.6	-36.5	3.89	3.64	3.50	3.40	3.35	3.68	4.51	5.11	5.44	5.79	6.18	6.60	7.07
0.5	-37	3.91	3.66	3.51	3.41	3.38	3.71	4.52	5.10	5.42	5.76	6.15	6.57	7.04
0.3	-37.3	3.94	3.69	3.55	3.45	3.41	3.75	4.57	5.13	5.44	5.78	6.20	6.60	7.08
0.3	-37.6	3.97	3.75	3.58	3.50	3.46	3.79	4.60	5.16	5.49	5.83	6.21	6.60	7.08
0.3	-37.9	4.02	3.78	3.65	3.57	3.53	3.86	4.65	5.23	5.52	5.88	6.26	6.66	7.13
0.3	-38.2	4.07	3.85	3.71	3.65	3.61	3.94	4.72	5.28	5.59	5.92	6.30	6.68	7.14
0.3	-38.5	4.15	3.93	3.79	3.72	3.69	4.06	4.82	5.36	5.65	5.98	6.37	6.77	7.19
0.3	-38.8	4.23	4.03	3.90	3.82	3.81	4.18	4.95	5.49	5.76	6.07	6.44	6.81	7.25
0.3	-39.1	4.36	4.15	4.04	3.96	3.98	4.35	5.12	5.65	5.91	6.21	6.50	6.89	7.35
0.3	-39.4	4.50	4.30	4.19	4.15	4.18	4.58	5.32	5.82	6.07	6.38	6.67	6.99	7.42
0.3	-39.7	4.65	4.49	4.42	4.38	4.44	4.88	5.62	6.11	6.34	6.62	6.89	7.19	7.55
0.3	-40	4.95	4.83	4.78	4.77	4.87	5.32	6.07	6.52	6.71	6.95	7.19	7.48	7.78

Table A3 - 11 – HEU fuel power density at day 42 (core power at 57.8 MW)

radial node width (cm)		0.3	0.3	0.3	0.3	1	1.734	1	0.3	0.3	0.3	0.3	0.3	0.3
distance (cm) from - inner edge of the fuel	0	0.3	0.6	0.9	1.2	2.2	3.934	4.934	5.234	5.534	5.834	6.134	6.434	6.734
- core center	14	14.29	14.57	14.85	15.13	16.01	17.43	18.19	18.42	18.64	18.86	19.07	19.29	19.5
axial node height (cm)	position to core midplane (cm)	volumetric heat generation rate (W/mm^3)												
	40													
0.3	39.7	8.57	8.61	8.62	8.59	8.59	8.56	8.61	8.57	8.58	8.53	8.48	8.43	8.32
0.3	39.4	8.43	8.42	8.34	8.30	8.22	8.18	8.31	8.36	8.38	8.42	8.38	8.37	8.29
0.3	39.1	8.27	8.23	8.12	8.03	7.90	7.84	8.01	8.14	8.17	8.23	8.24	8.26	8.20
0.3	38.8	8.11	8.04	7.87	7.78	7.58	7.52	7.74	7.94	7.96	8.04	8.09	8.10	8.09
0.3	38.5	7.98	7.82	7.67	7.54	7.32	7.24	7.49	7.72	7.82	7.92	7.98	8.04	8.04
0.3	38.2	7.88	7.66	7.49	7.31	7.08	6.98	7.29	7.54	7.65	7.77	7.87	7.92	7.99
0.3	37.9	7.75	7.53	7.31	7.16	6.88	6.77	7.09	7.38	7.53	7.65	7.74	7.85	7.87
0.3	37.6	7.61	7.37	7.17	6.96	6.70	6.58	6.95	7.24	7.39	7.54	7.66	7.76	7.83
0.3	37.3	7.52	7.30	7.05	6.85	6.54	6.41	6.80	7.12	7.28	7.45	7.57	7.71	7.77
0.3	37	7.45	7.18	6.94	6.71	6.40	6.27	6.68	7.00	7.19	7.36	7.51	7.64	7.69
0.3	36.7	7.37	7.10	6.84	6.62	6.28	6.16	6.58	6.93	7.14	7.28	7.44	7.60	7.66
0.3	36.4	7.28	7.00	6.73	6.52	6.19	6.04	6.49	6.84	7.03	7.21	7.38	7.51	7.61
0.3	36.1	7.24	6.94	6.65	6.44	6.09	5.95	6.40	6.79	6.97	7.14	7.32	7.47	7.56
0.3	35.8	7.17	6.86	6.58	6.35	6.01	5.88	6.34	6.71	6.90	7.09	7.24	7.42	7.53
0.3	35.5	7.09	6.79	6.51	6.29	5.94	5.83	6.29	6.67	6.87	7.07	7.24	7.38	7.49
3.6	31.9	6.87	6.56	6.29	6.06	5.73	5.62	6.11	6.51	6.71	6.91	7.10	7.25	7.37
3.6	28.3	6.72	6.44	6.18	5.97	5.65	5.57	6.09	6.48	6.68	6.87	7.04	7.20	7.29
3.6	24.7	6.79	6.52	6.28	6.09	5.79	5.72	6.23	6.61	6.80	6.98	7.14	7.27	7.34
3.6	21.1	6.93	6.69	6.48	6.28	5.99	5.93	6.43	6.80	6.98	7.14	7.28	7.39	7.43
3.6	17.5	7.08	6.86	6.64	6.46	6.19	6.14	6.63	6.97	7.14	7.30	7.42	7.51	7.52
3.6	13.9	7.24	7.03	6.83	6.65	6.37	6.32	6.80	7.14	7.30	7.44	7.55	7.62	7.62
3.6	10.3	7.38	7.18	6.98	6.79	6.52	6.47	6.95	7.28	7.43	7.58	7.68	7.74	7.72
3.6	6.7	7.52	7.32	7.11	6.93	6.64	6.58	7.06	7.39	7.55	7.69	7.80	7.84	7.81
3.6	3.1	7.69	7.47	7.24	7.04	6.73	6.66	7.14	7.48	7.64	7.78	7.88	7.95	7.92
3.6	-0.5	7.93	7.62	7.35	7.13	6.79	6.69	7.19	7.54	7.71	7.86	7.96	8.03	8.02
3.6	-4.1	8.17	7.79	7.47	7.21	6.82	6.69	7.18	7.55	7.72	7.89	8.01	8.10	8.11
3.6	-7.7	8.34	7.88	7.52	7.22	6.79	6.64	7.16	7.54	7.72	7.90	8.04	8.14	8.19
3.6	-11.3	8.44	7.91	7.50	7.16	6.70	6.53	7.06	7.47	7.67	7.87	8.04	8.17	8.24
3.6	-14.9	8.43	7.84	7.40	7.03	6.56	6.38	6.93	7.36	7.58	7.78	7.98	8.14	8.24
3.6	-18.5	8.31	7.67	7.20	6.83	6.34	6.16	6.73	7.18	7.42	7.66	7.88	8.08	8.24
3.6	-22.1	8.09	7.43	6.94	6.57	6.07	5.90	6.48	6.96	7.21	7.47	7.71	7.95	8.15
3.6	-25.7	7.76	7.08	6.60	6.22	5.74	5.59	6.19	6.68	6.96	7.23	7.50	7.78	8.03
3.6	-29.3	7.36	6.69	6.21	5.84	5.38	5.25	5.86	6.37	6.65	6.94	7.25	7.55	7.85
3.6	-32.9	6.90	6.23	5.77	5.42	4.98	4.88	5.52	6.06	6.35	6.65	6.98	7.31	7.66
3.6	-36.5	6.30	5.70	5.28	4.98	4.61	4.60	5.27	5.83	6.12	6.44	6.79	7.15	7.53
0.5	-37	5.83	5.30	4.99	4.76	4.48	4.57	5.27	5.81	6.13	6.47	6.80	7.17	7.59
0.3	-37.3	5.71	5.23	4.94	4.72	4.47	4.61	5.31	5.84	6.15	6.50	6.84	7.19	7.60
0.3	-37.6	5.62	5.18	4.93	4.70	4.50	4.66	5.38	5.92	6.19	6.59	6.87	7.23	7.60
0.3	-37.9	5.57	5.17	4.93	4.70	4.53	4.71	5.44	5.99	6.27	6.60	6.94	7.26	7.65
0.3	-38.2	5.54	5.15	4.93	4.77	4.61	4.81	5.53	6.04	6.35	6.65	6.97	7.29	7.72
0.3	-38.5	5.55	5.19	4.98	4.83	4.69	4.93	5.64	6.15	6.44	6.74	7.06	7.39	7.77
0.3	-38.8	5.57	5.24	5.06	4.91	4.82	5.08	5.78	6.26	6.54	6.83	7.12	7.48	7.83
0.3	-39.1	5.64	5.34	5.15	5.05	4.98	5.28	5.98	6.43	6.71	6.99	7.27	7.57	7.91
0.3	-39.4	5.72	5.48	5.32	5.24	5.20	5.53	6.22	6.66	6.92	7.16	7.41	7.70	8.03
0.3	-39.7	5.90	5.67	5.57	5.50	5.53	5.87	6.54	6.95	7.20	7.39	7.65	7.88	8.17
0.3	-40	6.17	6.02	5.97	5.95	5.98	6.39	7.02	7.39	7.59	7.75	7.92	8.15	8.38

Table A3 - 12 – HEU fuel power density at EOC, day 45.5 (core power at 57.8 MW)

radial node width (cm)		0.3	0.3	0.3	0.3	1	1.734	1	0.3	0.3	0.3	0.3	0.3	0.3
distance (cm) from - inner edge of the fuel	0	0.3	0.6	0.9	1.2	2.2	3.934	4.934	5.234	5.534	5.834	6.134	6.434	6.734
- core center	14	14.29	14.57	14.85	15.13	16.01	17.43	18.19	18.42	18.64	18.86	19.07	19.29	19.5
axial node height (cm)	position to core midplane (cm)	volumetric heat generation rate (W/mm^3)												
	40													
0.3	39.7	7.76	7.84	7.91	7.90	7.92	7.93	7.91	7.86	7.82	7.80	7.72	7.62	7.48
0.3	39.4	7.69	7.74	7.74	7.71	7.66	7.66	7.72	7.74	7.74	7.72	7.71	7.63	7.46
0.3	39.1	7.60	7.61	7.55	7.53	7.42	7.37	7.51	7.57	7.61	7.62	7.61	7.56	7.45
0.3	38.8	7.50	7.44	7.37	7.33	7.17	7.12	7.28	7.42	7.48	7.50	7.50	7.48	7.38
0.3	38.5	7.37	7.32	7.22	7.13	6.95	6.89	7.09	7.26	7.34	7.38	7.40	7.38	7.33
0.3	38.2	7.27	7.20	7.07	6.95	6.75	6.66	6.91	7.13	7.19	7.25	7.34	7.32	7.26
0.3	37.9	7.19	7.06	6.92	6.79	6.56	6.47	6.77	6.99	7.08	7.15	7.23	7.28	7.21
0.3	37.6	7.10	6.96	6.79	6.64	6.40	6.31	6.61	6.83	6.97	7.07	7.17	7.18	7.17
0.3	37.3	7.02	6.85	6.67	6.51	6.27	6.17	6.50	6.79	6.87	6.95	7.07	7.14	7.11
0.3	37	6.93	6.75	6.59	6.41	6.15	6.04	6.40	6.67	6.81	6.91	7.03	7.09	7.08
0.3	36.7	6.85	6.69	6.47	6.34	6.05	5.94	6.30	6.59	6.74	6.86	6.96	7.04	7.05
0.3	36.4	6.81	6.60	6.39	6.25	5.95	5.84	6.24	6.52	6.66	6.80	6.92	6.98	7.00
0.3	36.1	6.71	6.53	6.35	6.14	5.86	5.75	6.16	6.47	6.60	6.75	6.88	6.95	6.98
0.3	35.8	6.68	6.48	6.28	6.07	5.79	5.69	6.11	6.42	6.58	6.70	6.84	6.93	6.95
0.3	35.5	6.65	6.42	6.20	5.99	5.72	5.62	6.05	6.36	6.52	6.66	6.81	6.89	6.92
3.6	31.9	6.45	6.21	6.01	5.81	5.52	5.42	5.87	6.21	6.37	6.53	6.66	6.78	6.82
3.6	28.3	6.32	6.10	5.90	5.72	5.45	5.39	5.85	6.18	6.34	6.50	6.62	6.72	6.75
3.6	24.7	6.39	6.19	6.01	5.84	5.59	5.54	5.99	6.32	6.46	6.60	6.70	6.77	6.78
3.6	21.1	6.52	6.36	6.19	6.02	5.78	5.74	6.18	6.48	6.62	6.74	6.84	6.88	6.86
3.6	17.5	6.67	6.52	6.36	6.21	5.98	5.95	6.37	6.66	6.78	6.89	6.97	7.00	6.96
3.6	13.9	6.82	6.68	6.52	6.38	6.16	6.13	6.56	6.83	6.95	7.04	7.11	7.12	7.04
3.6	10.3	6.96	6.83	6.70	6.55	6.33	6.29	6.71	6.97	7.09	7.18	7.23	7.23	7.14
3.6	6.7	7.13	7.00	6.84	6.70	6.47	6.43	6.84	7.10	7.21	7.30	7.35	7.35	7.26
3.6	3.1	7.32	7.16	6.99	6.82	6.58	6.53	6.95	7.22	7.34	7.43	7.47	7.47	7.37
3.6	-0.5	7.58	7.36	7.16	6.97	6.68	6.61	7.03	7.31	7.43	7.53	7.59	7.59	7.51
3.6	-4.1	7.85	7.55	7.30	7.07	6.75	6.64	7.07	7.37	7.51	7.62	7.69	7.70	7.64
3.6	-7.7	8.08	7.72	7.40	7.14	6.76	6.62	7.08	7.40	7.55	7.67	7.76	7.80	7.76
3.6	-11.3	8.24	7.79	7.43	7.14	6.72	6.57	7.04	7.39	7.55	7.69	7.81	7.88	7.86
3.6	-14.9	8.32	7.80	7.40	7.08	6.63	6.46	6.96	7.32	7.51	7.68	7.81	7.91	7.94
3.6	-18.5	8.28	7.72	7.29	6.95	6.48	6.30	6.82	7.23	7.43	7.62	7.79	7.93	7.99
3.6	-22.1	8.18	7.57	7.12	6.75	6.27	6.10	6.64	7.07	7.30	7.51	7.71	7.88	8.02
3.6	-25.7	8.02	7.37	6.90	6.52	6.04	5.86	6.43	6.89	7.14	7.36	7.61	7.82	8.00
3.6	-29.3	7.82	7.14	6.65	6.26	5.77	5.60	6.19	6.68	6.93	7.19	7.46	7.72	7.95
3.6	-32.9	7.69	6.97	6.45	6.07	5.56	5.37	5.97	6.48	6.76	7.05	7.34	7.64	7.92
3.6	-36.5	7.80	7.02	6.49	6.07	5.53	5.34	5.94	6.47	6.75	7.05	7.38	7.70	8.03
0.5	-37	8.10	7.31	6.75	6.34	5.78	5.58	6.15	6.68	6.95	7.25	7.56	7.89	8.21
0.3	-37.3	8.21	7.42	6.86	6.45	5.89	5.69	6.25	6.75	7.05	7.32	7.66	7.97	8.30
0.3	-37.6	8.30	7.54	6.94	6.56	6.00	5.80	6.36	6.86	7.13	7.42	7.75	8.08	8.42
0.3	-37.9	8.44	7.63	7.08	6.66	6.14	5.95	6.48	6.95	7.22	7.53	7.80	8.15	8.46
0.3	-38.2	8.59	7.80	7.23	6.85	6.30	6.10	6.63	7.09	7.35	7.65	7.92	8.25	8.55
0.3	-38.5	8.75	7.96	7.43	7.01	6.50	6.30	6.81	7.27	7.52	7.79	8.06	8.35	8.66
0.3	-38.8	8.96	8.13	7.63	7.25	6.76	6.56	7.04	7.45	7.67	7.93	8.21	8.52	8.80
0.3	-39.1	9.13	8.37	7.89	7.55	7.06	6.88	7.32	7.68	7.92	8.14	8.37	8.65	8.92
0.3	-39.4	9.42	8.70	8.24	7.88	7.46	7.28	7.67	8.01	8.22	8.43	8.62	8.83	9.08
0.3	-39.7	9.74	9.13	8.71	8.36	7.98	7.79	8.14	8.42	8.56	8.73	8.92	9.11	9.28
0.3	-40	10.24	9.72	9.37	9.08	8.70	8.53	8.76	8.95	9.09	9.20	9.31	9.39	9.55

Table A3 - 13 – LEU fuel power density at BOC (core power at 57.8 MW)

radial node width (cm)		0.3	0.3	0.3	0.3	1	1.734	1	0.3	0.3	0.3	0.3	0.3	0.3
distance (cm) from - inner edge of the fuel	0	0.3	0.6	0.9	1.2	2.2	3.934	4.934	5.234	5.534	5.834	6.134	6.434	6.734
- core center	14	14.29	14.57	14.85	15.13	16.01	17.43	18.19	18.42	18.64	18.86	19.07	19.29	19.5
axial node height (cm)	**position to core midplane (cm)**	**volumetric heat generation rate (W/mm^3)**												
	44													
0.3	**43.7**	13.53	12.26	11.48	10.92	10.10	9.34	9.44	9.92	10.25	10.69	11.32	12.11	13.30
0.3	**43.4**	12.29	10.74	9.92	9.23	8.44	7.78	8.02	8.60	9.02	9.51	10.18	11.22	12.61
0.3	**43.1**	11.52	9.92	8.96	8.32	7.48	6.86	7.21	7.88	8.31	8.88	9.70	10.72	12.18
0.3	**42.8**	11.00	9.31	8.33	7.64	6.79	6.21	6.65	7.36	7.88	8.50	9.37	10.45	12.00
0.3	**42.5**	10.64	8.93	7.88	7.21	6.31	5.76	6.28	7.05	7.60	8.25	9.11	10.18	11.78
0.3	**42.2**	10.26	8.57	7.56	6.87	5.97	5.42	5.98	6.80	7.36	8.05	8.93	10.13	11.72
0.3	**41.9**	10.01	8.33	7.33	6.61	5.69	5.17	5.80	6.62	7.18	7.87	8.77	10.00	11.63
0.3	**41.6**	9.76	8.11	7.12	6.39	5.49	4.99	5.65	6.48	7.08	7.75	8.70	9.89	11.54
0.3	**41.3**	9.55	7.93	6.94	6.24	5.34	4.83	5.54	6.41	7.00	7.74	8.65	9.83	11.53
0.3	**41**	9.41	7.83	6.84	6.10	5.20	4.73	5.44	6.34	6.92	7.68	8.60	9.76	11.51
0.3	**40.7**	9.25	7.65	6.68	5.98	5.10	4.63	5.39	6.28	6.87	7.65	8.54	9.75	11.45
0.3	**40.4**	9.12	7.58	6.58	5.86	5.03	4.59	5.34	6.25	6.85	7.60	8.57	9.77	11.47
0.3	**40.1**	9.05	7.49	6.49	5.84	4.97	4.54	5.32	6.22	6.83	7.58	8.54	9.77	11.41
0.3	**39.8**	8.93	7.43	6.46	5.75	4.90	4.51	5.28	6.20	6.82	7.60	8.55	9.77	11.47
0.3	**39.5**	8.83	7.38	6.44	5.73	4.88	4.47	5.27	6.18	6.81	7.57	8.56	9.78	11.49
4	**35.5**	8.59	7.19	6.28	5.64	4.83	4.48	5.33	6.29	6.91	7.71	8.69	9.96	11.69
4	**31.5**	8.50	7.17	6.32	5.71	4.95	4.67	5.61	6.61	7.29	8.13	9.15	10.48	12.32
4	**27.5**	8.25	7.01	6.23	5.67	4.99	4.82	5.86	6.94	7.65	8.52	9.61	11.02	12.93
4	**23.5**	6.82	6.00	5.48	5.10	4.69	4.80	6.02	7.18	7.94	8.86	10.00	11.46	13.46
4	**19.5**	6.32	5.63	5.20	4.90	4.59	4.84	6.17	7.39	8.18	9.13	10.33	11.85	13.91
4	**15.5**	6.37	5.68	5.26	4.97	4.67	4.94	6.32	7.56	8.38	9.38	10.59	12.15	14.29
4	**11.5**	6.45	5.76	5.33	5.04	4.74	5.03	6.43	7.72	8.54	9.55	10.78	12.36	14.53
4	**7.5**	6.51	5.82	5.38	5.08	4.78	5.08	6.50	7.80	8.63	9.65	10.91	12.51	14.73
4	**3.5**	6.52	5.83	5.39	5.10	4.79	5.09	6.53	7.83	8.66	9.69	10.96	12.57	14.77
4	**-0.5**	6.49	5.80	5.37	5.08	4.77	5.07	6.50	7.80	8.64	9.66	10.93	12.53	14.73
4	**-4.5**	6.39	5.72	5.30	5.02	4.71	5.01	6.43	7.72	8.54	9.55	10.79	12.38	14.58
4	**-8.5**	6.27	5.60	5.19	4.90	4.62	4.92	6.30	7.58	8.39	9.38	10.61	12.17	14.32
4	**-12.5**	6.09	5.45	5.05	4.77	4.50	4.79	6.15	7.39	8.19	9.16	10.36	11.90	14.00
4	**-16.5**	5.85	5.24	4.85	4.59	4.33	4.62	5.94	7.15	7.92	8.87	10.04	11.51	13.56
4	**-20.5**	5.56	4.98	4.62	4.38	4.13	4.41	5.68	6.85	7.58	8.48	9.61	11.05	13.01
4	**-24.5**	5.21	4.67	4.33	4.11	3.88	4.17	5.39	6.50	7.21	8.07	9.15	10.51	12.39
4	**-28.5**	4.79	4.29	3.99	3.79	3.60	3.89	5.06	6.10	6.78	7.60	8.60	9.91	11.68
4	**-32.5**	4.23	3.82	3.57	3.40	3.25	3.57	4.69	5.69	6.32	7.10	8.07	9.28	10.96
4	**-36.5**	3.52	3.22	3.04	2.93	2.86	3.23	4.33	5.28	5.88	6.63	7.54	8.71	10.32
4	**-40.5**	3.15	2.88	2.74	2.66	2.63	3.03	4.11	5.03	5.62	6.34	7.22	8.36	9.90
0.5	**-41**	3.31	3.01	2.85	2.78	2.75	3.15	4.21	5.10	5.68	6.41	7.28	8.40	9.99
0.3	**-41.3**	3.39	3.08	2.94	2.86	2.83	3.24	4.29	5.20	5.74	6.47	7.33	8.42	10.03
0.3	**-41.6**	3.47	3.19	3.02	2.92	2.92	3.33	4.39	5.31	5.85	6.56	7.42	8.52	10.16
0.3	**-41.9**	3.59	3.29	3.13	3.05	3.04	3.45	4.49	5.36	5.96	6.65	7.55	8.66	10.21
0.3	**-42.2**	3.71	3.41	3.26	3.18	3.18	3.61	4.64	5.49	6.07	6.80	7.64	8.76	10.30
0.3	**-42.5**	3.86	3.58	3.43	3.36	3.38	3.83	4.85	5.75	6.27	6.95	7.83	8.91	10.46
0.3	**-42.8**	4.06	3.79	3.64	3.58	3.64	4.11	5.14	6.02	6.53	7.20	8.02	9.13	10.66
0.3	**-43.1**	4.34	4.05	3.93	3.89	3.97	4.47	5.51	6.36	6.87	7.51	8.32	9.40	10.95
0.3	**-43.4**	4.64	4.40	4.31	4.31	4.41	4.99	6.05	6.88	7.38	7.98	8.82	9.78	11.27
0.3	**-43.7**	5.11	4.92	4.86	4.90	5.06	5.74	6.83	7.65	8.14	8.76	9.44	10.32	11.79
0.3	**-44**	5.82	5.73	5.77	5.86	6.11	6.95	8.17	9.00	9.45	10.01	10.71	11.50	12.60

Table A3 - 14 – LEU fuel power density at day 1 (core power at 57.8 MW)

radial node width (cm)		0.3	0.3	0.3	0.3	1	1.734	1	0.3	0.3	0.3	0.3	0.3	0.3
distance (cm) from - inner edge of the fuel	0	0.3	0.6	0.9	1.2	2.2	3.934	4.934	5.234	5.534	5.834	6.134	6.434	6.734
- core center	14	14.29	14.57	14.85	15.13	16.01	17.43	18.19	18.42	18.64	18.86	19.07	19.29	19.5
axial node height (cm)	**position to core midplane (cm)**	**volumetric heat generation rate (W/mm^3)**												
	44													
0.3	**43.7**	13.80	12.43	11.68	11.01	10.17	9.41	9.54	10.05	10.39	10.90	11.46	12.31	13.54
0.3	**43.4**	12.47	10.95	10.02	9.32	8.47	7.79	8.08	8.65	9.04	9.61	10.38	11.34	12.79
0.3	**43.1**	11.68	10.05	9.05	8.35	7.48	6.83	7.21	7.86	8.31	8.95	9.73	10.86	12.35
0.3	**42.8**	11.16	9.43	8.39	7.66	6.79	6.17	6.66	7.34	7.86	8.54	9.38	10.47	12.15
0.3	**42.5**	10.77	8.99	7.94	7.19	6.28	5.69	6.23	7.01	7.55	8.25	9.13	10.30	11.95
0.3	**42.2**	10.38	8.65	7.59	6.86	5.94	5.36	5.95	6.77	7.29	8.02	8.94	10.11	11.85
0.3	**41.9**	10.10	8.37	7.31	6.59	5.65	5.10	5.74	6.59	7.17	7.88	8.85	10.06	11.76
0.3	**41.6**	9.89	8.13	7.11	6.38	5.45	4.90	5.58	6.46	7.06	7.80	8.74	9.95	11.66
0.3	**41.3**	9.68	8.00	6.94	6.20	5.29	4.77	5.47	6.35	6.96	7.73	8.66	9.90	11.61
0.3	**41**	9.52	7.87	6.83	6.07	5.17	4.67	5.39	6.29	6.89	7.62	8.62	9.89	11.59
0.3	**40.7**	9.42	7.74	6.71	6.01	5.07	4.58	5.34	6.24	6.84	7.61	8.59	9.88	11.60
0.3	**40.4**	9.33	7.65	6.66	5.92	4.98	4.54	5.30	6.19	6.84	7.58	8.57	9.83	11.61
0.3	**40.1**	9.19	7.58	6.57	5.84	4.94	4.48	5.25	6.18	6.77	7.57	8.60	9.82	11.59
0.3	**39.8**	9.08	7.52	6.51	5.81	4.90	4.45	5.22	6.17	6.76	7.60	8.57	9.83	11.61
0.3	**39.5**	9.06	7.44	6.45	5.76	4.88	4.42	5.23	6.18	6.78	7.57	8.56	9.84	11.58
4	**35.5**	8.84	7.33	6.37	5.70	4.84	4.44	5.31	6.28	6.93	7.75	8.76	10.07	11.86
4	**31.5**	8.93	7.48	6.55	5.89	5.04	4.69	5.61	6.65	7.34	8.19	9.26	10.63	12.51
4	**27.5**	9.34	7.83	6.89	6.19	5.34	4.99	5.97	7.06	7.79	8.68	9.80	11.24	13.22
4	**23.5**	9.76	8.21	7.21	6.50	5.61	5.25	6.28	7.41	8.17	9.11	10.28	11.78	13.86
4	**19.5**	10.07	8.48	7.46	6.73	5.81	5.45	6.51	7.68	8.48	9.44	10.65	12.21	14.35
4	**15.5**	10.25	8.64	7.59	6.85	5.93	5.57	6.67	7.88	8.68	9.67	10.91	12.50	14.70
4	**11.5**	10.19	8.60	7.57	6.84	5.93	5.59	6.73	7.96	8.77	9.77	11.04	12.66	14.88
4	**7.5**	9.49	8.05	7.13	6.47	5.67	5.45	6.64	7.89	8.71	9.73	10.99	12.61	14.84
4	**3.5**	7.39	6.47	5.90	5.48	5.02	5.12	6.45	7.73	8.54	9.56	10.83	12.46	14.67
4	**-0.5**	6.50	5.76	5.30	4.99	4.64	4.88	6.25	7.52	8.34	9.34	10.60	12.20	14.39
4	**-4.5**	6.19	5.50	5.07	4.76	4.46	4.72	6.07	7.32	8.14	9.13	10.36	11.93	14.08
4	**-8.5**	5.95	5.29	4.87	4.59	4.29	4.55	5.88	7.10	7.89	8.87	10.06	11.59	13.68
4	**-12.5**	5.69	5.06	4.67	4.39	4.11	4.37	5.66	6.86	7.61	8.55	9.71	11.19	13.22
4	**-16.5**	5.41	4.81	4.44	4.18	3.93	4.18	5.43	6.57	7.30	8.20	9.33	10.74	12.72
4	**-20.5**	5.11	4.55	4.20	3.96	3.71	3.97	5.16	6.25	6.95	7.81	8.88	10.25	12.11
4	**-24.5**	4.79	4.26	3.93	3.71	3.49	3.73	4.86	5.91	6.57	7.38	8.40	9.70	11.49
4	**-28.5**	4.45	3.96	3.66	3.45	3.24	3.48	4.56	5.54	6.18	6.95	7.91	9.13	10.81
4	**-32.5**	4.10	3.64	3.36	3.17	2.98	3.22	4.24	5.15	5.76	6.49	7.40	8.55	10.14
4	**-36.5**	3.78	3.35	3.08	2.91	2.75	2.97	3.94	4.82	5.38	6.07	6.94	8.03	9.56
4	**-40.5**	3.66	3.22	2.96	2.79	2.62	2.85	3.77	4.62	5.16	5.84	6.67	7.73	9.21
0.5	**-41**	3.84	3.37	3.09	2.92	2.75	2.99	3.89	4.74	5.29	5.93	6.74	7.80	9.29
0.3	**-41.3**	3.93	3.45	3.19	3.02	2.85	3.07	3.97	4.79	5.34	6.00	6.83	7.87	9.36
0.3	**-41.6**	4.00	3.53	3.28	3.11	2.93	3.16	4.07	4.87	5.42	6.06	6.86	7.98	9.42
0.3	**-41.9**	4.11	3.65	3.36	3.19	3.04	3.27	4.17	5.00	5.53	6.17	6.98	8.07	9.54
0.3	**-42.2**	4.26	3.77	3.51	3.34	3.20	3.42	4.32	5.14	5.70	6.29	7.13	8.15	9.68
0.3	**-42.5**	4.44	3.94	3.68	3.53	3.37	3.64	4.52	5.31	5.82	6.49	7.26	8.30	9.86
0.3	**-42.8**	4.65	4.15	3.90	3.77	3.64	3.93	4.79	5.59	6.11	6.72	7.49	8.56	10.02
0.3	**-43.1**	4.89	4.41	4.18	4.05	3.99	4.31	5.19	5.94	6.41	7.01	7.79	8.79	10.29
0.3	**-43.4**	5.20	4.78	4.61	4.48	4.46	4.84	5.72	6.46	6.94	7.52	8.23	9.19	10.63
0.3	**-43.7**	5.68	5.33	5.14	5.09	5.11	5.59	6.50	7.24	7.66	8.21	8.89	9.76	11.05
0.3	**-44**	6.49	6.19	6.13	6.10	6.22	6.82	7.85	8.59	9.00	9.50	10.10	10.83	11.97

Table A3 - 15 – LEU fuel power density at day 5 (core power at 57.8 MW)

radial node width (cm)		0.3	0.3	0.3	0.3	1	1.734	1	0.3	0.3	0.3	0.3	0.3	0.3
distance (cm) from - inner edge of the fuel	0	0.3	0.6	0.9	1.2	2.2	3.934	4.934	5.234	5.534	5.834	6.134	6.434	6.734
- core center	14	14.29	14.57	14.85	15.13	16.01	17.43	18.19	18.42	18.64	18.86	19.07	19.29	19.5
axial node height (cm)	**position to core midplane (cm)**	**volumetric heat generation rate (W/mm^3)**												
	44													
0.3	**43.7**	13.26	12.08	11.31	10.73	9.95	9.28	9.43	9.91	10.21	10.68	11.26	12.03	13.15
0.3	**43.4**	12.02	10.62	9.77	9.14	8.35	7.72	7.97	8.53	8.95	9.51	10.10	11.06	12.46
0.3	**43.1**	11.37	9.82	8.88	8.23	7.38	6.79	7.16	7.79	8.22	8.79	9.55	10.60	12.05
0.3	**42.8**	10.87	9.24	8.25	7.60	6.71	6.14	6.60	7.32	7.75	8.40	9.20	10.25	11.76
0.3	**42.5**	10.45	8.79	7.82	7.12	6.22	5.67	6.20	6.96	7.44	8.11	8.95	10.07	11.61
0.3	**42.2**	10.14	8.52	7.46	6.77	5.85	5.32	5.89	6.70	7.21	7.90	8.79	9.89	11.48
0.3	**41.9**	9.87	8.25	7.20	6.49	5.58	5.06	5.70	6.52	7.07	7.76	8.64	9.82	11.35
0.3	**41.6**	9.62	8.04	7.00	6.26	5.36	4.86	5.53	6.35	6.95	7.66	8.57	9.70	11.38
0.3	**41.3**	9.41	7.85	6.81	6.10	5.22	4.71	5.44	6.27	6.85	7.56	8.52	9.67	11.29
0.3	**41**	9.26	7.72	6.68	5.98	5.09	4.60	5.33	6.21	6.81	7.53	8.44	9.62	11.21
0.3	**40.7**	9.14	7.59	6.59	5.90	5.00	4.52	5.25	6.17	6.77	7.52	8.40	9.58	11.24
0.3	**40.4**	9.05	7.49	6.51	5.80	4.92	4.46	5.23	6.12	6.70	7.45	8.43	9.57	11.22
0.3	**40.1**	8.94	7.42	6.46	5.74	4.85	4.41	5.18	6.06	6.68	7.43	8.39	9.56	11.25
0.3	**39.8**	8.85	7.34	6.37	5.69	4.81	4.38	5.16	6.06	6.69	7.45	8.37	9.60	11.25
0.3	**39.5**	8.81	7.30	6.35	5.64	4.77	4.36	5.16	6.08	6.69	7.50	8.41	9.58	11.26
4	**35.5**	8.59	7.16	6.24	5.58	4.75	4.37	5.21	6.16	6.81	7.59	8.56	9.78	11.49
4	**31.5**	8.70	7.30	6.41	5.75	4.95	4.61	5.52	6.53	7.19	8.01	9.04	10.33	12.08
4	**27.5**	9.10	7.67	6.74	6.09	5.25	4.91	5.88	6.94	7.63	8.49	9.57	10.91	12.75
4	**23.5**	9.54	8.06	7.10	6.40	5.53	5.18	6.20	7.30	8.04	8.93	10.04	11.45	13.36
4	**19.5**	9.90	8.38	7.38	6.68	5.77	5.41	6.46	7.61	8.37	9.29	10.45	11.90	13.88
4	**15.5**	10.17	8.60	7.58	6.85	5.94	5.56	6.64	7.82	8.59	9.55	10.72	12.20	14.22
4	**11.5**	10.28	8.71	7.68	6.95	6.01	5.64	6.74	7.94	8.73	9.70	10.90	12.40	14.47
4	**7.5**	10.27	8.70	7.68	6.93	6.01	5.65	6.75	7.98	8.76	9.73	10.94	12.44	14.51
4	**3.5**	9.99	8.47	7.48	6.77	5.88	5.55	6.68	7.89	8.67	9.65	10.84	12.36	14.41
4	**-0.5**	8.94	7.62	6.78	6.19	5.45	5.29	6.48	7.70	8.48	9.43	10.63	12.12	14.16
4	**-4.5**	6.82	6.01	5.50	5.14	4.73	4.88	6.18	7.39	8.17	9.13	10.31	11.78	13.79
4	**-8.5**	6.06	5.38	4.95	4.66	4.35	4.60	5.91	7.12	7.88	8.82	9.97	11.42	13.37
4	**-12.5**	5.71	5.07	4.67	4.41	4.13	4.38	5.66	6.82	7.57	8.47	9.57	10.98	12.87
4	**-16.5**	5.38	4.79	4.42	4.17	3.90	4.16	5.39	6.51	7.23	8.10	9.18	10.53	12.36
4	**-20.5**	5.06	4.49	4.16	3.91	3.67	3.93	5.11	6.18	6.86	7.70	8.71	10.01	11.76
4	**-24.5**	4.72	4.20	3.87	3.66	3.44	3.69	4.81	5.83	6.48	7.26	8.25	9.48	11.15
4	**-28.5**	4.37	3.89	3.59	3.38	3.18	3.43	4.49	5.45	6.07	6.82	7.73	8.90	10.47
4	**-32.5**	4.02	3.58	3.30	3.12	2.94	3.17	4.17	5.08	5.66	6.36	7.24	8.33	9.83
4	**-36.5**	3.71	3.29	3.04	2.86	2.70	2.93	3.88	4.74	5.28	5.96	6.78	7.83	9.25
4	**-40.5**	3.60	3.17	2.92	2.74	2.58	2.80	3.72	4.55	5.08	5.72	6.52	7.54	8.94
0.5	**-41**	3.79	3.34	3.06	2.89	2.73	2.94	3.82	4.66	5.16	5.80	6.60	7.63	9.03
0.3	**-41.3**	3.90	3.43	3.15	2.95	2.81	3.02	3.90	4.72	5.23	5.88	6.71	7.72	9.09
0.3	**-41.6**	3.99	3.52	3.23	3.05	2.89	3.11	4.00	4.80	5.32	5.95	6.78	7.79	9.13
0.3	**-41.9**	4.07	3.61	3.33	3.16	3.01	3.25	4.13	4.92	5.40	6.06	6.87	7.88	9.24
0.3	**-42.2**	4.21	3.74	3.47	3.30	3.17	3.40	4.28	5.07	5.55	6.18	6.98	7.98	9.37
0.3	**-42.5**	4.38	3.91	3.66	3.50	3.36	3.62	4.47	5.23	5.75	6.38	7.13	8.11	9.52
0.3	**-42.8**	4.57	4.11	3.87	3.71	3.61	3.88	4.75	5.49	6.00	6.60	7.31	8.33	9.70
0.3	**-43.1**	4.82	4.38	4.15	4.03	3.94	4.26	5.12	5.88	6.35	6.92	7.66	8.61	9.93
0.3	**-43.4**	5.16	4.77	4.56	4.44	4.40	4.77	5.62	6.36	6.81	7.38	8.10	8.98	10.31
0.3	**-43.7**	5.62	5.28	5.11	5.01	5.07	5.51	6.41	7.07	7.51	8.02	8.66	9.53	10.72
0.3	**-44**	6.40	6.13	6.06	6.06	6.17	6.72	7.69	8.39	8.77	9.23	9.77	10.52	11.57

Table A3 - 16 – LEU fuel power density at day 12 (core power at 57.8 MW)

radial node width (cm)		0.3	0.3	0.3	0.3	1	1.734	1	0.3	0.3	0.3	0.3	0.3	0.3
distance (cm) from - inner edge of the fuel	0	0.3	0.6	0.9	1.2	2.2	3.934	4.934	5.234	5.534	5.834	6.134	6.434	6.734
- core center	14	14.29	14.57	14.85	15.13	16.01	17.43	18.19	18.42	18.64	18.86	19.07	19.29	19.5
axial node height (cm)	position to core midplane (cm)	volumetric heat generation rate (W/mm^3)												
	44													
0.3	43.7	12.78	11.75	11.10	10.60	9.93	9.33	9.51	9.91	10.22	10.63	11.12	11.82	12.81
0.3	43.4	11.76	10.37	9.65	9.09	8.37	7.83	8.12	8.63	9.01	9.47	10.08	10.93	12.13
0.3	43.1	11.04	9.63	8.78	8.17	7.46	6.90	7.28	7.89	8.31	8.86	9.56	10.48	11.71
0.3	42.8	10.55	9.11	8.19	7.56	6.77	6.25	6.72	7.42	7.87	8.46	9.25	10.21	11.52
0.3	42.5	10.14	8.71	7.80	7.11	6.26	5.78	6.30	7.04	7.51	8.13	8.89	9.90	11.31
0.3	42.2	9.86	8.36	7.44	6.75	5.93	5.42	6.00	6.76	7.30	7.93	8.76	9.78	11.16
0.3	41.9	9.62	8.08	7.20	6.47	5.65	5.15	5.77	6.56	7.08	7.72	8.57	9.64	11.08
0.3	41.6	9.39	7.92	6.98	6.26	5.42	4.95	5.61	6.43	6.98	7.65	8.46	9.53	10.98
0.3	41.3	9.23	7.71	6.80	6.11	5.26	4.79	5.48	6.33	6.87	7.56	8.42	9.50	10.91
0.3	41	9.10	7.62	6.67	5.98	5.13	4.67	5.37	6.24	6.80	7.49	8.37	9.43	10.87
0.3	40.7	8.94	7.47	6.53	5.87	5.02	4.57	5.32	6.18	6.75	7.47	8.32	9.41	10.87
0.3	40.4	8.80	7.39	6.44	5.74	4.93	4.50	5.25	6.14	6.74	7.45	8.30	9.38	10.87
0.3	40.1	8.72	7.31	6.39	5.75	4.88	4.46	5.21	6.09	6.67	7.38	8.25	9.38	10.83
0.3	39.8	8.63	7.24	6.33	5.65	4.81	4.42	5.19	6.08	6.67	7.39	8.27	9.35	10.83
0.3	39.5	8.60	7.17	6.28	5.59	4.78	4.36	5.17	6.05	6.62	7.38	8.25	9.36	10.83
4	35.5	8.36	7.03	6.16	5.53	4.73	4.37	5.20	6.13	6.73	7.47	8.38	9.50	11.00
4	31.5	8.43	7.13	6.29	5.68	4.91	4.58	5.49	6.47	7.09	7.86	8.79	9.94	11.50
4	27.5	8.78	7.46	6.61	5.98	5.19	4.88	5.84	6.85	7.52	8.31	9.27	10.48	12.10
4	23.5	9.21	7.82	6.94	6.28	5.47	5.15	6.14	7.20	7.88	8.72	9.72	10.96	12.62
4	19.5	9.58	8.16	7.24	6.56	5.71	5.37	6.40	7.49	8.20	9.06	10.10	11.39	13.09
4	15.5	9.86	8.40	7.46	6.77	5.89	5.54	6.60	7.72	8.45	9.32	10.38	11.71	13.44
4	11.5	10.02	8.54	7.59	6.88	5.99	5.64	6.73	7.87	8.61	9.51	10.58	11.90	13.66
4	7.5	10.06	8.59	7.63	6.92	6.03	5.68	6.77	7.93	8.66	9.57	10.65	11.98	13.76
4	3.5	10.02	8.54	7.57	6.88	5.99	5.66	6.74	7.90	8.64	9.54	10.61	11.94	13.73
4	-0.5	9.81	8.34	7.40	6.72	5.86	5.54	6.63	7.78	8.52	9.40	10.48	11.80	13.58
4	-4.5	9.27	7.88	7.00	6.35	5.56	5.32	6.44	7.58	8.31	9.18	10.25	11.56	13.29
4	-8.5	7.40	6.43	5.82	5.38	4.87	4.91	6.11	7.25	7.97	8.84	9.88	11.18	12.88
4	-12.5	5.96	5.28	4.87	4.58	4.28	4.51	5.76	6.89	7.59	8.44	9.47	10.73	12.40
4	-16.5	5.45	4.86	4.49	4.23	3.97	4.23	5.46	6.55	7.23	8.05	9.04	10.26	11.88
4	-20.5	5.08	4.52	4.18	3.95	3.71	3.98	5.15	6.20	6.84	7.64	8.60	9.77	11.34
4	-24.5	4.72	4.21	3.89	3.67	3.46	3.72	4.83	5.83	6.45	7.20	8.12	9.24	10.74
4	-28.5	4.37	3.89	3.59	3.39	3.20	3.45	4.52	5.45	6.05	6.76	7.63	8.69	10.13
4	-32.5	4.01	3.56	3.30	3.12	2.94	3.18	4.18	5.07	5.61	6.30	7.13	8.14	9.49
4	-36.5	3.69	3.28	3.03	2.86	2.69	2.93	3.88	4.73	5.26	5.90	6.68	7.65	8.96
4	-40.5	3.59	3.16	2.91	2.74	2.58	2.81	3.72	4.53	5.04	5.66	6.42	7.37	8.64
0.5	-41	3.76	3.31	3.04	2.88	2.72	2.94	3.83	4.60	5.13	5.74	6.52	7.47	8.74
0.3	-41.3	3.87	3.41	3.14	2.97	2.81	3.04	3.91	4.71	5.19	5.80	6.55	7.50	8.80
0.3	-41.6	3.95	3.49	3.23	3.06	2.90	3.12	3.99	4.77	5.29	5.89	6.63	7.55	8.85
0.3	-41.9	4.05	3.58	3.32	3.16	3.00	3.24	4.12	4.87	5.39	5.94	6.73	7.66	8.92
0.3	-42.2	4.20	3.72	3.46	3.29	3.16	3.40	4.26	5.03	5.52	6.10	6.82	7.80	9.04
0.3	-42.5	4.35	3.85	3.63	3.45	3.35	3.62	4.47	5.19	5.71	6.29	6.97	7.88	9.16
0.3	-42.8	4.56	4.12	3.87	3.71	3.60	3.88	4.73	5.45	5.93	6.49	7.22	8.13	9.31
0.3	-43.1	4.79	4.35	4.13	4.01	3.95	4.25	5.09	5.80	6.23	6.84	7.48	8.34	9.56
0.3	-43.4	5.13	4.72	4.50	4.40	4.39	4.75	5.57	6.30	6.71	7.21	7.85	8.70	9.88
0.3	-43.7	5.55	5.18	5.06	5.00	5.01	5.45	6.32	7.00	7.40	7.87	8.44	9.17	10.29
0.3	-44	6.30	6.03	5.98	5.96	6.04	6.57	7.50	8.19	8.55	8.96	9.47	10.10	11.01

Table A3 - 17 – LEU fuel power density at day 18 (core power at 57.8 MW)

radial node width (cm)		0.3	0.3	0.3	0.3	1	1.734	1	0.3	0.3	0.3	0.3	0.3	0.3
distance (cm) from - inner edge of the fuel	0	0.3	0.6	0.9	1.2	2.2	3.934	4.934	5.234	5.534	5.834	6.134	6.434	6.734
- core center	14	14.29	14.57	14.85	15.13	16.01	17.43	18.19	18.42	18.64	18.86	19.07	19.29	19.5
axial node height (cm)	position to core midplane (cm)	volumetric heat generation rate (W/mm^3)												
	44													
0.3	43.7	12.43	11.48	10.93	10.51	9.91	9.42	9.65	10.04	10.33	10.68	11.15	11.73	12.59
0.3	43.4	11.40	10.31	9.55	9.15	8.44	7.98	8.30	8.76	9.15	9.57	10.15	10.84	11.91
0.3	43.1	10.77	9.56	8.82	8.26	7.53	7.05	7.47	8.05	8.40	8.94	9.56	10.42	11.55
0.3	42.8	10.35	8.99	8.21	7.62	6.86	6.40	6.90	7.54	7.96	8.49	9.24	10.10	11.25
0.3	42.5	9.98	8.63	7.77	7.17	6.38	5.89	6.46	7.15	7.62	8.19	8.91	9.85	11.09
0.3	42.2	9.71	8.32	7.43	6.83	5.99	5.53	6.12	6.86	7.37	7.96	8.71	9.69	10.91
0.3	41.9	9.42	8.09	7.16	6.55	5.70	5.24	5.88	6.69	7.18	7.83	8.60	9.55	10.86
0.3	41.6	9.21	7.85	6.95	6.29	5.47	5.02	5.69	6.48	7.04	7.69	8.48	9.43	10.73
0.3	41.3	9.07	7.69	6.80	6.12	5.30	4.86	5.54	6.37	6.94	7.57	8.36	9.36	10.69
0.3	41	8.91	7.55	6.65	5.97	5.16	4.73	5.45	6.28	6.83	7.52	8.32	9.31	10.54
0.3	40.7	8.78	7.41	6.53	5.87	5.05	4.62	5.36	6.23	6.74	7.44	8.23	9.24	10.60
0.3	40.4	8.66	7.32	6.43	5.79	4.95	4.54	5.30	6.17	6.70	7.36	8.22	9.22	10.57
0.3	40.1	8.55	7.20	6.36	5.72	4.88	4.49	5.25	6.12	6.70	7.34	8.20	9.20	10.53
0.3	39.8	8.49	7.14	6.27	5.65	4.83	4.44	5.21	6.08	6.66	7.35	8.15	9.17	10.47
0.3	39.5	8.40	7.06	6.24	5.60	4.78	4.41	5.19	6.08	6.61	7.31	8.16	9.16	10.50
4	35.5	8.15	6.89	6.07	5.48	4.71	4.37	5.20	6.11	6.69	7.38	8.21	9.23	10.59
4	31.5	8.18	6.96	6.17	5.59	4.84	4.55	5.45	6.39	6.98	7.70	8.56	9.61	11.00
4	27.5	8.50	7.27	6.46	5.88	5.12	4.83	5.77	6.75	7.37	8.11	9.01	10.09	11.51
4	23.5	8.91	7.63	6.80	6.18	5.40	5.10	6.08	7.09	7.73	8.50	9.41	10.53	11.98
4	19.5	9.25	7.94	7.07	6.44	5.63	5.33	6.34	7.39	8.05	8.84	9.78	10.92	12.41
4	15.5	9.52	8.17	7.31	6.66	5.82	5.50	6.54	7.61	8.28	9.09	10.05	11.20	12.73
4	11.5	9.71	8.35	7.45	6.79	5.94	5.62	6.67	7.76	8.45	9.28	10.25	11.42	12.96
4	7.5	9.81	8.42	7.52	6.86	5.99	5.67	6.74	7.84	8.52	9.35	10.33	11.52	13.05
4	3.5	9.83	8.43	7.51	6.84	5.99	5.67	6.74	7.84	8.54	9.36	10.33	11.53	13.08
4	-0.5	9.75	8.34	7.43	6.76	5.92	5.60	6.67	7.77	8.46	9.29	10.27	11.45	13.00
4	-4.5	9.56	8.16	7.27	6.60	5.77	5.47	6.53	7.61	8.30	9.11	10.08	11.27	12.79
4	-8.5	9.12	7.78	6.91	6.27	5.50	5.24	6.31	7.38	8.07	8.85	9.81	10.98	12.49
4	-12.5	7.74	6.66	5.97	5.48	4.91	4.86	5.98	7.05	7.72	8.50	9.44	10.58	12.07
4	-16.5	5.86	5.19	4.78	4.50	4.19	4.40	5.58	6.63	7.30	8.06	8.98	10.11	11.55
4	-20.5	5.21	4.63	4.28	4.05	3.81	4.06	5.23	6.25	6.89	7.64	8.53	9.61	11.03
4	-24.5	4.79	4.26	3.94	3.73	3.52	3.78	4.90	5.88	6.48	7.20	8.05	9.09	10.46
4	-28.5	4.40	3.93	3.64	3.43	3.24	3.50	4.55	5.48	6.05	6.74	7.55	8.55	9.85
4	-32.5	4.02	3.58	3.33	3.14	2.97	3.22	4.23	5.11	5.65	6.29	7.07	8.02	9.27
4	-36.5	3.71	3.29	3.05	2.88	2.72	2.96	3.91	4.75	5.27	5.88	6.63	7.55	8.76
4	-40.5	3.60	3.18	2.92	2.76	2.61	2.84	3.75	4.57	5.06	5.67	6.39	7.27	8.46
0.5	-41	3.78	3.34	3.07	2.90	2.74	2.98	3.87	4.67	5.15	5.73	6.43	7.32	8.52
0.3	-41.3	3.87	3.41	3.16	3.00	2.83	3.07	3.97	4.74	5.23	5.83	6.52	7.40	8.61
0.3	-41.6	3.97	3.50	3.25	3.07	2.93	3.17	4.05	4.81	5.29	5.88	6.61	7.47	8.63
0.3	-41.9	4.09	3.63	3.35	3.17	3.05	3.29	4.16	4.94	5.38	5.99	6.71	7.55	8.73
0.3	-42.2	4.22	3.72	3.48	3.32	3.18	3.44	4.31	5.07	5.53	6.11	6.80	7.64	8.81
0.3	-42.5	4.37	3.91	3.66	3.48	3.37	3.64	4.51	5.26	5.72	6.27	6.94	7.83	8.98
0.3	-42.8	4.55	4.10	3.85	3.73	3.64	3.91	4.76	5.48	5.95	6.48	7.17	8.00	9.13
0.3	-43.1	4.79	4.35	4.13	4.02	3.96	4.28	5.13	5.79	6.23	6.76	7.41	8.26	9.29
0.3	-43.4	5.09	4.70	4.53	4.44	4.40	4.76	5.60	6.27	6.68	7.17	7.76	8.55	9.55
0.3	-43.7	5.52	5.18	5.06	4.98	5.01	5.44	6.28	6.90	7.29	7.73	8.31	8.98	9.96
0.3	-44	6.19	5.98	5.92	5.90	5.99	6.50	7.37	8.00	8.36	8.77	9.27	9.83	10.64

Table A3 - 18 – LEU fuel power density at day 24 (core power at 57.8 MW)

radial node width (cm)		0.3	0.3	0.3	0.3	1	1.734	1	0.3	0.3	0.3	0.3	0.3	0.3
distance (cm) from - inner edge of the fuel	0	0.3	0.6	0.9	1.2	2.2	3.934	4.934	5.234	5.534	5.834	6.134	6.434	6.734
- core center	14	14.29	14.57	14.85	15.13	16.01	17.43	18.19	18.42	18.64	18.86	19.07	19.29	19.5
axial node height (cm)	position to core midplane (cm)	volumetric heat generation rate (W/mm^3)												
	44													
0.3	43.7	12.17	11.31	10.91	10.54	10.04	9.62	9.90	10.30	10.52	10.90	11.29	11.81	12.51
0.3	43.4	11.32	10.29	9.70	9.20	8.62	8.21	8.58	9.09	9.41	9.78	10.29	10.98	11.90
0.3	43.1	10.73	9.60	8.84	8.38	7.72	7.30	7.72	8.29	8.69	9.15	9.75	10.49	11.51
0.3	42.8	10.29	9.06	8.30	7.72	7.04	6.62	7.10	7.77	8.16	8.69	9.33	10.17	11.21
0.3	42.5	9.91	8.67	7.86	7.26	6.54	6.11	6.67	7.39	7.80	8.38	9.05	9.92	11.04
0.3	42.2	9.61	8.35	7.56	6.92	6.14	5.72	6.32	7.05	7.53	8.12	8.87	9.68	10.85
0.3	41.9	9.39	8.08	7.29	6.62	5.84	5.41	6.04	6.81	7.28	7.90	8.62	9.55	10.73
0.3	41.6	9.14	7.84	7.03	6.41	5.61	5.17	5.84	6.61	7.17	7.76	8.52	9.38	10.59
0.3	41.3	8.96	7.68	6.84	6.21	5.42	4.98	5.69	6.50	6.98	7.67	8.41	9.28	10.53
0.3	41	8.80	7.52	6.70	6.08	5.26	4.85	5.58	6.41	6.92	7.57	8.32	9.21	10.42
0.3	40.7	8.68	7.40	6.56	5.94	5.14	4.73	5.47	6.30	6.85	7.50	8.24	9.17	10.38
0.3	40.4	8.53	7.28	6.46	5.83	5.04	4.63	5.39	6.24	6.78	7.45	8.21	9.16	10.34
0.3	40.1	8.46	7.20	6.39	5.75	4.97	4.56	5.33	6.21	6.75	7.43	8.19	9.09	10.30
0.3	39.8	8.38	7.17	6.30	5.68	4.90	4.52	5.29	6.15	6.72	7.38	8.13	9.07	10.26
0.3	39.5	8.32	7.10	6.24	5.62	4.84	4.48	5.28	6.11	6.68	7.28	8.12	9.02	10.27
4	35.5	8.01	6.83	6.05	5.47	4.72	4.41	5.24	6.12	6.67	7.34	8.12	9.06	10.29
4	31.5	7.99	6.85	6.10	5.55	4.83	4.56	5.44	6.35	6.93	7.58	8.39	9.35	10.57
4	27.5	8.27	7.10	6.35	5.80	5.08	4.81	5.74	6.67	7.26	7.95	8.76	9.73	10.99
4	23.5	8.62	7.43	6.66	6.09	5.34	5.07	6.03	7.00	7.60	8.32	9.14	10.13	11.40
4	19.5	8.95	7.73	6.93	6.33	5.57	5.28	6.28	7.28	7.90	8.63	9.47	10.47	11.77
4	15.5	9.22	7.97	7.15	6.54	5.75	5.46	6.48	7.50	8.13	8.87	9.73	10.73	12.06
4	11.5	9.40	8.13	7.29	6.68	5.88	5.58	6.61	7.65	8.29	9.04	9.91	10.93	12.25
4	7.5	9.50	8.22	7.38	6.75	5.94	5.65	6.69	7.74	8.39	9.14	10.02	11.06	12.38
4	3.5	9.55	8.25	7.39	6.77	5.96	5.66	6.70	7.75	8.40	9.16	10.03	11.07	12.40
4	-0.5	9.52	8.22	7.36	6.73	5.91	5.61	6.65	7.70	8.34	9.10	9.97	11.01	12.34
4	-4.5	9.44	8.11	7.25	6.61	5.80	5.51	6.54	7.59	8.23	8.98	9.86	10.88	12.21
4	-8.5	9.23	7.91	7.05	6.42	5.62	5.35	6.37	7.40	8.04	8.79	9.65	10.69	12.00
4	-12.5	8.81	7.52	6.70	6.09	5.34	5.11	6.13	7.14	7.77	8.49	9.35	10.36	11.68
4	-16.5	7.67	6.58	5.90	5.40	4.81	4.73	5.79	6.79	7.40	8.11	8.95	9.96	11.24
4	-20.5	5.70	5.04	4.64	4.36	4.06	4.25	5.37	6.36	6.96	7.67	8.49	9.47	10.74
4	-24.5	4.92	4.39	4.06	3.84	3.62	3.88	4.99	5.94	6.52	7.20	8.00	8.95	10.19
4	-28.5	4.48	3.98	3.69	3.50	3.30	3.57	4.63	5.54	6.09	6.75	7.51	8.44	9.64
4	-32.5	4.09	3.63	3.37	3.19	3.02	3.28	4.28	5.15	5.67	6.29	7.04	7.93	9.08
4	-36.5	3.75	3.34	3.09	2.92	2.76	3.02	3.97	4.80	5.30	5.89	6.60	7.46	8.57
4	-40.5	3.63	3.21	2.96	2.80	2.65	2.89	3.81	4.61	5.09	5.67	6.38	7.20	8.29
0.5	-41	3.80	3.38	3.12	2.95	2.79	3.03	3.92	4.71	5.18	5.75	6.45	7.27	8.38
0.3	-41.3	3.89	3.43	3.18	3.01	2.88	3.11	4.00	4.80	5.25	5.82	6.52	7.28	8.43
0.3	-41.6	3.98	3.51	3.26	3.11	2.97	3.21	4.10	4.83	5.31	5.89	6.55	7.37	8.47
0.3	-41.9	4.09	3.63	3.38	3.21	3.08	3.34	4.19	4.94	5.43	6.00	6.67	7.51	8.52
0.3	-42.2	4.21	3.75	3.50	3.35	3.22	3.49	4.36	5.12	5.56	6.12	6.78	7.58	8.62
0.3	-42.5	4.36	3.93	3.67	3.52	3.42	3.69	4.54	5.27	5.71	6.26	6.89	7.68	8.74
0.3	-42.8	4.55	4.12	3.89	3.75	3.67	3.96	4.81	5.52	5.97	6.50	7.06	7.88	8.87
0.3	-43.1	4.80	4.37	4.18	4.06	4.00	4.32	5.17	5.84	6.26	6.74	7.37	8.09	9.11
0.3	-43.4	5.10	4.72	4.55	4.45	4.43	4.80	5.63	6.24	6.67	7.12	7.69	8.41	9.34
0.3	-43.7	5.53	5.16	5.05	4.98	5.02	5.44	6.26	6.90	7.22	7.64	8.17	8.79	9.68
0.3	-44	6.13	5.96	5.89	5.84	5.96	6.46	7.33	7.88	8.20	8.55	8.96	9.50	10.22

Table A3 - 19 – LEU fuel power density at day 30 (core power at 57.8 MW)

radial node width (cm)		0.3	0.3	0.3	0.3	1	1.734	1	0.3	0.3	0.3	0.3	0.3	0.3
distance (cm) from - inner edge of the fuel	0	0.3	0.6	0.9	1.2	2.2	3.934	4.934	5.234	5.534	5.834	6.134	6.434	6.734
- core center	14	14.29	14.57	14.85	15.13	16.01	17.43	18.19	18.42	18.64	18.86	19.07	19.29	19.5
axial node height (cm)	position to core midplane (cm)	volumetric heat generation rate (W/mm^3)												
	44													
0.3	43.7	11.90	11.26	10.85	10.51	10.08	9.81	10.12	10.49	10.76	11.10	11.40	11.82	12.47
0.3	43.4	11.06	10.20	9.69	9.32	8.79	8.45	8.85	9.34	9.61	10.02	10.49	11.02	11.82
0.3	43.1	10.55	9.55	8.95	8.50	7.89	7.56	8.01	8.54	8.93	9.36	9.89	10.61	11.48
0.3	42.8	10.13	9.10	8.40	7.93	7.23	6.85	7.39	7.99	8.41	8.90	9.48	10.21	11.15
0.3	42.5	9.81	8.69	7.94	7.46	6.71	6.33	6.92	7.59	8.05	8.56	9.19	9.95	10.96
0.3	42.2	9.54	8.40	7.63	7.06	6.31	5.91	6.53	7.25	7.73	8.27	8.94	9.71	10.77
0.3	41.9	9.31	8.12	7.31	6.74	5.99	5.59	6.26	7.02	7.51	8.07	8.73	9.54	10.58
0.3	41.6	9.07	7.88	7.09	6.48	5.72	5.34	6.04	6.79	7.30	7.90	8.59	9.41	10.48
0.3	41.3	8.89	7.68	6.89	6.28	5.52	5.14	5.86	6.63	7.16	7.71	8.44	9.33	10.35
0.3	41	8.73	7.50	6.74	6.12	5.36	4.98	5.70	6.51	7.01	7.64	8.35	9.20	10.29
0.3	40.7	8.60	7.38	6.62	6.00	5.23	4.85	5.62	6.43	6.94	7.53	8.24	9.11	10.17
0.3	40.4	8.45	7.28	6.51	5.92	5.14	4.75	5.53	6.37	6.91	7.47	8.21	9.07	10.15
0.3	40.1	8.33	7.22	6.38	5.80	5.03	4.67	5.45	6.30	6.81	7.41	8.15	9.03	10.09
0.3	39.8	8.27	7.07	6.30	5.71	4.95	4.60	5.40	6.25	6.79	7.35	8.09	8.93	10.06
0.3	39.5	8.19	7.02	6.21	5.65	4.89	4.55	5.33	6.21	6.71	7.36	8.06	8.93	10.03
4	35.5	7.87	6.76	6.02	5.46	4.74	4.44	5.27	6.13	6.67	7.28	8.00	8.86	9.95
4	31.5	7.80	6.72	6.02	5.49	4.80	4.55	5.41	6.29	6.84	7.47	8.18	9.05	10.13
4	27.5	8.01	6.94	6.23	5.71	5.02	4.78	5.68	6.58	7.14	7.77	8.51	9.37	10.46
4	23.5	8.33	7.23	6.50	5.96	5.27	5.02	5.96	6.88	7.44	8.08	8.84	9.71	10.81
4	19.5	8.63	7.49	6.75	6.20	5.49	5.24	6.20	7.15	7.72	8.39	9.15	10.01	11.13
4	15.5	8.88	7.73	6.97	6.40	5.66	5.40	6.39	7.36	7.95	8.62	9.38	10.27	11.38
4	11.5	9.06	7.87	7.12	6.54	5.79	5.53	6.53	7.52	8.10	8.77	9.54	10.44	11.55
4	7.5	9.18	8.00	7.21	6.63	5.87	5.60	6.61	7.60	8.20	8.89	9.66	10.56	11.67
4	3.5	9.24	8.04	7.25	6.66	5.89	5.61	6.64	7.63	8.24	8.92	9.70	10.60	11.73
4	-0.5	9.26	8.04	7.24	6.65	5.87	5.59	6.61	7.61	8.20	8.88	9.67	10.57	11.71
4	-4.5	9.22	7.99	7.18	6.58	5.80	5.52	6.53	7.51	8.11	8.79	9.59	10.49	11.64
4	-8.5	9.12	7.86	7.03	6.43	5.66	5.40	6.40	7.38	7.98	8.65	9.44	10.35	11.49
4	-12.5	8.89	7.63	6.82	6.22	5.47	5.21	6.20	7.17	7.75	8.43	9.19	10.10	11.23
4	-16.5	8.50	7.29	6.50	5.92	5.20	4.97	5.94	6.88	7.45	8.11	8.89	9.78	10.90
4	-20.5	7.70	6.58	5.87	5.37	4.75	4.62	5.59	6.51	7.08	7.74	8.49	9.38	10.50
4	-24.5	5.81	5.10	4.66	4.35	4.00	4.13	5.17	6.07	6.63	7.27	8.02	8.89	9.98
4	-28.5	4.70	4.17	3.86	3.65	3.45	3.70	4.75	5.64	6.18	6.80	7.52	8.37	9.45
4	-32.5	4.20	3.74	3.48	3.29	3.11	3.37	4.38	5.23	5.75	6.35	7.05	7.88	8.92
4	-36.5	3.82	3.40	3.16	2.99	2.83	3.09	4.06	4.87	5.37	5.95	6.61	7.41	8.44
4	-40.5	3.69	3.26	3.02	2.86	2.70	2.95	3.88	4.67	5.16	5.72	6.37	7.16	8.18
0.5	-41	3.88	3.43	3.18	2.99	2.85	3.10	4.00	4.80	5.23	5.81	6.47	7.23	8.24
0.3	-41.3	3.95	3.52	3.24	3.10	2.94	3.19	4.09	4.85	5.32	5.88	6.52	7.27	8.26
0.3	-41.6	4.03	3.59	3.34	3.17	3.04	3.30	4.18	4.92	5.40	5.94	6.58	7.33	8.30
0.3	-41.9	4.15	3.70	3.45	3.28	3.15	3.41	4.29	5.07	5.52	6.03	6.67	7.44	8.40
0.3	-42.2	4.27	3.83	3.59	3.43	3.31	3.57	4.45	5.18	5.62	6.13	6.75	7.51	8.48
0.3	-42.5	4.42	3.99	3.75	3.58	3.50	3.77	4.64	5.35	5.80	6.31	6.91	7.63	8.63
0.3	-42.8	4.61	4.17	3.95	3.82	3.72	4.04	4.87	5.57	6.00	6.48	7.06	7.81	8.73
0.3	-43.1	4.84	4.45	4.22	4.11	4.05	4.39	5.22	5.88	6.31	6.73	7.30	7.99	8.87
0.3	-43.4	5.13	4.76	4.60	4.51	4.50	4.86	5.68	6.28	6.64	7.12	7.61	8.28	9.11
0.3	-43.7	5.54	5.20	5.08	5.03	5.08	5.47	6.29	6.88	7.24	7.60	8.07	8.67	9.43
0.3	-44	6.13	5.94	5.89	5.87	5.96	6.46	7.27	7.83	8.11	8.44	8.81	9.32	9.90

Table A3 - 20 – LEU fuel power density at day 36 (core power at 57.8 MW)

radial node width (cm)		0.3	0.3	0.3	0.3	1	1.734	1	0.3	0.3	0.3	0.3	0.3	0.3
distance (cm) from - inner edge of the fuel	0	0.3	0.6	0.9	1.2	2.2	3.934	4.934	5.234	5.534	5.834	6.134	6.434	6.734
- core center	14	14.29	14.57	14.85	15.13	16.01	17.43	18.19	18.42	18.64	18.86	19.07	19.29	19.5
axial node height (cm)	position to core midplane (cm)	volumetric heat generation rate (W/mm^3)												
	44													
0.3	43.7	11.44	10.90	10.57	10.32	10.01	9.84	10.22	10.59	10.80	11.05	11.35	11.70	12.17
0.3	43.4	10.77	10.02	9.60	9.27	8.83	8.57	9.02	9.45	9.77	10.09	10.49	10.94	11.60
0.3	43.1	10.29	9.42	8.85	8.53	7.97	7.71	8.19	8.73	9.03	9.43	9.89	10.45	11.24
0.3	42.8	9.85	9.00	8.40	7.94	7.32	7.00	7.56	8.18	8.55	8.99	9.53	10.14	10.95
0.3	42.5	9.58	8.57	7.95	7.45	6.81	6.48	7.06	7.71	8.15	8.65	9.17	9.86	10.75
0.3	42.2	9.32	8.28	7.61	7.08	6.41	6.05	6.70	7.39	7.81	8.31	8.89	9.63	10.54
0.3	41.9	9.11	8.04	7.34	6.80	6.09	5.72	6.39	7.10	7.57	8.08	8.71	9.42	10.37
0.3	41.6	8.86	7.80	7.09	6.53	5.83	5.45	6.15	6.90	7.34	7.90	8.55	9.30	10.24
0.3	41.3	8.69	7.63	6.89	6.33	5.62	5.23	5.96	6.74	7.24	7.77	8.43	9.18	10.08
0.3	41	8.59	7.44	6.71	6.15	5.41	5.06	5.82	6.59	7.07	7.67	8.28	9.02	9.98
0.3	40.7	8.41	7.28	6.57	6.03	5.27	4.92	5.69	6.46	6.98	7.55	8.20	8.98	9.92
0.3	40.4	8.25	7.17	6.44	5.89	5.14	4.80	5.56	6.38	6.90	7.46	8.13	8.91	9.84
0.3	40.1	8.19	7.11	6.35	5.78	5.06	4.71	5.50	6.32	6.81	7.42	8.04	8.81	9.80
0.3	39.8	8.08	7.01	6.26	5.70	4.97	4.65	5.43	6.27	6.80	7.35	7.98	8.78	9.74
0.3	39.5	7.96	6.91	6.18	5.65	4.92	4.58	5.37	6.21	6.73	7.29	7.97	8.75	9.68
4	35.5	7.65	6.63	5.94	5.41	4.72	4.44	5.26	6.09	6.60	7.18	7.84	8.61	9.56
4	31.5	7.53	6.54	5.89	5.38	4.74	4.51	5.36	6.20	6.70	7.29	7.94	8.70	9.65
4	27.5	7.71	6.73	6.07	5.58	4.94	4.72	5.60	6.46	6.98	7.55	8.20	8.95	9.90
4	23.5	7.99	6.99	6.33	5.82	5.17	4.95	5.86	6.73	7.25	7.84	8.50	9.25	10.19
4	19.5	8.26	7.24	6.57	6.05	5.38	5.15	6.09	6.98	7.51	8.10	8.76	9.51	10.45
4	15.5	8.49	7.45	6.76	6.23	5.55	5.32	6.27	7.17	7.71	8.30	8.97	9.73	10.67
4	11.5	8.67	7.61	6.91	6.38	5.68	5.45	6.42	7.33	7.87	8.47	9.14	9.90	10.83
4	7.5	8.81	7.73	7.01	6.48	5.77	5.53	6.50	7.43	7.98	8.58	9.25	10.02	10.96
4	3.5	8.89	7.79	7.07	6.53	5.81	5.57	6.55	7.48	8.03	8.65	9.32	10.09	11.04
4	-0.5	8.95	7.83	7.08	6.54	5.81	5.56	6.55	7.48	8.03	8.65	9.33	10.09	11.05
4	-4.5	8.96	7.81	7.06	6.50	5.76	5.51	6.49	7.42	7.96	8.59	9.28	10.06	11.03
4	-8.5	8.93	7.74	6.97	6.40	5.66	5.41	6.39	7.32	7.87	8.49	9.18	9.96	10.94
4	-12.5	8.81	7.61	6.83	6.26	5.52	5.27	6.23	7.15	7.70	8.32	9.01	9.80	10.78
4	-16.5	8.59	7.37	6.61	6.03	5.31	5.08	6.02	6.91	7.45	8.08	8.77	9.57	10.56
4	-20.5	8.22	7.04	6.29	5.75	5.06	4.84	5.76	6.64	7.16	7.77	8.47	9.25	10.24
4	-24.5	7.67	6.56	5.85	5.34	4.70	4.52	5.43	6.29	6.81	7.41	8.08	8.88	9.85
4	-28.5	6.52	5.62	5.03	4.63	4.14	4.10	5.03	5.88	6.38	6.96	7.64	8.41	9.38
4	-32.5	4.76	4.20	3.88	3.65	3.41	3.60	4.58	5.42	5.91	6.49	7.15	7.92	8.89
4	-36.5	4.05	3.60	3.34	3.15	2.99	3.24	4.21	5.03	5.50	6.06	6.72	7.46	8.43
4	-40.5	3.85	3.41	3.15	2.98	2.83	3.08	4.03	4.82	5.29	5.84	6.48	7.23	8.16
0.5	-41	4.00	3.55	3.31	3.12	2.97	3.22	4.15	4.90	5.37	5.91	6.55	7.28	8.22
0.3	-41.3	4.11	3.65	3.37	3.24	3.07	3.32	4.22	4.98	5.44	5.97	6.58	7.35	8.28
0.3	-41.6	4.21	3.73	3.45	3.30	3.16	3.43	4.32	5.06	5.53	6.06	6.66	7.41	8.33
0.3	-41.9	4.31	3.86	3.59	3.42	3.28	3.54	4.44	5.19	5.62	6.16	6.76	7.46	8.37
0.3	-42.2	4.44	3.96	3.70	3.57	3.44	3.71	4.59	5.34	5.75	6.26	6.89	7.57	8.46
0.3	-42.5	4.57	4.14	3.89	3.73	3.62	3.92	4.80	5.48	5.90	6.42	6.99	7.67	8.57
0.3	-42.8	4.76	4.34	4.09	3.98	3.88	4.18	5.06	5.71	6.13	6.59	7.14	7.82	8.67
0.3	-43.1	4.99	4.60	4.39	4.26	4.21	4.54	5.38	6.00	6.39	6.87	7.39	8.05	8.84
0.3	-43.4	5.28	4.90	4.72	4.64	4.64	5.00	5.82	6.46	6.78	7.19	7.70	8.25	9.01
0.3	-43.7	5.68	5.33	5.22	5.17	5.19	5.62	6.41	6.97	7.33	7.69	8.09	8.63	9.27
0.3	-44	6.28	6.03	5.96	5.96	6.06	6.55	7.33	7.82	8.11	8.43	8.83	9.22	9.71

Table A3 - 21 – LEU fuel power density at day 42 (core power at 57.8 MW)

radial node width (cm)		0.3	0.3	0.3	0.3	1	1.734	1	0.3	0.3	0.3	0.3	0.3	0.3
distance (cm) from - inner edge of the fuel	0	0.3	0.6	0.9	1.2	2.2	3.934	4.934	5.234	5.534	5.834	6.134	6.434	6.734
- core center	14	14.29	14.57	14.85	15.13	16.01	17.43	18.19	18.42	18.64	18.86	19.07	19.29	19.5
axial node height (cm)	position to core midplane (cm)	volumetric heat generation rate (W/mm^3)												
	44													
0.3	43.7	10.75	10.34	10.08	9.91	9.65	9.59	9.93	10.30	10.49	10.68	10.95	11.21	11.57
0.3	43.4	10.18	9.59	9.25	8.96	8.61	8.48	8.89	9.29	9.58	9.85	10.18	10.57	11.06
0.3	43.1	9.76	9.09	8.63	8.30	7.86	7.65	8.13	8.64	8.92	9.29	9.67	10.16	10.72
0.3	42.8	9.45	8.65	8.15	7.78	7.24	7.00	7.54	8.14	8.43	8.83	9.29	9.80	10.50
0.3	42.5	9.18	8.31	7.78	7.35	6.75	6.49	7.08	7.70	8.06	8.44	8.97	9.52	10.30
0.3	42.2	8.92	8.03	7.44	6.96	6.35	6.07	6.69	7.31	7.75	8.20	8.69	9.33	10.04
0.3	41.9	8.70	7.77	7.14	6.63	6.05	5.71	6.39	7.08	7.50	7.96	8.52	9.08	9.89
0.3	41.6	8.48	7.56	6.92	6.41	5.76	5.45	6.13	6.82	7.27	7.80	8.31	9.02	9.79
0.3	41.3	8.33	7.36	6.73	6.24	5.55	5.23	5.96	6.70	7.11	7.63	8.20	8.85	9.63
0.3	41	8.18	7.24	6.54	6.06	5.38	5.05	5.77	6.55	6.97	7.51	8.08	8.76	9.55
0.3	40.7	8.08	7.09	6.44	5.91	5.22	4.90	5.65	6.42	6.88	7.39	8.00	8.63	9.44
0.3	40.4	7.93	6.98	6.31	5.78	5.09	4.79	5.55	6.34	6.76	7.32	7.89	8.57	9.37
0.3	40.1	7.84	6.87	6.19	5.70	4.98	4.69	5.46	6.25	6.65	7.21	7.80	8.49	9.32
0.3	39.8	7.73	6.77	6.12	5.61	4.92	4.62	5.37	6.15	6.60	7.14	7.73	8.47	9.29
0.3	39.5	7.67	6.68	6.04	5.55	4.84	4.54	5.33	6.09	6.56	7.11	7.71	8.38	9.20
4	35.5	7.33	6.39	5.76	5.28	4.63	4.38	5.18	5.96	6.43	6.97	7.56	8.22	9.04
4	31.5	7.18	6.28	5.68	5.22	4.62	4.42	5.24	6.03	6.50	7.02	7.59	8.26	9.05
4	27.5	7.33	6.43	5.84	5.39	4.80	4.61	5.46	6.25	6.72	7.24	7.82	8.47	9.25
4	23.5	7.58	6.68	6.07	5.62	5.01	4.82	5.70	6.51	6.98	7.50	8.07	8.71	9.50
4	19.5	7.84	6.92	6.31	5.84	5.22	5.02	5.92	6.73	7.21	7.74	8.31	8.94	9.71
4	15.5	8.05	7.11	6.49	6.01	5.38	5.19	6.10	6.94	7.42	7.95	8.51	9.14	9.92
4	11.5	8.23	7.28	6.64	6.16	5.52	5.32	6.24	7.10	7.58	8.11	8.68	9.32	10.09
4	7.5	8.36	7.40	6.76	6.27	5.62	5.42	6.35	7.20	7.69	8.22	8.80	9.44	10.20
4	3.5	8.49	7.49	6.84	6.33	5.68	5.47	6.41	7.27	7.77	8.32	8.88	9.53	10.32
4	-0.5	8.57	7.56	6.89	6.38	5.70	5.48	6.44	7.30	7.79	8.33	8.93	9.58	10.37
4	-4.5	8.65	7.60	6.89	6.38	5.69	5.46	6.42	7.28	7.79	8.33	8.93	9.57	10.38
4	-8.5	8.67	7.57	6.86	6.32	5.62	5.40	6.35	7.23	7.73	8.29	8.88	9.55	10.36
4	-12.5	8.62	7.50	6.77	6.23	5.53	5.29	6.24	7.10	7.60	8.16	8.78	9.46	10.30
4	-16.5	8.50	7.36	6.62	6.08	5.38	5.15	6.08	6.94	7.44	8.00	8.63	9.32	10.16
4	-20.5	8.28	7.13	6.40	5.87	5.18	4.96	5.86	6.72	7.22	7.77	8.40	9.09	9.96
4	-24.5	7.97	6.84	6.12	5.60	4.93	4.72	5.61	6.44	6.95	7.50	8.12	8.83	9.70
4	-28.5	7.56	6.46	5.76	5.25	4.63	4.45	5.31	6.12	6.61	7.17	7.79	8.49	9.38
4	-32.5	7.03	6.00	5.34	4.87	4.28	4.12	4.97	5.76	6.24	6.78	7.41	8.12	9.00
4	-36.5	6.29	5.36	4.77	4.35	3.85	3.78	4.62	5.40	5.88	6.41	7.03	7.73	8.61
4	-40.5	4.93	4.30	3.92	3.65	3.35	3.48	4.39	5.17	5.64	6.17	6.78	7.50	8.38
0.5	-41	4.57	4.05	3.72	3.52	3.33	3.55	4.47	5.27	5.73	6.25	6.85	7.55	8.42
0.3	-41.3	4.62	4.06	3.78	3.61	3.41	3.64	4.58	5.36	5.79	6.32	6.92	7.59	8.49
0.3	-41.6	4.69	4.15	3.89	3.68	3.50	3.74	4.66	5.43	5.87	6.40	6.99	7.66	8.52
0.3	-41.9	4.73	4.25	3.98	3.80	3.62	3.87	4.80	5.54	5.98	6.47	7.04	7.73	8.57
0.3	-42.2	4.86	4.36	4.11	3.93	3.78	4.03	4.93	5.68	6.09	6.59	7.19	7.86	8.67
0.3	-42.5	5.00	4.52	4.27	4.10	3.97	4.25	5.15	5.86	6.24	6.73	7.28	7.96	8.74
0.3	-42.8	5.17	4.72	4.48	4.32	4.21	4.53	5.38	6.06	6.49	6.93	7.47	8.12	8.90
0.3	-43.1	5.40	4.98	4.76	4.64	4.55	4.87	5.72	6.37	6.72	7.20	7.72	8.31	9.06
0.3	-43.4	5.69	5.31	5.10	4.99	4.99	5.34	6.15	6.78	7.12	7.50	7.98	8.55	9.21
0.3	-43.7	6.09	5.71	5.58	5.53	5.56	5.97	6.74	7.31	7.61	7.96	8.39	8.84	9.43
0.3	-44	6.64	6.45	6.37	6.34	6.45	6.87	7.62	8.12	8.36	8.66	8.97	9.37	9.82

Table A3 - 22 – LEU fuel power density at EOC, day 48 (core power at 57.8 MW)

radial node width (cm)		0.3	0.3	0.3	0.3	1	1.734	1	0.3	0.3	0.3	0.3	0.3	0.3
distance (cm) from - inner edge of the fuel	0	0.3	0.6	0.9	1.2	2.2	3.934	4.934	5.234	5.534	5.834	6.134	6.434	6.734
- core center	14	14.29	14.57	14.85	15.13	16.01	17.43	18.19	18.42	18.64	18.86	19.07	19.29	19.5
axial node height (cm)	position to core midplane (cm)	volumetric heat generation rate (W/mm^3)												
	44													
0.3	43.7	9.94	9.63	9.45	9.32	9.14	9.10	9.46	9.76	9.95	10.07	10.27	10.48	10.70
0.3	43.4	9.52	9.04	8.76	8.58	8.25	8.13	8.56	8.93	9.17	9.38	9.63	9.96	10.32
0.3	43.1	9.20	8.62	8.23	7.95	7.61	7.44	7.91	8.34	8.61	8.94	9.21	9.53	10.02
0.3	42.8	8.91	8.27	7.80	7.51	7.06	6.84	7.36	7.88	8.17	8.51	8.88	9.29	9.81
0.3	42.5	8.65	7.93	7.48	7.08	6.60	6.35	6.93	7.45	7.81	8.19	8.61	9.04	9.62
0.3	42.2	8.44	7.66	7.20	6.75	6.20	5.97	6.57	7.15	7.52	7.89	8.39	8.87	9.47
0.3	41.9	8.21	7.45	6.91	6.48	5.90	5.63	6.28	6.89	7.27	7.71	8.16	8.69	9.32
0.3	41.6	8.04	7.23	6.69	6.28	5.64	5.35	6.04	6.67	7.06	7.52	7.97	8.52	9.17
0.3	41.3	7.89	7.08	6.49	6.06	5.44	5.15	5.85	6.52	6.90	7.34	7.86	8.42	9.07
0.3	41	7.78	6.91	6.32	5.90	5.25	4.97	5.69	6.38	6.79	7.26	7.75	8.31	9.00
0.3	40.7	7.66	6.79	6.21	5.76	5.10	4.83	5.56	6.26	6.67	7.12	7.62	8.21	8.90
0.3	40.4	7.55	6.68	6.10	5.62	4.98	4.72	5.46	6.16	6.57	7.02	7.54	8.13	8.80
0.3	40.1	7.45	6.60	5.99	5.54	4.89	4.61	5.36	6.08	6.50	6.93	7.46	8.05	8.79
0.3	39.8	7.35	6.49	5.88	5.45	4.80	4.53	5.28	5.98	6.42	6.89	7.43	7.97	8.72
0.3	39.5	7.29	6.43	5.82	5.34	4.73	4.47	5.22	5.94	6.36	6.84	7.39	7.98	8.65
4	35.5	6.97	6.13	5.55	5.11	4.51	4.28	5.06	5.79	6.22	6.69	7.22	7.79	8.48
4	31.5	6.82	6.02	5.47	5.04	4.49	4.30	5.10	5.83	6.24	6.72	7.22	7.79	8.47
4	27.5	6.96	6.14	5.61	5.20	4.65	4.48	5.30	6.04	6.47	6.93	7.43	7.98	8.63
4	23.5	7.20	6.37	5.83	5.41	4.86	4.69	5.53	6.27	6.69	7.15	7.65	8.19	8.84
4	19.5	7.43	6.60	6.05	5.62	5.05	4.89	5.74	6.50	6.93	7.39	7.88	8.41	9.04
4	15.5	7.64	6.79	6.24	5.80	5.23	5.06	5.93	6.69	7.12	7.58	8.07	8.59	9.24
4	11.5	7.83	6.97	6.40	5.96	5.37	5.20	6.07	6.85	7.29	7.75	8.24	8.76	9.38
4	7.5	7.97	7.10	6.53	6.08	5.48	5.30	6.19	6.97	7.42	7.88	8.36	8.89	9.52
4	3.5	8.09	7.20	6.62	6.15	5.55	5.37	6.28	7.07	7.51	7.98	8.48	8.99	9.62
4	-0.5	8.23	7.30	6.68	6.22	5.60	5.41	6.32	7.12	7.56	8.04	8.54	9.08	9.72
4	-4.5	8.34	7.37	6.74	6.25	5.61	5.42	6.33	7.14	7.58	8.07	8.58	9.12	9.78
4	-8.5	8.41	7.39	6.74	6.25	5.58	5.38	6.30	7.11	7.57	8.05	8.57	9.14	9.81
4	-12.5	8.42	7.38	6.69	6.18	5.52	5.31	6.22	7.04	7.51	8.00	8.54	9.11	9.81
4	-16.5	8.38	7.31	6.61	6.08	5.42	5.20	6.11	6.92	7.39	7.90	8.45	9.04	9.76
4	-20.5	8.26	7.16	6.46	5.94	5.27	5.05	5.94	6.76	7.23	7.75	8.29	8.92	9.66
4	-24.5	8.07	6.97	6.26	5.74	5.07	4.86	5.73	6.54	7.02	7.54	8.11	8.73	9.49
4	-28.5	7.80	6.70	5.99	5.49	4.84	4.63	5.49	6.29	6.75	7.28	7.86	8.50	9.29
4	-32.5	7.48	6.41	5.72	5.22	4.58	4.39	5.23	6.02	6.49	7.00	7.58	8.24	9.04
4	-36.5	7.23	6.16	5.48	4.98	4.35	4.16	4.98	5.75	6.22	6.74	7.33	8.00	8.81
4	-40.5	7.27	6.15	5.45	4.93	4.30	4.10	4.90	5.68	6.14	6.66	7.25	7.93	8.75
0.5	-41	7.61	6.47	5.76	5.20	4.57	4.36	5.14	5.90	6.34	6.86	7.42	8.11	8.90
0.3	-41.3	7.72	6.57	5.86	5.35	4.71	4.50	5.26	6.02	6.45	7.01	7.55	8.20	9.00
0.3	-41.6	7.87	6.70	5.98	5.46	4.84	4.65	5.38	6.12	6.56	7.07	7.64	8.27	9.07
0.3	-41.9	7.99	6.85	6.16	5.64	5.02	4.81	5.55	6.26	6.69	7.17	7.73	8.38	9.11
0.3	-42.2	8.16	7.03	6.30	5.84	5.22	5.03	5.73	6.44	6.84	7.35	7.85	8.50	9.25
0.3	-42.5	8.31	7.21	6.54	6.06	5.49	5.30	5.98	6.62	7.07	7.52	8.01	8.63	9.34
0.3	-42.8	8.59	7.47	6.80	6.30	5.80	5.66	6.29	6.93	7.33	7.78	8.22	8.82	9.51
0.3	-43.1	8.85	7.77	7.13	6.72	6.21	6.09	6.69	7.26	7.64	8.04	8.47	9.03	9.67
0.3	-43.4	9.20	8.21	7.59	7.24	6.76	6.66	7.20	7.73	8.03	8.40	8.79	9.30	9.87
0.3	-43.7	9.62	8.73	8.24	7.89	7.49	7.38	7.89	8.31	8.60	8.94	9.24	9.64	10.17
0.3	-44	10.31	9.60	9.23	8.96	8.58	8.47	8.85	9.22	9.40	9.65	9.87	10.18	10.58

Table A3 - 23 – HEU and LEU power density evolution at location presenting at least once the peak value. When highlighted in yellow, values represent the peak.

HEU power density (W/mm^3)							LEU power density (W/mm^3)			
time (days)	outer edge			inner edge		envelope	time (days)	outer edge		envelope
	midplane	top	bottom	top	bottom			midplane	top	
0	14.36	11.93	8.68	9.26	3.26	14.36	**0**	14.77	13.30	14.77
1	14.38	12.29	8.09	9.72	3.58	14.38	**1**	14.88	13.54	14.88
2	14.27	12.32	8.03	9.79	3.62	14.27	**2**	14.83	13.37	14.83
3	14.13	12.33	7.96	9.82	3.61	14.13	**3**	14.72	13.30	14.72
4	13.97	12.27	7.93	9.91	3.63	13.97	**4**	14.60	13.21	14.60
5	13.81	12.29	7.89	10.01	3.64	13.81	**5**	14.51	13.15	14.51
6	13.65	12.30	7.87	10.10	3.66	13.65	**6**	14.40	13.06	14.40
9	13.17	12.44	7.78	10.37	3.74	13.17	**9**	14.08	12.92	14.08
12	12.68	12.55	7.74	10.75	3.80	12.68	**12**	13.76	12.81	13.76
15	12.16	12.56	7.62	11.09	3.85	12.56	**15**	13.43	12.70	13.43
18	11.69	12.65	7.62	11.45	3.93	12.65	**18**	13.08	12.59	13.08
21	11.20	12.52	7.53	11.70	4.03	12.52	**21**	12.76	12.62	12.76
24	10.72	12.35	7.53	11.72	4.12	12.35	**24**	12.40	12.51	12.51
27	10.24	11.96	7.50	11.60	4.26	11.96	**27**	12.08	12.47	12.47
30	9.76	11.38	7.54	11.25	4.42	11.38	**30**	11.73	12.47	12.47
33	9.25	10.66	7.65	10.65	4.65	10.66	**33**	11.38	12.30	12.30
36	8.73	9.86	7.78	9.97	4.95	9.97	**36**	11.04	12.17	12.17
39	8.21	9.09	8.01	9.23	5.34	9.23	**39**	10.66	11.92	11.92
42	7.72	8.32	8.38	8.57	6.17	8.57	**42**	10.32	11.57	11.57
43	7.55	8.06	8.58	8.34	7.40	8.58	**43**	10.17	11.40	11.40
44	7.37	7.83	8.95	8.10	8.89	8.95	**44**	10.05	11.24	11.24
45	7.22	7.58	9.39	7.85	9.88	9.88	**45**	9.94	11.14	11.14
45.5	7.14	7.48	9.55	7.76	10.24	10.24	**46**	9.80	10.92	10.92
							47	9.70	10.77	10.77
							48	9.62	10.70	10.70

A4. Tabulated Values of Section 4.4

Table A4 - 1 – Experimental device reactivity worth total and when flooded

experimental device	HEU - worth (pcm) - cold	HEU - worth (pcm) - hot	LEU - worth (pcm) - cold	flooded beam tube	HEU - worth (pcm) - hot	LEU - worth (pcm) - cold
H2	40	24	29	**H2**	544	632
IH3	68	54	57	**IH3**	276	409
H12	77	71	74	**H12**	55	207
H4	83	75	76	**H3**	286	421
H1	115	117	121	**H4**	94	239
H8	144	125	126	**H8**	39	183
H6-7	150	131	134	**H6-7**	70	219
H3	154	141	150	**H1**	70	200
VX7	206	203	191	**VX7**	290	441
H5	287	277	284	**H5**	205	356
H9	299	297	288	**H9**	80	224
H11	358	317	308	**VX4**	70	222
VX4	380	342	328	**H11**	243	372
H5 + horizontal cold source	399	405	397	**H13**	53	190
H13	461	453	455	**H5 + source**	270	355
Hot Source	649	562	603	**H10**	130	269
H10	787	779	717			
vertical cold source	821	817	784			

Table A4 - 2 – Detailed reactivity effect of passage from room temperature to full power (57.8 MW) conditions

In-pile components		from cold to hot conditions reactivity effect (pcm)		
type	**location**	**Effect of…**	**HEU**	**LEU**
Heavy water	**reflector**	**density**	-328	-251
		elastic	53	50
		doppler	72	70
		combined	-249	-154
	fuel element	**density**	-36	-42
		elastic	16	-14
		doppler	22	2
		combined	-48	-71
	central cavity	**density**	11	-6
		elastic	15	4
		doppler	41	35
		combined	39	35
	all	**density**	-314	-302
		elastic	44	59
		doppler	71	111
		combined	-260	-165
structures	**fuel**	**elastic**	8	3
		doppler	-16	-167
		combined	-32	-150
	hot source	**elastic**	18	-37
		doppler	81	74
		combined	141	66
	others	**elastic**	35	-8
		doppler	-24	39
		combined	-2	-4
entire reactor		**density**	-314	-302
		elastic	16	-37
		doppler	-33	-133
		combined	-240	-252

Table A4 - 3 – Control Element (CE) reactivity worth at BOC in cold conditions and during irradiation at full power condition

CE worth (pcm), cold, BOC			CE worth (pcm) during core depletion			
CE distance from fully withdrawn position (cm)	**HEU core**	**LEU core**	**HEU core, CE distance from fully withdrawn position (cm)**	**HEU core**	**LEU core, CE distance from fully withdrawn position (cm)**	**LEU core**
0	128	136	**25**	277	**47**	217
5	132	159	**42**	265	**50**	212
10	166	171	**44**	265	**52**	210
15	193	196	**45**	276	**53**	203
20	224	201	**47**	260	**54**	213
25	243	213	**48**	260	**55**	205
30	263	219	**48**	259	**58**	200
35	272	217	**50**	274	**60**	187
40	272	212	**52**	243	**62**	181
45	261	197	**54**	247	**65**	171
50	239	185	**55**	212	**67**	161
55	216	170	**57**	243	**70**	157
60	191	150	**59**	235	**73**	147
65	163	135	**62**	221	**75**	131
70	134	117	**65**	188	**78**	130
75	106	101	**69**	195	**82**	118
80	82	85	**74**	167	**86**	111
85	53	67	**80**	146	**92**	87
90	24	62	**87**	111	**94**	64
95	21	60	**90**	91	**96**	73
			95	73	**98**	78
			100	73	**101**	61
			105	52	**103**	61
			111	44	**106**	77
					108	69
					112	56
					115	34

Table A4 - 4 – Core reactivity change due to the insertion of the safety rods

distance of insertion (cm)	BOC, cold condition		BOC, cold condition, H10 flooded	
	HEU core	LEU core	HEU core	LEU core
0	0	0	0	0
20	-452	-495	-450	-516
34	-1417	-1590	-1411	-1591
40	-2223	-2484	-2197	-2467
42	-2574	-2837	-2578	-2815
59	-7310	-7054	-7255	-6967
72.5	-13446	-12064	-13394	-12015
77.5	-16254	-14368	-16266	-14394
93	-22493	-22984	-22490	-22976
120	-35996	-32714	-35845	-32619

Nuclear Engineering Division
Argonne National Laboratory
9700 South Cass Avenue, Bldg. 208
Argonne, IL 60439

www.anl.gov

Argonne National Laboratory is a U.S. Department of Energy
laboratory managed by UChicago Argonne, LLC